Identification of Critical Active-Site Groups and Catalytic Steps Governing Desulfonation by Alkanesulfonate Monooxygenase

by

John Michael Robbins

A dissertation submitted to the Graduate Faculty of
Auburn University
in partial fulfillment of the
requirements for the Degree of
Doctor of Philosophy

Auburn, Alabama
December 8, 2012

Approved by

Holly R. Ellis, Chair, Associate Professor of Chemistry and Biochemistry
Douglas C. Goodwin, Associate Professor of Chemistry and Biochemistry
David M. Stanbury, Professor of Chemistry and Biochemistry
Peter D. Livant, Associate Professor of Chemistry and Biochemistry

Abstract

The alkanesulfonate monooxygenase enzyme (SsuD) catalyzes the oxygenolytic cleavage of a carbon-sulfur bond of sulfonated substrates. A mechanism involving acid-base catalysis is proposed for the desulfonation mechanism by SsuD. In the proposed mechanism, base catalysis is involved in abstracting a proton from an alkane peroxyflavin intermediate, while acid catalysis is needed for the protonation of the $FMNO^-$ intermediate. The catalytic mechanism for SsuD was evaluated using several kinetic approaches including steady-state pH dependence studies, solvent deuterium and substrate deuterium kinetic isotope effects, temperature dependent studies, and single turnover kinetics. The pH dependence of k_{cat} indicated SsuD requires a group with a pK_a of 6.6 ± 0.1 to be deprotonated and a second group with a pK_a of 9.5 ± 0.1 to be protonated for catalysis, while the pH dependence of k_{cat}/K_m indicated SsuD requires a single group with a pK_a of 6.9 ± 0.1 to be deprotonated in order for the reaction to commit through the first irreversible step. Each observed isotope effect on the k_{cat} and k_{cat}/K_m kinetic parameter was determined by analyzing the pH dependence of the solvent deuterium and substrate deuterium isotope effects, the latter obtained in both H_2O and D_2O. Labeled and unlabeled substrate yielded a solvent isotope effect on k_{cat} of 0.75 ± 0.04 and 2.4 ± 0.2, respectively. The observed substrate isotope effect on k_{cat} in H_2O was 3.0 ± 0.2. Each isotope effect on k_{cat}/K_m was within an experimental error of one indicating product release to be the rate-limiting step. This result was reinforced by

proton inventories exhibiting dome-shaped curves indicating large commitments to catalysis. Results from single-turnover experiments show increased stability of the C4a-(hydro)peroxyflavin intermediate in D_2O, but that the overall rate of flavin oxidation by SsuD monitored at 370 and 450 nm was not altered in the deuterated solvent. The deuterated substrate failed to stabilize the C4a-(hydro)peroxyflavin intermediate under single-turnover conditions. These combined results have identified key chemical steps of the proposed catalytic mechanism by implicating Arg226 as playing a critical role in catalysis as well as the quantification of catalytic commitment factors.

Acknowledgements

I would like to express my sincere appreciation to my advisor, Dr. Holly R. Ellis, for heroically mentoring me for the past five years here at Auburn University. Words cannot express how grateful I am for her guidance and encouragement throughout my graduate school career. I will be forever indebted to her for teaching me the skills, reinforcing the attitude, and the providing the opportunities necessary to succeed as a researcher. I would also like to express my gratitude to Dr. Douglas C. Goodwin, Dr. David M. Stanbury, and Dr. Peter D. Livant for agreeing to be on my committee and critique my dissertation; their willingness to engage in meaningful discussion, supply advice, and provide constructive criticism proved integral to my research. A special thanks to Dr. Goodwin for the use of his stopped-flow instrument, to Dr. Evert Duin for the use of his anaerobic glove box, and to Dr. Livant for the use of his lab when I needed to synthesize a deuterated substrate essential to my success on this project. Thanks to my former and current lab mates, Dr. Xuanzhi Zhan, Dr. Russell Carpenter, Dr. Erin Imsand, Dr. Jingyuan "Bear" Xiong, Catherine Njeri, and Paritosh Dayal for their meaningful discussions and help during my studies. Lastly, thanks to the Department of Chemistry and Biochemistry and the National Science Foundation for financial support of this research.

Table of Contents

List of Tables

List of Schemes

List of Figures

CHAPTER ONE

Literature Review

1.1 Mechanistic Enzymology

Biochemistry is a broad field of study. The scope of modern biochemistry entails elements of physical organic chemistry, inorganic chemistry, modern molecular biology, microbiology, and medicine. The origins of the modern field emerged in Germany around 1870 with Felix Hoppe-Seyler's establishment of *physiologische Chemie* (*1*). Prior to this point, any chemistry dealing with substances obtained from the tissues and fluids of animals and plants was considered to be an extension of organic chemistry (*1*). However, separate but parallel investigations by medical physiologists and laboratory chemists into the process of fermentation led to the first of many branches within the field of biochemistry (*1*, *2*). The opposing disciplines gave rise to different approaches: the organic chemists tended to approach problems in the field with an emphasis on structure and chemical properties of substances isolated from biological substances, while the medical establishment focused on the physiological role of such substances (*1*). As a result, the modern biochemist is presented with a variety of tools and approaches with which to the study the chemical processes of living organisms. Of these approaches, it is those employed by the mechanistic enzymologists that seek to identify and understand the boundary that distinguishes a living organism from a random collection of

thermodynamically stable molecules. What is the chemistry of life? In what way does life manipulate the laws of thermodynamics so that only a handful of molecules can be used to govern a vast array of chemical processes? How does an organism catalyze such a wide range of reactions at room temperature, neutral pH, and at high rates with impeccable precision and efficiency? Mechanistic enzymology serves to answer these questions and provide a broader understanding of the biological and chemical sciences as a whole.

The origins of mechanistic enzymology can be traced back to 1894, when Emil Fischer demonstrated that an enzyme he called "invertin" acted only on α-D-glucosides, while another enzyme termed "emulsin" acted only on β-D-glucosides (*2*). Although, the term "enzyme" had already been coined in 1877 from the Greek word for "in leaven", in reference to the rising of bread as it baked, Fischer's discovery was the first evidence of enzyme selectivity; this finding resulted in his infamous "lock and key" metaphor which was used to describe enzyme-substrate interactions (*2–4*). However, Fischer's discovery failed to resolve a debate within the scientific community at the time: Louis Pasteur claimed that certain biological processes, such as fermentation, were catalyzed by a vital force inherent to life itself which he referred to as the "fungus of fermentation" (*2*, *5*). On the other hand, others argued fermentation was purely a chemical process brought about by the transfer of unstable properties from the ferment to the fermenting substance, thus leading to its breakdown (*2*, *5*). Eduard Buchner presented evidence for and against both claims in 1897 when he observed that yeast extract was capable of carrying out fermentation of sugar to alcohol and carbon dioxide outside of a living cell (*2*, *5*, *6*). The discovery was a milestone in that it demonstrated that fermentation was not a process

possible exclusively to living organsims but the result of a chemical he called "zymase" being present in the yeast extract (*2*, *5*, *6*). The finding would lead to the discovery and eventual elucidation of the first biochemical pathway, fermentation (*2*, *7*, *8*). Modern enzymology was born.

The first part of the 20th century gave way to the development of the basic tools and principles of enzyme characterization that are now the foundation of mechanistic enzymology. By end of the 19th century, colloid and physical organic chemistry techniques had become a prominent feature of biological thought and experimental investigation (*1*). The same approaches that were used to purify compounds and study organic reaction mechanisms were applied to the study of enzyme reactions. Buchner's identification of "zymase" sparked widespread interest in the process of enzyme catalysis and eventually led to Arthur Harden's discovery of "cozymase" in 1904 when he passed yeast extract through a gel filtration column to yield two separate fractions incapable of producing fermentation (*2*, *5*, *7–9*). Amazingly, he discovered activity could be restored simply by recombining the two fractions (*5*, *9*). By the late 1920's, Hans von Euler had determined the structure of "cozymase" to be that of an organic molecule, nicotinamide adenine dinucleotide (Figure 1.1) (*2*, *5*, *10–14*). Harden and Euler would eventually share the Nobel Prize in Chemistry for their work on coenzymes in 1929 (*2*, *5*).

In 1913, L. Michaelis and M. L. Menten helped to develop the groundbreaking equation that would bear their name by detailing the kinetic behavior of enzyme catalyzed reactions (equation 1.1) (*2*, *15*):

$$v = \frac{k_{cat}[E_0][S]}{K_m + [S]} \qquad \text{(equation 1.1)}$$

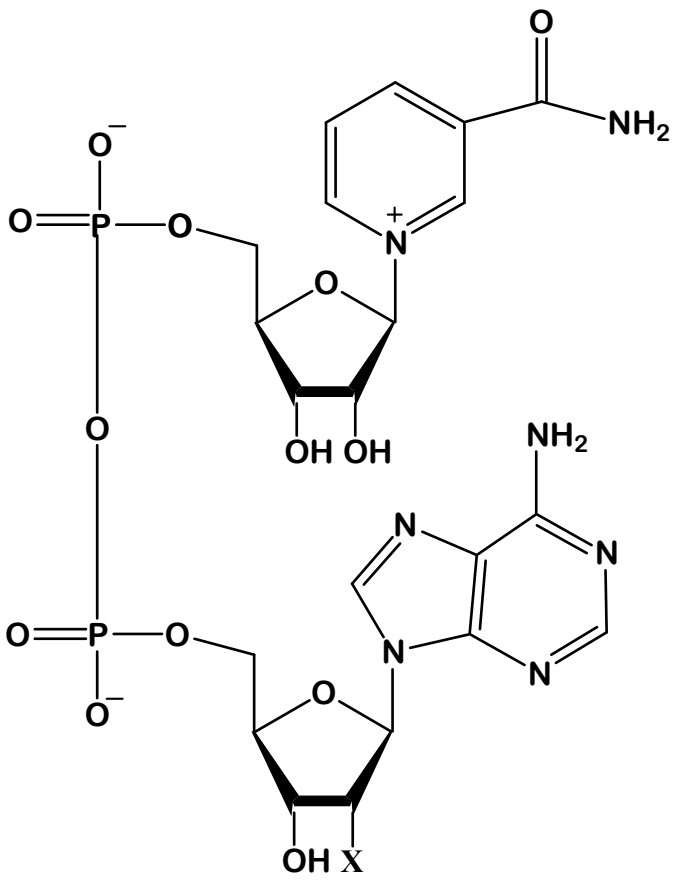

X = OH

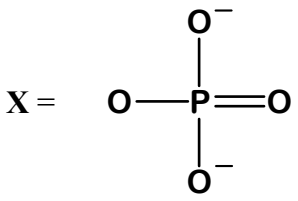

NAD **NADPH**

Figure 1.1. Structures of nicotinamide adenine dinucleotide (NAD) and nicotinamide adenine dinucleotide phosphate (NADPH)

where v is the rate of the enzyme reaction, [E_0] equals total enzyme concentration, [S] is the concentration of substrate, k_{cat} represents the sum of all first-order rate constants in the conversion of substrate to product, and K_m represents the substrate concentration at which the reaction rate is half of maximal rate of the reaction (V_{max}). Twelve years later, G. E. Briggs and J. B. S. Haldane applied the steady-state approximation to enzyme catalysis after rationalizing that the concentration of the enzyme-substrate complex would reach steady-state after a few catalytic turnovers and remain constant over time (*2*, *16*). This rationalization would be embodied by the Michaelis constant, K_m, which encompasses not only the dissociation constant for substrate binding but for product formation as well. The Michaelis-Menten equation would become the underlying foundation of enzyme kinetics. Even today, the Michaelis-Menten equation and the k_{cat} and k_{cat}/K_m catalytic parameters therein continue to serve as the standard descriptors of an enzyme's kinetic properties (*2*, *17*, *18*).

By 1930, enzyme studies had become prevalent enough for J. B. S. Haldane to publish the first comprehensive book on the subject (*2*, *8*, *19*). With the development of the continuous-flow method in 1923 and the stopped-flow method in 1934, even more advanced characterizations of enzymes became possible as absolute rate constants associated with enzyme catalysis could now be determined (*2*, *20*, *21*). The detection of these individual rate-constants would lead to the derivation of more complex kinetic mechanisms and provide evidence of catalytic intermediates in enzyme reactions. However, kinetic analysis remained the primary method to study enzyme behavior since it was still unclear as to the chemical composition of the biological catalysts themselves (*2*, *8*). Before the successful crystallization of urease in 1926, it was still not even

generally accepted that biological catalysis was dependent on a chemical species (*2*, *22*). It would not be until the successful crystallization of pepsin, trypsin, and chymotrypsin by John Northrop in the 1930's that enzymes would be conclusively identified as proteins (*2*, *23–25*).

Much of 1930's and 1940's were focused on purification, identification, and characterization of enzymes and coenzymes as well as the synthesis of the latter (*1*, *2*, *8*). The major vitamins (A, B_1, C, D, and E) and their relationship to food and nutrition had been characterized as early as 1925, but it was not until the elucidation and successful synthesis of the nucleotide coenzymes such as ATP, NAD, and FAD that the link between the vitamins and coenzymes became apparent (*1*, *2*, *8*, *26–28*). The elucidation and synthesis of these cofactors resulted in a boon for physical organic and synthetic chemists (*1*, *8*, *26*, *28*). The dependence of enzymatic activity on certain coenzymes, or cofactors, suggested that these molecules were participating directly in the chemical mechanisms of the enzyme-catalyzed reaction (*1*, *2*, *26*, *28*). As a result, organic chemical mechanisms could be proposed for enzymatic reactions and analyzed using traditional physical organic techniques (*1*, *2*, *26*). Meanwhile, work on metalloenzymes was still in its infancy during this period as Linus Pauling was just beginning to explore the chemistry governing the transport of molecular oxygen by hemoglobin (*1*, *2*, *26*, *29*, *30*). Therefore, mechanistic enzymology was predominantly limited to an understanding of enzymes as organic catalysts employing organic-like reaction mechanisms throughout much of the early 20th century (*1*, *2*, *26*, *31*).

The second half of the 20th century produced two technological advances that had a major impact on mechanistic enzymology: X-ray crystallography and advanced

molecular biology techniques. X-ray crystallography provided a tool to identify specific interactions occurring between the enzyme and the reactants, while the polymerase chain reaction (PCR) resulted in a rapid, inexpensive, and efficient method to mutate functional groups and probe the mechanistic effect. Prior to these advances, the geometry of the enzyme active-site and the definitive roles of enzyme functional groups in catalysis were largely speculative (*1*, *2*, *7*, *8*, *20*, *21*, *26*, *28–30*). In many cases, the enzyme interactions were simply disregarded in the development of proposed chemical mechanism altogether (*1*, *2*, *26*, *29*, *30*). However, Watson and Crick's successful elucidation of the double-helical structure of DNA by X-Ray diffraction in 1953 opened the door to the technique's application to proteins in the late 1950's (*1*, *2*, *26*, *32*). When the technique was used successfully to obtain high-resolution three-dimensional structures of sperm whale myoglobin in 1957 and horse hemoglobin in 1959, mechanistic enzymologists realized that they now had a tool to investigate the role of enzyme interactions on the reaction mechanism of enzyme catalysis (*2*, *26*, *33*, *34*). The successful crystallization and determination of chicken egg lysozyme by David Phillips in 1965 provided the first glimpse into the previously mysterious world of enzymatic structural characteristics (*1*, *26*, *35*). The structure revealed a large cleft on the enzyme that was later shown to accommodate the polysaccharide strand of the peptidoglycan substrate (*35*, *36*). After the three-dimensional structure of the enzyme co-crystallized with substrate was determined, a close examination of the points of contact between the substrate and the enzyme revealed two amino acid residues, Asp52 and Glu35, were positioned in close proximity above and below the fourth and fifth sugars of the polysaccharide chain of the substrate (*36–38*). Although previous characterizations of lysozyme had already demonstrated that

the enzyme catalyzed the cleavage of this glycosidic bond at this position, the enzyme's lack of a cofactor limited the ability to propose a meaningful reaction mechanism in terms of catalysis (*35–38*). The revelation of the aspartate and glutamate residues near the active site provided a basis for the proposal of two mechanisms: Glu35 protonates the departing hydroxy group while Asp52 either stabilizes the resulting carbonium ion (Figure 1.2, Path A) or acts as a nucleophile forming a covalent adduct (Figure 1.2, Path B) (*36*, *39*). Although the discovery provided the first direct evidence of an amino-acid residue being involved in catalysis as well as the idea that an enzyme can activate the substrate by inducing distortion or strain, it failed to distinguish between the two possible mechanisms (*36*, *39*). Later, additional kinetic analysis would demonstrated the covalent adduct be to be the correct mechanism (*40*). Nevertheless, structural determination via X-ray crystallography, when possible, has become a standard tool of the mechanistic enzymologist despite its limitations.

The other major technological innovation that served to impact the field of mechanistic enzymology stemmed from advances in molecular biology (*1*, *2*, *26*). Although X-ray crystallography proved instrumental in providing a structural template for the development of hypothetical catalytic reaction schemes, there were few tools available with which to investigate a specific enzyme's structural features, such as the role of a particular amino acid residue; mechanistic probes were limited to substrate analogues, isotope effects, or post translational modifications to the enzyme (*1*, *2*, *26*). Furthermore, X-ray crystallography was limited to enzymes that could be naturally expressed to high enough concentrations to yield at least 10 mg of pure protein (*2*). The

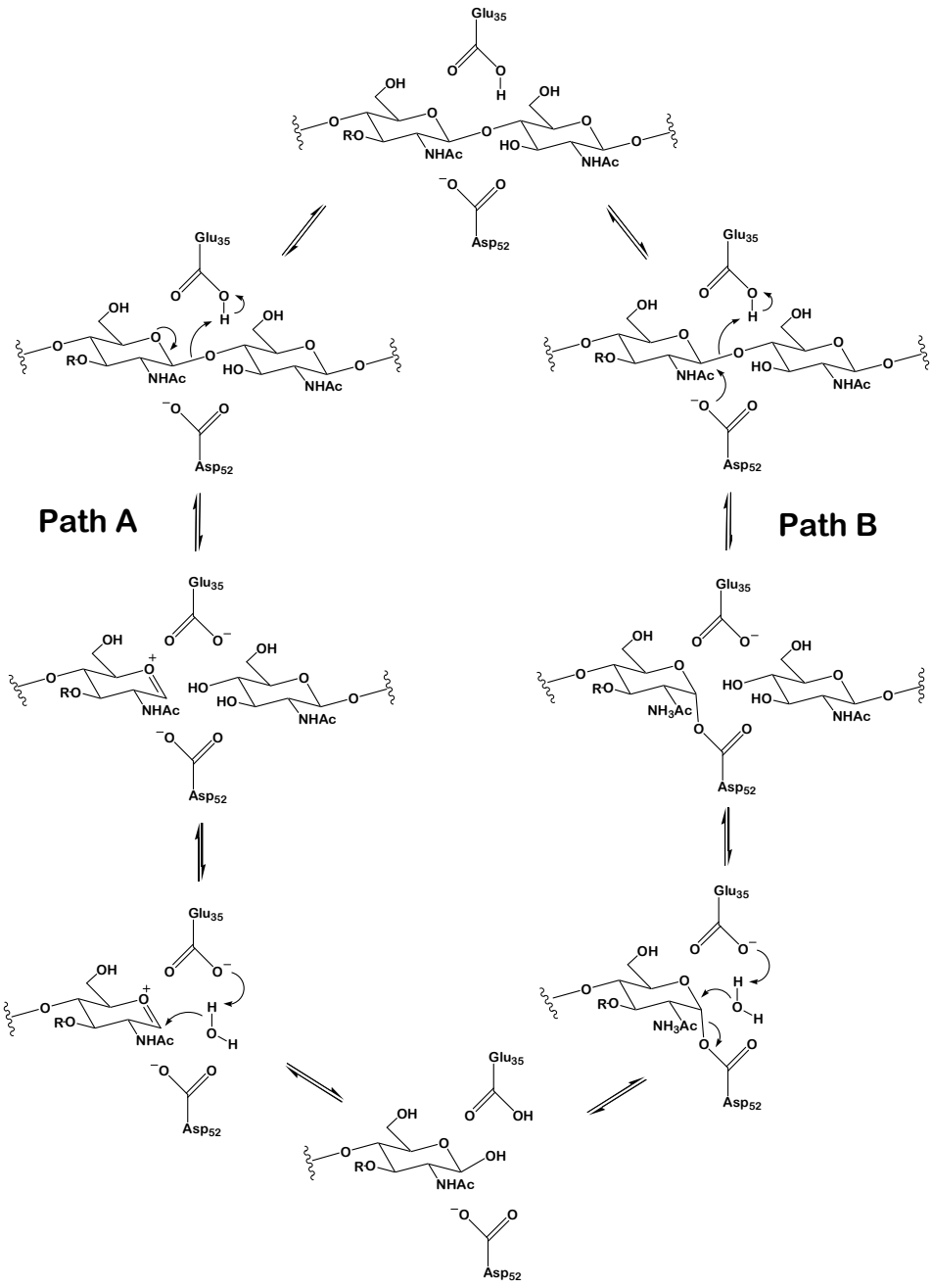

Figure 1.2. The catalytic mechanism for lysozyme adapted from reference (*40*). The Phillips mechanism (Path A) was originally proposed from the three-dimensional structure, but kinetic analysis eventually demonstrated the Koshland mechanism via a covalent adduct (path B) to be the correct mechanism.

successful cloning of the first recombinant gene, *E. coli recA*, in 1977 and its over-expression in 1980 meant that biochemical studies were no longer limited to those proteins that could be naturally expressed and purified; the door had been opened for the study of a plethora of enzymes previously not subject to X-ray crystallography or basic characterization (*1*, *2*, *26*). By 1982, Michael Smith had developed a technique to generate enzyme variants with controlled site-directed mutations to particular amino acid positions (*41–43*). The technique was used to make a series of *B. stearothermophilis* tyrosyl ^{t}RNA synthetase variants in which the sidechains of certain functional groups, identified from the X-ray crystal structure, were removed because they were believed to be involved in hydrogen-bonding interactions with the substrate (*42–44*). The elimination of these hydrogen bonding interactions produced an unexpected result: K_m was increased while k_{cat} was decreased compared to wild-type (*44*). The result provided the first evidence indicating that the binding energy in an enzymatic reaction favors catalysis by increasinhg k_{cat} rather than by promoting tighter substrate binding (*44*). Molecular biology allowed mechanistic enzymologists to explore the complexity of enzymatic machinery. The discovery and development of the PCR method by Mullis in 1983 permitted the rapid amplication of nucleotide sequences for cloning or analytical purposes such as site-directed mutagenesis (*45*). In the following decades, various approaches to site-directed mutagenesis, including the Kunkel method in 1987, were developed in an effort to standardize the process and increase efficiency (*46*). Today, the systematization of PCR procedures has allowed the mechanistic enzymologist to clone recombinant genes and generate enzyme variants quickly, efficiently, and relatively

inexpensively with minimal training or expertise, permitting more emphasis on the exploration of various enzyme reaction mechanisms.

As mechanistic enzymologists began to be able to focus on the enzyme structural features and their relationships to catalysis, the distinction between mechanistic enzymology and the traditional physical organic and inorganic chemistry fields became more defined. Interestingly, this same phenomenon that began to distinguish an enzymologist from the organic chemist began to divide the traditional biochemist from the molecular biologist: the term "molecular biology" was actually the result of physicists attempting to explain the "nature of life" using a quantum mechanical model independent from chemistry (*1*). This seemingly innocuous distinction would result in an undeniable tension between biochemists and molecular biologists after the 1950's, a tension that would result in the change of the name of the American Society of Biological Chemists to the American Society of Biochemistry and Molecular Biology in 1987 (*1*).

Today, the field of biochemistry remains internally divided and grossly misunderstood by the outside disciplines. Although the modern biochemist is often required to demonstrate an effective understanding of both fundamental chemistry and biology in order to receive a Ph.D., they are commonly viewed as "narrow-minded specialists, who are neither a proper chemist or proper biologist and who are interested only in the petty details of metabolic pathways (*1*)". A. V. Hill was once quoted stating, "The trouble with so many biochemists or physiological chemists, or whatever one calls them, is that they either know no chemistry or no physiology or no biology (*47*)." However, this hostile and unfair assessment is ironic in that many of these same individuals are often purported in the very same statement to possess little if any

understanding of fundamental biochemistry. The hypocrisy of such statements serves little to advance either discipline; hopefully, such criticisms will become a thing of the past as advances in mechanistic enzymology help to further blur the distinctions between all of these fields. Therefore, this dissertation has been styled to address the subject of the two-component alkanesulfonate monooxygenase system from the chemical approach followed by the physiological approach before diving into the pure mechanistic enzymology governing the research therein.

1.2 Flavin Dependent Enzymes-Early History

The story of flavin dependent enzymes begins in 1879 with Winter Blyth's observation of lactochrome, a distinctly yellow-pigmented compound isolated from milk whey (*48*). Twenty years later during a completely unrelated set of studies, Otto Kühling was investigating the redox properties of a class of compounds that would eventually be known as alloxazines (*49*). However, Blyth's and Kühling's discoveries would remain in relative obscurity until 1926 when Joseph Goldberger discovered that the human disease pellagra was caused by a deficiency in a dietary factor belonging to the same complex as vitamin B_1; this antipellagra factor was subsequently labeled vitamin B_2 (*50*). In 1933, Richard Kühn and his associates isolated a B-complex dietary factor from milk that was described as orange-pigmented, but lacking antipellagra activity; the resulting compound was referred to as lactoflavin, derived from the latin words for *lacto* "milk" and *flavus* "yellow", and was identified as vitamin B_2 despite its lack of antipellagra activity (*1*, *51*). As a result, Goldberger's factor would be renamed vitamin B_6 or modern day pyridoxal 5'-phosphate (*27*, *52*). Interestingly, vitamin B_6 would continue to be studied as Goldberger antipellagra factor throughout the 20^{th} century until it was finally determined

that it was actually vitamin B_3, niacin, that was acting as the true antipellagra factor (Figure 1.3) (*27*, *28*, *53*, *54*). While Richard Kühn was working to isolate and synthesize the yellow pigment, Albert Szent-György observed that a yellow pigment in animal tissues, which he coined cytoflave, could be eliminated and regenerated through reversible oxidation-reduction (*55*). During this same period, it was observed by a competing group that some animal tissues emitted green fluorescent light after being irradiated with ultraviolet light; they coined these pigments lyochrome (*56*). By this time, the yellow pigment was suspected to be the result of a coenzyme; efforts were undertaken to isolate the compound from its enzyme counterpart much like Euler had done with co-zymase a quarter century before. By 1935, the pigment was identified as a flavin phosphate following a successful attempt to reversibly separate it from the old yellow enzyme without denaturation (*57*). These independent chemical and spectral studies on the yellow pigment eventually led Warburg and Christian to determine it to be one of Kühling's alloxazine compounds through X-ray crystallography (*58*). Following the successful synthesis of riboflavin-5'-monophosphate by Richard Kühn's Lab in 1936, it was demonstrated that catalytic activity could be achieved by combining the synthetic flavin compound with the apo-enzyme (*59*). It was concluded that riboflavin-5'-monophosphate served as a "prosthetic group" integral to the protein itself, giving rise to the term "flavoprotein" (*60*, *61*). In accordance with the terminology at the time, riboflavin-5'-monophosphate was referred to as flavin mononucleotide (FMN), with *nucleotide* referring to any nitrogenous compound linked to a sugar phosphate (*1*, *60*, *61*). By 1938, Warburg and Christian had also solved the structure of the flavin adenine dinucleotide (FAD) coenzyme integral to D-amino acid oxidase (*62*). It was now clear

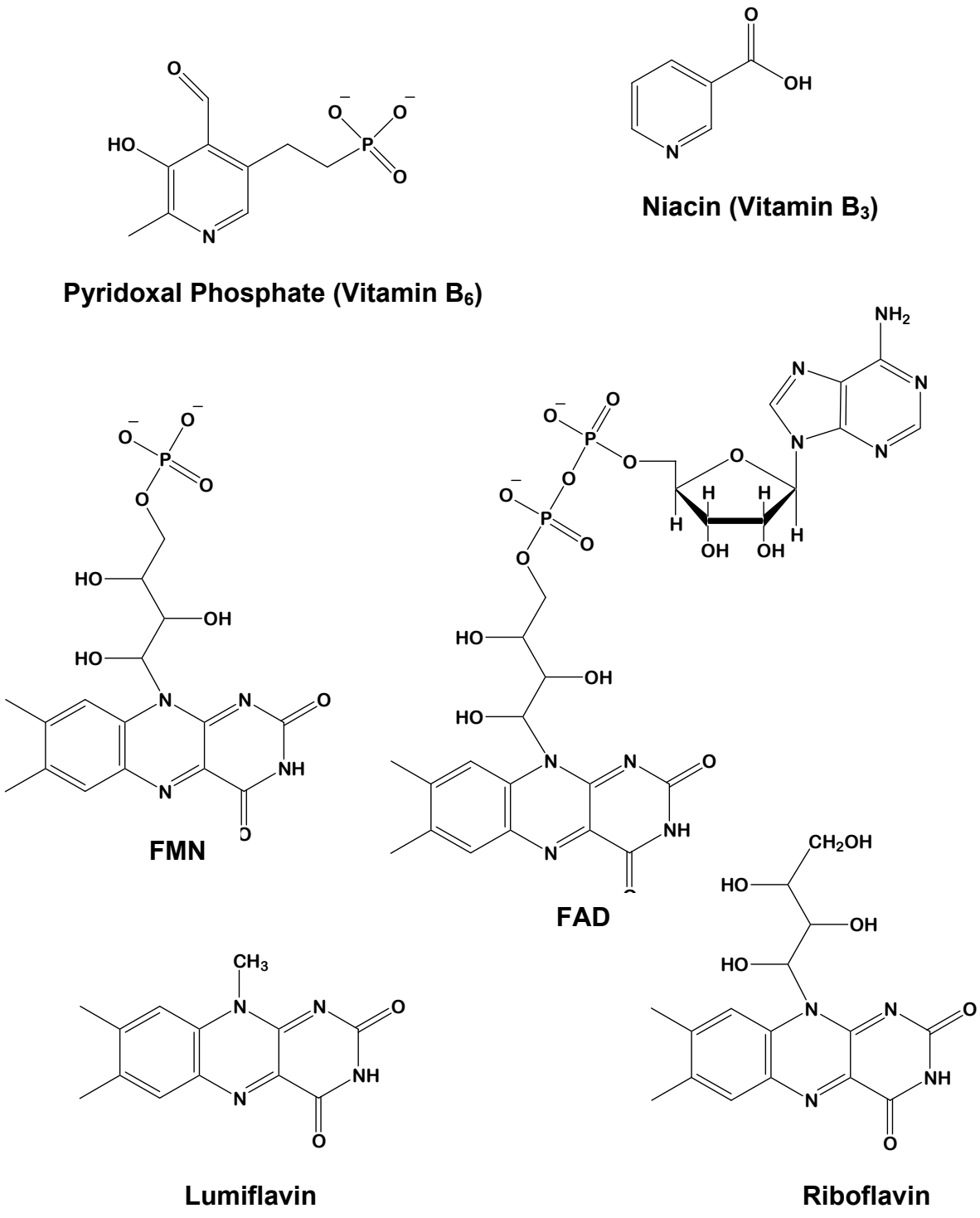

Figure 1.3. Structures of pyridoxal phosphate, Niacin, Lumiflavin, riboflavin, FMN, and FAD.

that biologically relevant flavocompounds came in two forms, FMN and FAD, with the riboflavin (vitamin B_2) component being integral to each form (Figure 1.3) (*28*, *61*).

1.3 The Chemical Relevance to the Study of Alkanesulfonate Monooxygenase System

The core molecular structure of any flavin compound was determined to be lumiflavin or 7,8-dimethylisoalloxazine and a numbering system corresponding to the positions of the isoalloxazine ring of the flavin was established (Figure 1.4) (*63*). The functional diversity of the flavin cofactor in biological systems was found to be related to the covalent linkage of the *nucleotide* group covalently linked to the N10 position of the isoalloxazine ring. In riboflavin, the *nucleotide* group was determined to be a ribityl sugar (Figure 1.3). In FMN, the ribityl sugar was found to include a phosphate group attached to the terminal hydroxyl group by an ester linkage, while FAD included an additional adenosine monophosphate group linked to the terminal phosphate of FMN (Figure 1.3) (*61*). For the most part, these *nucleotide* groups have been determined to anchor the flavin moiety in the protein and/or to enhance the solubility of the flavin moiety in solution as riboflavin is not soluble in water (*61*). Nevertheless, the specific chemical properties of the flavin moiety were shown to be dependent on its micro-environment within the flavoprotein (*64*). In most flavoproteins, the flavin cofactor was determined to be only tightly bound to the enzyme. However, flavoproteins had been found to contain covalently bound flavin moieties linked through either the C6 position via a cysteine amino acid residue or through the 8*α*-methyl group via a tyrosine, histidine, or cysteine amino acid residue (*63*).

1.3.1 Flavin Oxidases, Flavin Dehydrogenases, Flavin Reductases, and Controversy

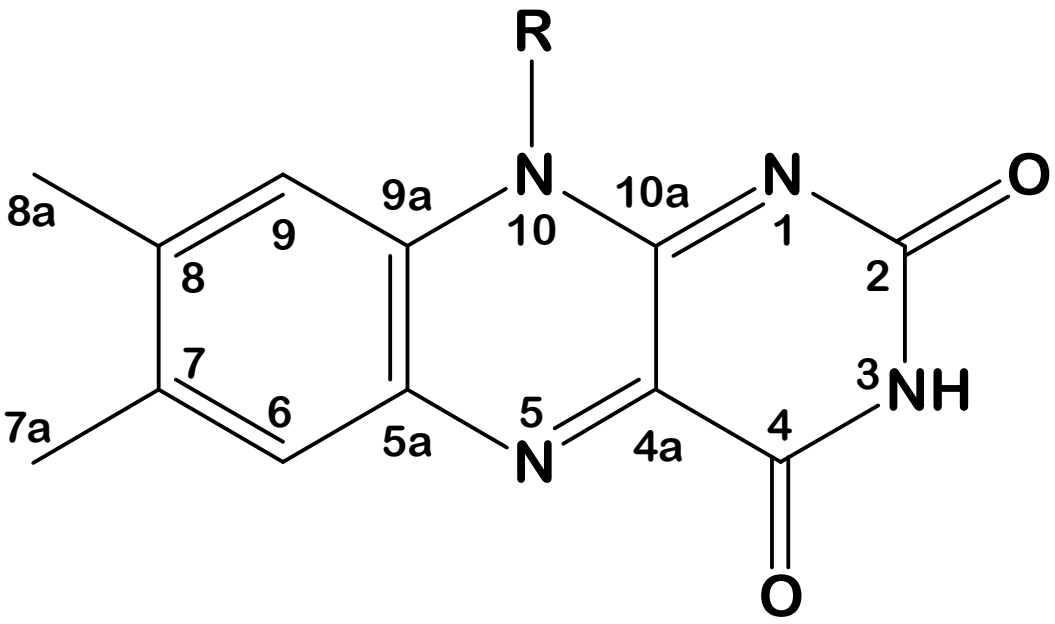

Figure 1.4. Flavin isoalloxazine ring numbering system.

Although the structures of the two major flavocompounds had been elucidated, the mechanisms of action of the flavin redox coenzymes continued to stir controversy (*2*, *60*, *61*, *65*). Throughout the 1960's, the characterizations of an increasing number of flavoenzymes demonstrating a diverse range of reactions resulted in the classification of flavoproteins into four distinct groups: flavin oxidases, flavin dehydrogenases, flavin reductases, and flavin oxygenases (Figure 1.5) (*2*, *60*, *61*, *65–69*). Flavin oxidases, such as D-amino acid oxidase, react with molecular oxygen to yield an oxidized product and H_2O_2 (*66*). In these enzymes, the flavin accepts two electrons from the substrate to form reduced flavin prior to the formation of the anionic flavin semiquinone intermediate required for the one electron transfer to molecular oxygen prior to the formation of H_2O_2 (Figure 1.5) (*61*). Flavin dehydrogenases, such as succinate dehydrogenase, transfer a pair of electrons and a proton from the substrate to the flavin cofactor in order to form a dehydrogenated product (*67*, *70*). This process can result in either the generation of carbon-carbon double bonds as in the succinate dehydrogenase or the condensation of an alcohol to aldehyde as in the case of alcohol dehydrogenase (*61*, *67*, *71*). Flavin reductases, such as glutathione reductase, catalyze the reduction of flavin by catalyzing the transfer of electrons from a pyridine nucleotide such as NADH or NADPH to an oxidized flavin substrate (*61*, *68*). Flavin oxygenases, such as *p*-hydroxybenzoate hydroxylase, insert one atom of molecular oxygen into a substrate while producing water with the other oxygen atom.

The flavin coenzyme was proposed to mediate redox reactions by governing the transfer of one or two electrons during catalysis; this electron transfer results in the formation of three redox states: a fully oxidized flavin, a flavin semiquinone, and the

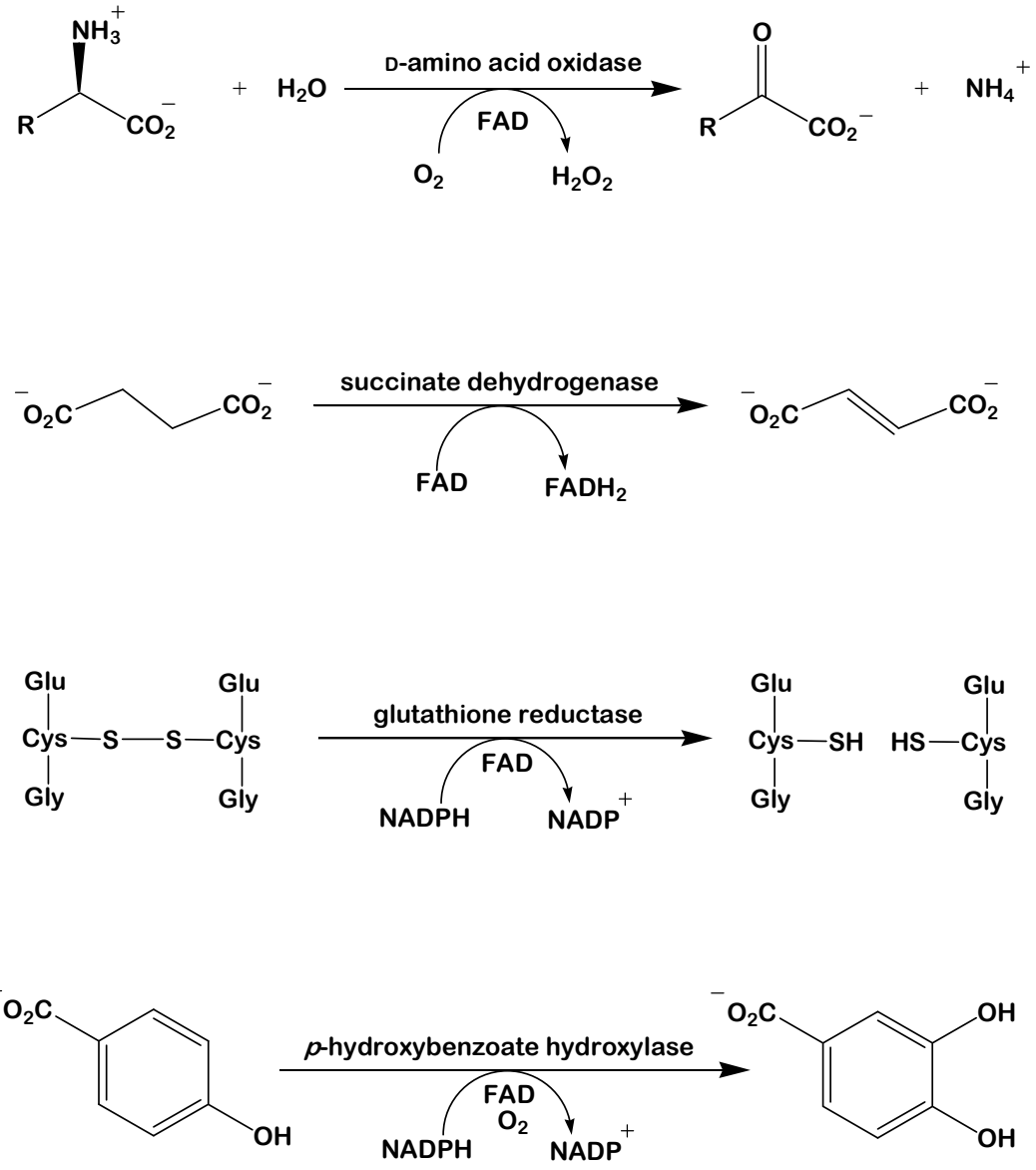

Figure 1.5. Reactions catalyzed by flavoenzymes

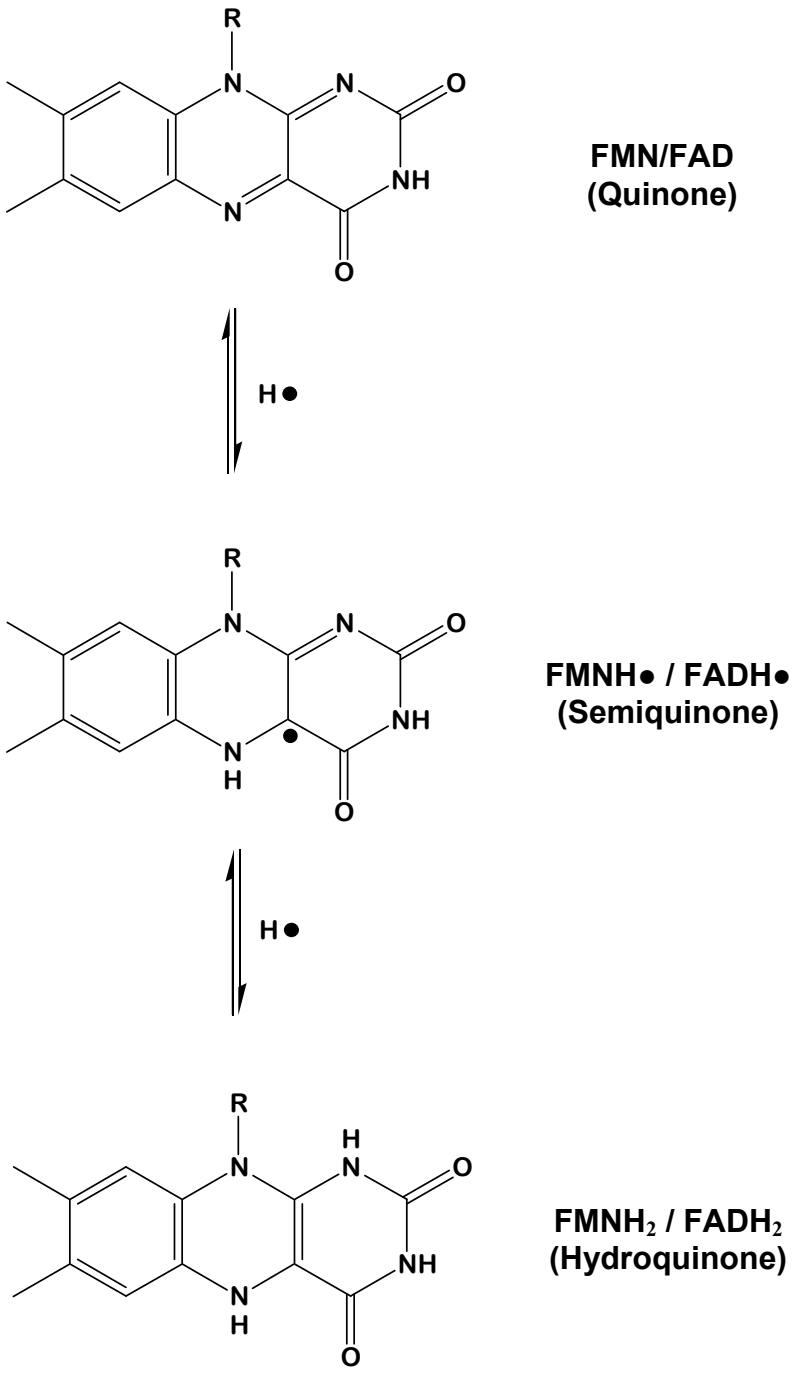

Figure 1.6. The redox states of flavin coenzymes

fully reduced flavin (Figure 1.6) (*2*, *60*, *61*, *65–69*). The ability of the flavin to exist in three different oxidation states was discovered by the observation that distinct spectral intermediates could be generated during oxidation-reduction reactions (*60*, *61*, *63*, *65*, *72*, *73*). A characteristic absorbance spectrum with maxima at 370 and 450 nm is observed for fully oxidized flavin as well as a fluorescence emission peak at 520 nm. Alternatively, the flavin semiquinone exhibits a broad absorbance peak in the 600 nm region, while the fully reduced flavin does not display any fluorescence or absorbance in the visible region (Figure 1.7) (*74*).

Although it was generally accepted that the flavin could exist in these three redox states, the mechanism by which the three states are interconverted during the dehydrogenase reactions was, and to many still is, a subject of intense controversy (*2*, *60*, *61*, *65–69*, *72*, *75*, *76*). To many, the hydride transfer mechanism was considered the most plausible mechanism due to its simplicity as well as its similarity to the established mechanism for NAD-NADH oxidation-reduction (Figure 1.8) (*2*, *61*, *77*). Throughout the 1970's however, evidence demonstrating that the C4a position of flavin was susceptible to nucleophilic attack by thiols and dioxygen began to become commonplace, especially for monooxygenase reactions (*60*, *65*, *71*, *77*). Alternatively, studies on D-amino acid oxidase during this period complicated the debate further by providing evidence that the substrate forms an α-carbanion intermediate performing a nucleophilic attack on the N5 position of the flavin (*77–80*). Nevertheless, it was Tom Bruice's emphatic defense of the radical mechanism that would result in the debate's escalation into what some would refer to as a virtual scientific conflict. Bruice argued, and eventually provided evidence,

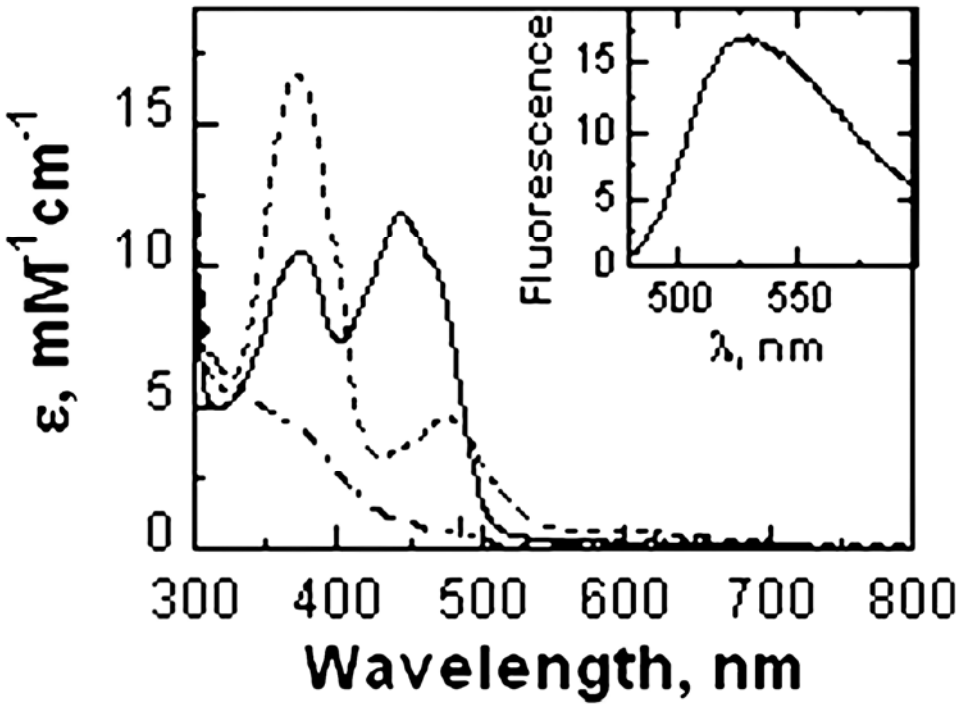

Figure 1.7. UV absorbance spectra of the three-different redox states of a flavin coenzyme: fully reduced flavin (— • —), flavin semiquinone (— —), and fully-oxidized flavin (——). The fluorescence emission spectrum of the flavin semiquinone when excited at 444 nm (inset). This research originally appeared in reference (*74*).

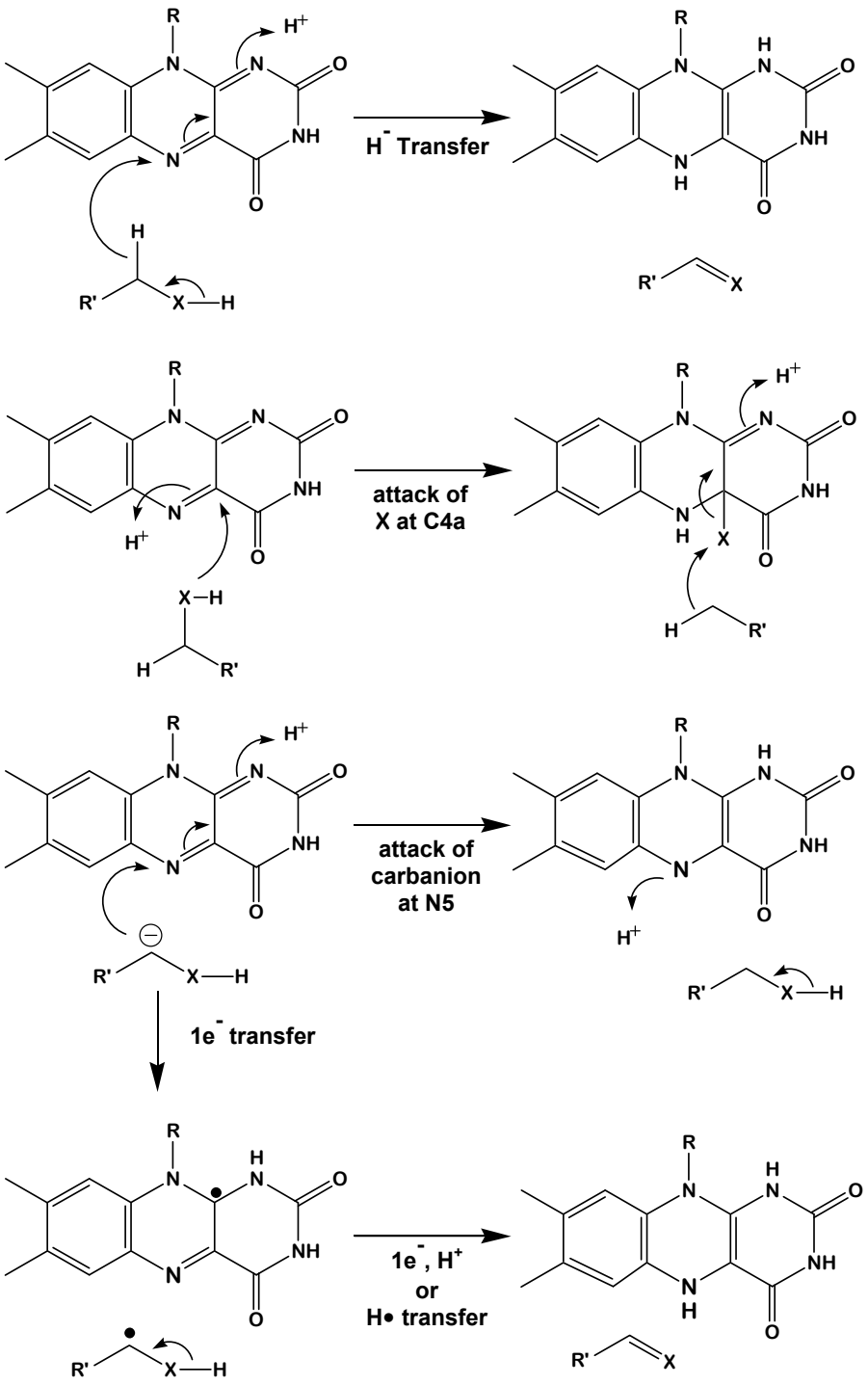

Figure 1.8. Proposed mechanisms for flavin dehydrogenation. The details governing the dehydrogenation mechanism remains an area of active dispute. Figure adapted from reference (*2*).

that flavin oxidation-reduction reactions proceed by radical formation and that the catalytic oxidation of alcohols by flavin involve the attack of an enamine upon a carbonyl oxygen (*2*, *77*, *81*, *82*). The plethora of conflicting data and interpretations from competing groups has caused deep divisions within the flavin community regarding the mechanism of flavin-dependent dehydrogenation (*2*, *61*, *77*). Alternatively, the mechanism governing oxygen activation by flavin-dependent monooxygenases has been well established (*60*, *61*, *65*, *72*, *77*, *83*, *84*).

1.3.2 Flavin dependent monooxygenases

The mechanism by which a flavin oxygenase, such as *p*-hydroxybenzoate hydroxylase (PHBH), inserts one atom of molecular oxygen into a substrate while producing water with the other is one of the most studied reactions in enzymology (*2*, *60*, *61*, *65*, *72*, *75*, *77*, *81*, *83–88*). In general, the oxidized flavoenzyme will first form a complex with NAD(P)H, which will serve to reduce the flavin cofactor prior to the release of $NADP^+$ (Scheme 1.1). The reduced flavoenzyme then reacts with molecular oxygen to generate a C4a-(hydro)peroxyflavin intermediate ($FlOO^-$ or FlOOH). This intermediate then serves to insert one atom of oxygen into the substrate while releasing the other oxygen atom in the form of H_2O (Scheme 1.1). At this point, the product is released making room for another NAD(P)H to bind so that the catalytic cycle can repeat.

Flavin dependent monooxygenases were the first monooxygenases to be studied in detail (*2*, *60*, *72*, *77*). W.B. Sutton is credited with identifying the first of these enzymes in 1954 when he observed decarboxylation of lactate to acetate in *Mycobacterium phlei* extracts (*89*). His group subsequently identified this enzyme as

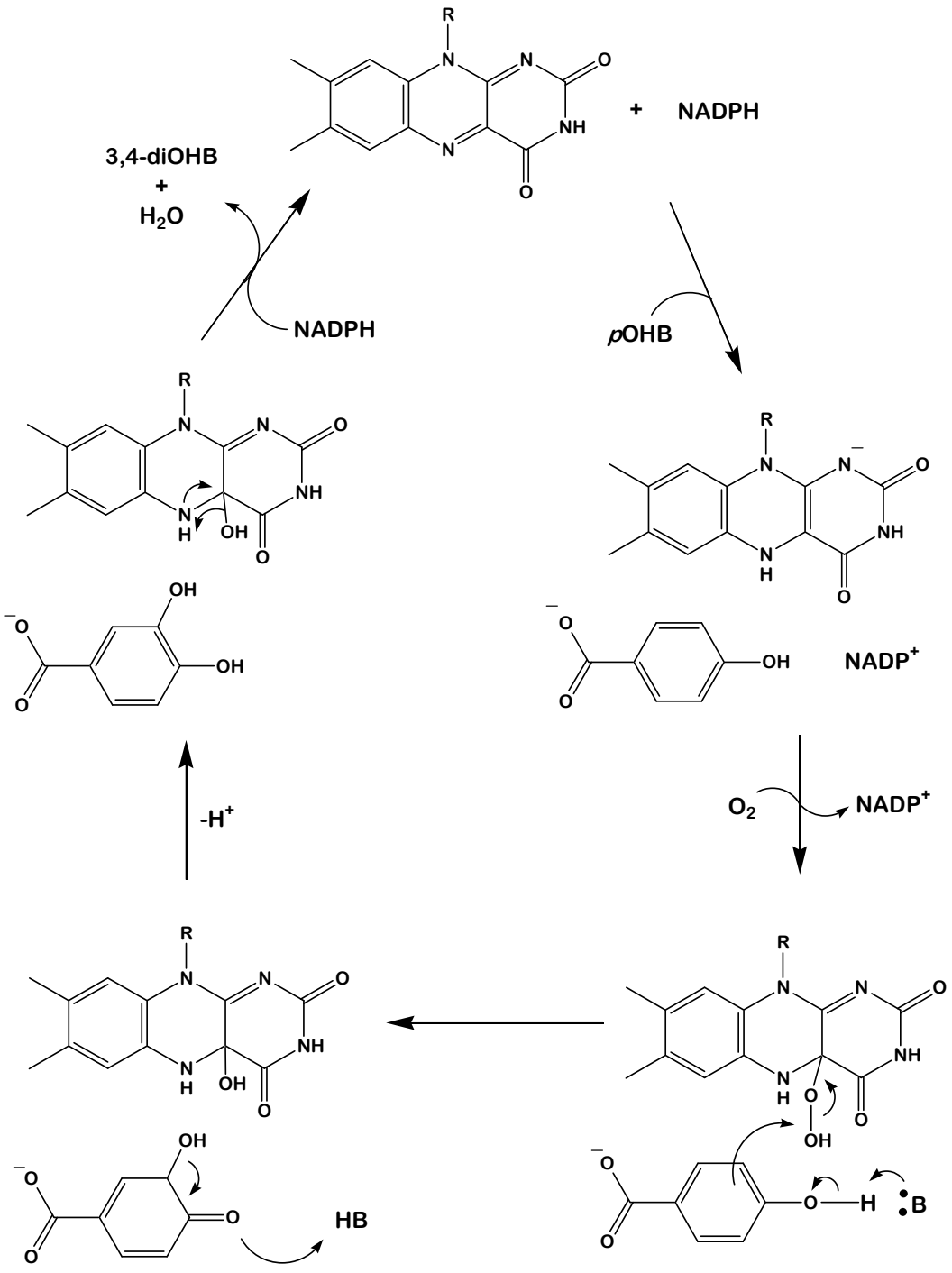

Scheme 1.1. The catalytic cycle of PHBH, a typical mechanism for a "cautious" flavin dependent monooxygenase enzyme. A conformational change traps NADPH in the active site until the substrate can bind.

lactate monooxygenase, and determined that catalysis resulted in the incorporation of ^{18}O into acetate and water from $^{18}O_2$ (*90*, *91*). Although several more flavin-dependent monooxygenases would be identified and characterized throughout the ensuing years, it would not be until Strickland and Massey's elucidation of the kinetic mechanism of melilotate hydroxylase in 1973 using pre-steady-state kinetic analysis that the fundamental properties of flavin-oxygen catalysis would become established (*2*, *60*, *85*). In these studies, Massey detected the formation of what he proposed to be a flavo-oxygen intermediate developing during catalysis. Nevertheless, it would not be until their work with *p*-hydroxybenzoate hydroxylase in 1976 that Massey and his co-workers would claim they had amassed sufficient evidence to support the formation of a C4a-hydroperoxide species serving as the hydroxylating intermediate during a monooxygenase reaction (*60*, *65*, *72*, *86*). Although chemical models supported the formation of the C4a-hydroperoxide species, Massey's work continued to face intense scrutiny as many doubted that such an intermediate could exist (*60*, *61*, *72*, *75*, *83*, *87*, *88*).

Massey proposed the intermediate while investigating the reaction of free reduced flavin with molecular oxygen (*88*). By this time, Tom Bruice and coworkers had been studying extensively the reaction of molecular oxygen with free reduced flavin (*72*). He had concluded that the reaction resulted in an accumulation of the superoxide anion and flavin radicals; the oxidation reaction occurs extremely fast and is autocatalytic (Scheme 1.2) (*65*, *72*, *73*, *77*). The initial reaction of reduced flavin with dioxygen proceeds first through the transfer of an electron from a singlet reduced flavin to a triplet O_2 to yield a

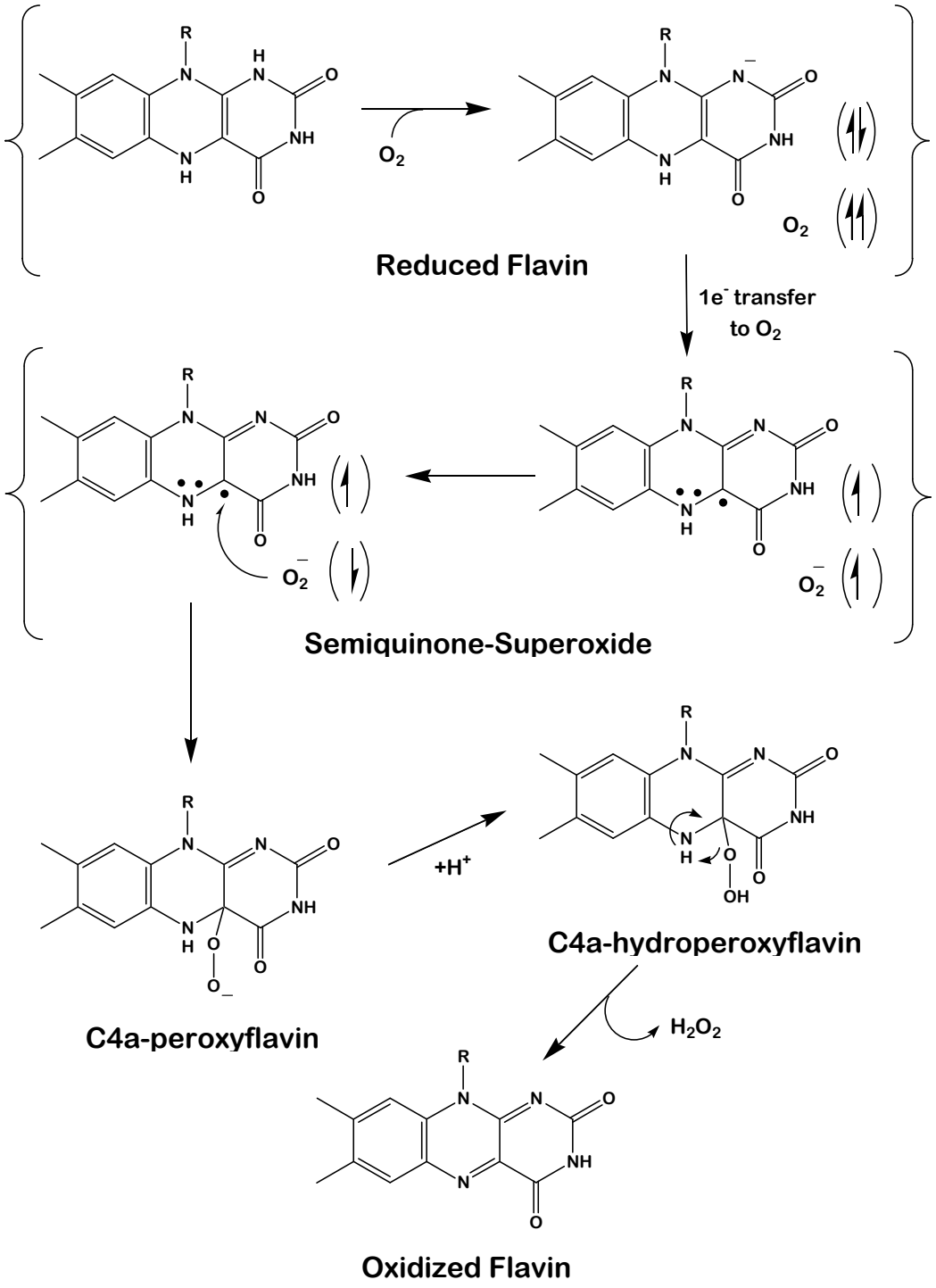

Scheme 1.2. Activation of molecular oxygen by flavin

caged radical pair (Scheme 1.2). Spin inversion of this radical pair collapses to form the flavin hydroperoxide intermediate, which then heterolytically dissociates into H_2O_2 and oxidized flavin (*75*). Through pulse radiolysis experiments, it was determined that the neutral flavin radical could react with excess O_2^- to produce $FlOO^-$ prior to formation of the FlOOH intermediate at neutral pH; the observation and exponential decay of an absorbance peak at 540 nm was attributed to the neutral flavin radical intermediate (*92*, *93*). Observation of this flavin radical in combination with prior studies by Massey provided additional support for the formation of the flavin C4a-hydroperoxide intermediate (*87*, *88*).

1.3.3 Mechanism of Flavin Dependent Monooxygenases

The initial step to oxygen activation in all flavin-dependent monooxygenases involved the one-electron reduction of molecular oxygen producing a caged radical pair (*60*, *65*, *72*). The pair then collapses to form the C4a-peroxide intermediate ($FlOO^-$) which can be protonated to generate the C4a-hydroperoxide intermediate (FlOOH) (Scheme 1.2). The enzyme will favor one of these intermediates depending on the nature of the reaction: typically, the C4a-peroxide intermediate is favored in reactions involving a Baeyer-Villiger rearrangement prior to a nucleophilic attack of the peroxide on the substrate, while the C4a-hydroperoxide intermediate is favored for reactions involving aromatic hydroxylation via electrophilic attack (*60*, *65*, *72*, *94*). For instance, cyclohexanone monooxygenase performs a nucleophilic attack on a cyclic ketone substrate through a C4a-peroxyflavin intermediate in order to incorporate an oxygen atom into its lactone product, while *p*-hydroxybenzoate hydroxylase has been shown to utilize an electrophilic attack on the aromatic ring substrate via a C4a-hydroperoxyflavin

intermediate in order to incorporate a hydroxyl group onto the aromatic ring (*69*, *86*, *95*, *96*). Interestingly, these reactions produce remarkably similar results despite relying on two contrasting mechanisms.

1.3.3.1 C4a-hydroperoxyflavin and the "Cautious Monooxygenase" Strategy

Among the first of the flavin monooxygenases to be extensively characterized was *p*-hydroxybenzoate hydroxylase (PHBH); investigations into its catalytic mechanism have resulted in it being one of the best understood of the flavin monooxygenases (*60*, *65*, *69*, *86*). The enzyme's mechanism exhibits features that are shared by all aromatic hydroxylases, as well as some features that are uniquely adapted to PHBH. It requires a non-covalently bound FAD prosthetic group to catalyze the hydroxylation of *p*-hydroxybenzoate (pOHB) to 3,4-dihydroxybenzoate generating NADPH and O_2 (*65*, *86*, *97*). PHBH and related enzymes are known as "cautious monooxygenases" in reference to the control mechanism they employ to prevent the wasteful oxidation of NAD(P)H when the substrate is absent. A "cautious monooxygenase" requires a hydroxylatable substrate to be bound in order to allow rapid flavin reduction (*65*, *98*). Therefore, C4a-hydroperoxide formation from the reduced enzyme is triggered by the presence of the substrate to be hydroxylated. For the PHBH reaction, the enzyme commits to catalysis in the reductive half-reaction, but only when pOHB is bound. At this point, a conformational change of the enzyme kinetically traps the pOHB subtrate in the active site ensuring its availability for hydroxylation by electrophilic aromatic substitution in the oxidative half-reaction (Scheme 1.1).

The details pertaining to how oxygen is inserted to the aromatic pOHB substrate was a subject of intense debate for many years (*65*). In accord with classic electrophilic

aromatic substitutions from organic chemistry, the site of enzymatic hydroxylation is always *ortho* or *para* to an electron-donating ring substituent (*99*). Although flavoproteins were only known to hydroxylate aromatic substrates that have electron-donating substituents, there was doubt as to whether the C4a-hydroperoxide was a strong enough electrophile to drive the reaction (*65*, *86*, *100–102*). Over the next few decades, however, proponents of simple electrophilic aromatic substitution had collected enough experimental data to reinforce their claim (*60*, *65*, *86*, *100–103*). The final proposed mechanism considers that the intermediate in the electrophilic substitution reaction is non-aromatic; oxygen transfer to the 3-position of pOHB creates an sp^3-hybridized carbon, and the activating -OH group becomes a carbonyl. What is fascinating is how the highly controlled enzyme system utilizes a proton-transfer network consisting of Tyr201, Tyr385, two water molecules, and His72 in order to abstract the phenolic proton of pOHB so that the unstable protonated carbonyl will form without exposing the active site to solvent (*65*, *103*). PHBH serves as an excellent example of how an enzyme can exhibit control over an organic reaction.

1.3.3.2 C4a-peroxyflavin and the "Bold Monooxygenase" Strategy

A "bold monooxygenase" differs from its "cautious monooxygenase" counterpart by promoting rapid flavin reduction and subsequent hydroperoxide formation regardless of the presence of a hydroxylatable substrate. Despite this seemingly reckless strategy, these enzymes still manage to prevent futile NAD(P)H oxidase activity by effectively protecting the flavin hydroperoxide from elimination and stalling the catalytic cycle until a competent substrate is encountered (*65*). Early efforts to understand this strategy focused on the catalytic mechanism employed by cyclohexanone monooxygenase

from *Acinetobacter* (Scheme 1.3) (*95*, *96*). As a result, cyclohexanone monooxygenase became one of the most studied examples of an enzyme utilizing the "bold monooxygenase" strategy. Structures of related "bold monooxygenases" include phenylacetone monooxygenase from *Thermobifida fusca* and cyclohexanone monooxygenase from *Rhodococcus*. A common feature of many "bold monooxygenases" is the insertion of a single oxygen atom of a substrate via a Baeyer-Villiger rearrangement (*65*, *94*). Each provides evidence of the origin of the kinetic behavior characteristic of this group of enzymes (*104*, *105*). Interestingly, Baeyer-Villiger monooxygenases are not closely related to aromatic hydroxylases in sequence or structure, but resemble instead disulfide oxidoreductases (*106*). The active site cleft is between an NADPH binding domain and an FAD-binding domain; the two domains are joined by a signature sequence for Baeyer-Villiger monooxygenases (*106*). Mechanistically, these enzymes have been shown to use flavin peroxides as nucleophiles in Baeyer-Villiger oxidations of ketones to esters. Unlike the "cautious monooxygenase", the presence of the ketone substrate makes no difference in the rate of flavin reduction. Also, $NADP^+$ remains bound to the enzyme after flavin reduction (*95*). The reduced enzyme–$NADP^+$ complex then reacts with oxygen rapidly to form the flavin C4a-peroxide (*65*, *96*). Interestingly, this adduct remains stabilized in the absence of the ketone substrate with a half-life of 5 min before decaying to H_2O_2. In contrast, the flavin hydroperoxides of aromatic hydroxylases without substrate generally decay within milliseconds (*65*). The stability of the C4a-peroxyflavin intermediate of Baeyer–Villiger monooxygenases has been shown to depend on the presence of bound $NADP^+$ as fully

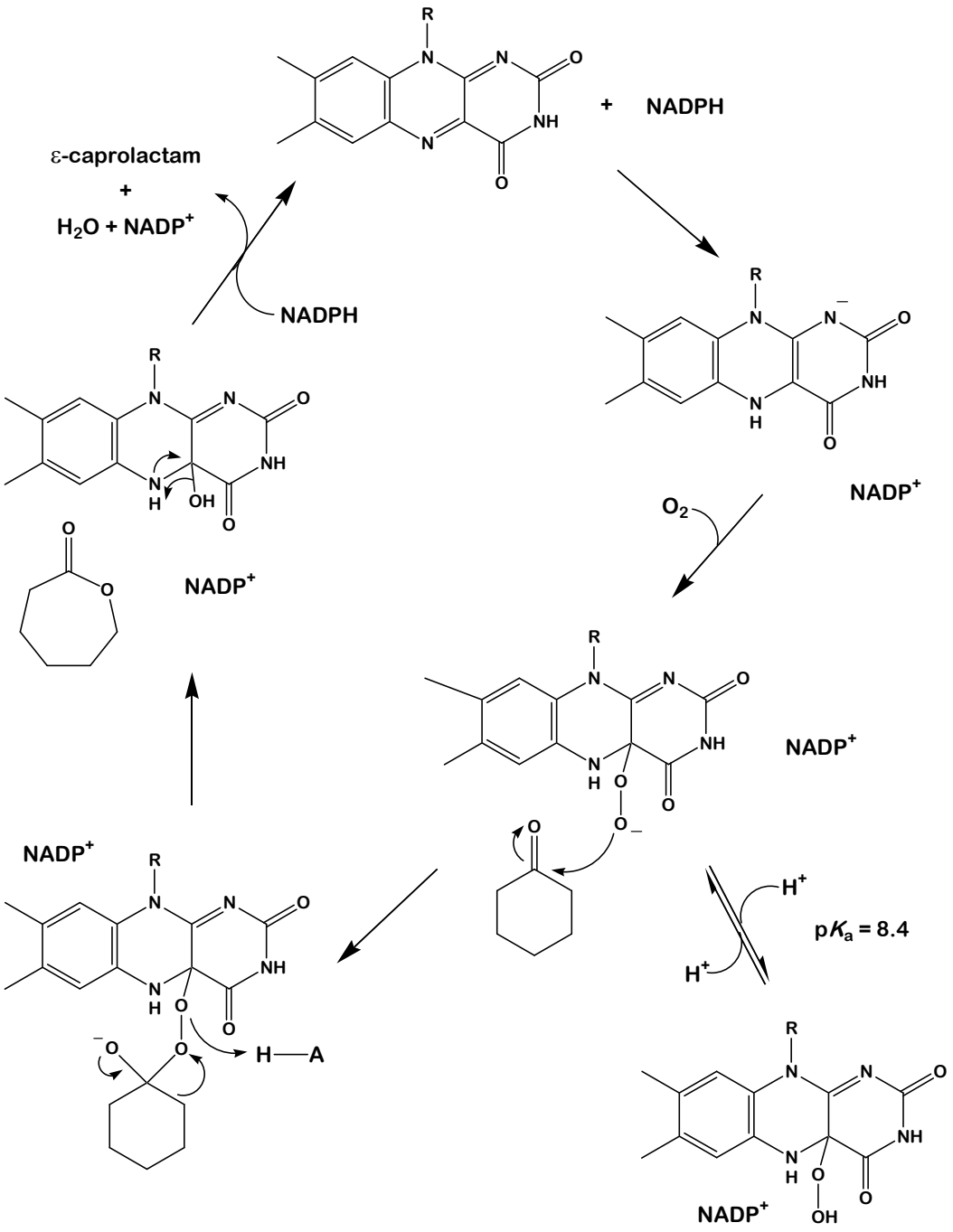

Scheme 1.3. The catalytic cycle of cyclohexanone monooxygenase, a typical mechanism for a "bold monooxygenase" enzyme utilizing a Baeyer-Villiger mechanism. Note: the $NADP^+$ must be bound in order to stabilize the formation of the C4a-hydroperoxide intermediate in the absence of substrate.

oxidized enzyme will form within seconds if it is absent (*65*, *95*, *96*, *103*). The three-dimensional structures for the free oxidized enzyme and NADP complexes show that a conformational change regulates this stability: after hydride transfer from NADPH, domain rotation moves the nicotinamide ring to a position that blocks access to N5 of FAD, preventing the breakdown of the C4a-hydroperoxide to H_2O_2.

Similar to the case with *p*-hydroxybenzoate hydroxylase, there was considerable debate within enzymology and organic chemistry as to whether the C4a-peroxyflavin intermediate was capable of serving as a nucleophile for the Baeyer-Villiger reaction. By 2001, however, a series of cleverly engineered studies using a stopped-flow spectrophotometer to conduct pH jump-experiments were conclusive in demonstrating that it was a C4a-flavinperoxide, and not a C4a-flavinhydroperoxide, acting as the nucleophile that attacks the carbonyl of the substrate (*96*). Separate experiments demonstrated that $NADP^+$ binds to the oxidized enzyme in a two-step process involving a conformational change; the reverse rate constant was consistent with that measured for proton transfers to the oxygen adducts, suggesting that the same conformational change controls release from the active site (*96*). One of the most fascinating observations from this study was the identification of the distinct absorbance maxima at 366 and 383 nm corresponding to the C4a-peroxyflavin and the C4a-hydroperoxyflavin intermediate, respectively. Now, there was spectral evidence for the existence of each intermediate, and a value of 8.4 was determined for the pK_a of the C4a-hydroperoxyflavin intermediate (*96*).

1.3.4 Flavin-Dependent Two-Component Monooxygenase Systems: Chemical Meets Physiological

Although the most extensively studied flavin dependent monooxygenases are composed of a single polypeptide and a single flavin as a prosthetic group, an increasing number of two-component systems utilizing flavin have been identified over the last few decades (*65*, *107*). In these systems, the flavin serves as substrate rather than a tightly bound prosthetic group. As a result, the monooxygenase is dependent on another enzyme, a flavin reductase, to generate and supply the reduced flavin required for monooxygenase activity. Two different kinds of reductases can supply flavin to the monooxygenase: in one reductase, a single flavin substrate is reduced by NAD(P)H before being transferred to the monooxygenase, while the other reductase consists of a prosthetic group flavin that is reduced first by a NAD(P)H before transferring the electrons to a second flavin substrate (*107*, *108*). Also, just like their single component counterparts, some two-component systems have been reported to use a C4a-(hydro)peroxyflavin intermediate as an electrophile while others use it as a nucleophile; some use FAD, while others use FMN (*107*). The similarities shared between these two-component systems and their single component counterparts prompts speculation and debate as to which system evolved from the other.

Several FAD-dependent two component monooxygenase systems have been identified including *p*-hydroxyphenylacetate hydroxylase (HpaA), styrene monooxygenase (SMOA), 2,4,6-trichlorophenol monooxygenase (2,4,6-TCP), 2,4,5-trichlorophenol monooxygenase (TftD), isobutylamine *N*-hydroxylase (VlmH), rebeccamycin halogenase (RebH), and phenol monooxygenase (PheA2) (*109–115*). Many of these FAD-dependent enzymes are involved in hydroxylating aromatic compounds, and have been proposed to use a C4a-hydroperoxyflavin as the oxygenating

intermediate. Out of these systems, HpaA is among the best characterized (*109*, *116*, *117*). The C_2 monomer of HpaA is interesting in that it is capable of utilizing both $FADH_2$ and $FMNH_2$ in order to carry out the hydroxylation of p-hydroxyphenylacetate (pHPA) to 3,4-dihydroxyphenylacetate (DHPA) (Scheme 1.3) (*116*, *117*). Although the hydroxylation reaction carried out by HpaA is remarkably similar to that the "cautious monooxygenase" PHBH, the two-component nature of the HpaA system exempts it from utilizing the "cautious monooxygenase" strategy as NAD(P)H does not bind to the monooxygenase component. Nevertheless, HpaA appears to be just an effective a catalyst as its single-component counterpart, though the exact details of its mechanism are still under investigation.

By far, the best characterized FMN-dependent monooxygenase is bacterial luciferase: the enzyme was the first of the flavin-dependent two-component enzymes to be identified, and detailed studies of its catalytic system have been instrumental in establishing the fundamental properties of the two-component monooxygenases (*118–120*). This enzyme is found in several bacterial organisms ranging from aquatic to terrestrial environments including *Vibrio harveyii*, *Vibrio fischeri*, *Photobacterium leiognathi*, and *Photobacterium phosphorium* (*121*). The reaction catalyzed by bacterial luciferase utilizes a long-chain aliphatic aldehyde substrate, reduced flavin, and dioxygen to produce an aliphatic carboxylic acid and bioluminescence in the form of blue-green light (Scheme 1.4) (*118–120*, *122–124*). The light emission comes from the decomposition of the C4a-aldehydeperoxyflavin intermediate (*123*, *125*). There are two other members of the bacterial luciferase family based on similar structural properties, long-chain alkane monooxygensase (LadA) and alkanesulfonate monooxygenase (SsuD).

LadA has been identified from *Geobacillus thermodenitrificans* and catalyzes the initial reaction in the terminal oxidation pathway of long-chain alkanes ranging in length from C15 to C36 to the corresponding primary alcohol (Scheme 1.2) (*126*, *127*). The SsuD enzyme differs from both LadA and bacterial luciferase in that the mechanism is not the oxidation of a long-chain alkane or aldehyde, but involves C–S bond cleavage: SsuD catalyzes the desulfonation of alkanesulfonate to sulfite and the corresponding aldehyde (Scheme 1.4) (*128*, *129*). Chemically, the oxygenolytic cleavage of a carbon-sulfur bond via a C4a-(hydro)peroxyflavin intermediate is of mechanistic interest; the details of this process will be the primary focus of the investigations presented in later chapters of this dissertation. Physiologically, the enzyme system is believed to be expressed only during times of sulfur starvation, yet the gene corresponding to it has been found ubiquitously throughout known bacterial species (*129*). The conservation of this gene throughout bacterial genomes indicates that SsuD may serve an alternative but previously uncharacterized role in these organisms.

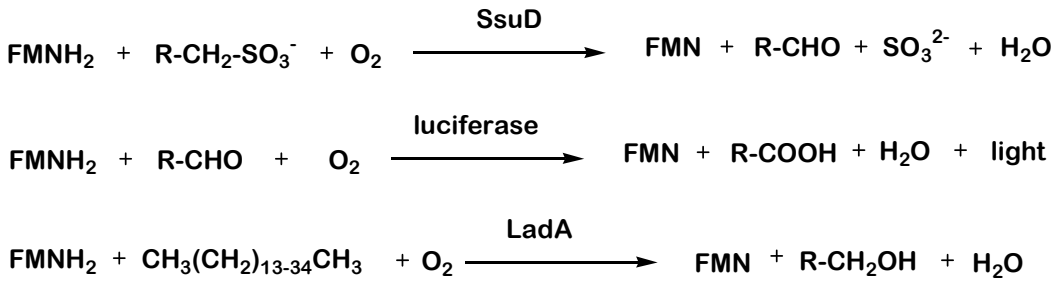

Scheme 1.4. The members of the bacterial luciferase family, and the reactions they catalyze.

1.4 The Physiological Relevance to the Study of Alkanesulfonate Monooxygenase System

FMN dependent two-component monooxygenases are responsible for catalyzing a diverse range of reactions from the oxidation of environmental aromatic and polycyclic compounds for use as carbon sources, the biosynthesis of antibiotics, bioluminescence, the oxidation of long-chain alkanes, and the desulfurization of sulfonated compounds (Table 1.1) (*107*). Nevertheless, all of these enzymes share key mechanistic features: they are dependent on reduced FMN supplied from an FMN reductase, and their mechanisms involve the formation of a C4a-(hydro)peroxyflavin intermediate that is responsible for the oxygenation of the substrate. At least two FMN-dependent monooxygenases have been characterized that are involved in the synthesis of antibiotics, ActVA and SnaA. The ActVA monooxygenase is linked to the last step in actinorhodin biosynthesis (*130*, *131*). Actinorhodin is a polyketide antibiotic first identified in *Streptomyces coelicolor*. The ActVA enzyme hydroxylates dihydrokalafungin (DHK), and eventually leads to the actinorhodin product. SnaA (PII_A synthase) is the other FMN-dependent monooxygenase involved in antibiotic synthesis. It has been identified in several *Streptomyces* species and has been linked to the synthesis of the polyunsaturated cyclic peptolide pristinamycin II_A (PII_A), an inhibitor of protein synthesis (*132*, *133*). The PII_A synthase enzyme catalyzes the oxidation of the dehydroproline residue in PII_B to form PII_A.

Other two-component monooxygenases are linked to the breakdown of chelating agents such as NTA and EDTA. It is believed the organism breaks down these compounds in order to provide free carbon and nitrogen as sources of energy. The FMN-

Enzyme	Reaction(s) catalyzed
LuxA/B or bacterial luciferase	**Oxidation of long-chain alkanes with the emission of blue-green light**
SsuD	**Desulfonation of alkanesulfonates**
ActVA	**Actinorhodin biosynthesis**
HpaH/C_2	**Hydroxylation of *p*-hydroxyphenylacetate**
EmoA/EDTA-Mo	**EDTA degradation**
NtaA/NTA-Mo	**Nitrilotriacetate degradation**
SnaA or PII_A synthase	**Pristinamycin biosynthesis**
LadA	**Oxidation of long-chain alkanes**
Dsz/SoxA and C	**Dibenzothiophene degradation**

Table 1.1. FMN dependent monooxygenase enzymes from two-component systems. Table adapted with permission from (*107*).

dependent monooxygenase NtaA (NTA-Mo) characterized from *Chelatobacter heintzii* ATCC 29600 catalyzes the conversion of NTA to iminodiacetate and glyoxylate (*134–136*). Interestingly, the enzyme uses an Mg^{2+}-NTA complex as its substrate, with different metals capable of substituting for Mg^{2+} in the reaction. A number of bacteria phylogenetically related to *Mesorhizobium* and *Agrobacterium* species have also been discovered that are capable of EDTA degradation (Figure 1.9) (*137*). The EDTA-degrading monooxygenase EmoA (Emo-Mo) catalyzes the oxidation of EDTA to ethylenediaminetriacetate (ED3A) and glyoxylate followed by the further oxidation of ED3A to ethylenediaminediacetate (Figure 1.9) (*138*, *139*). It can also degrade NTA and diethylenetriaminepentaacetate (DTPA) with or without chelated metals (*139*). What is interesting about these particular systems is the origin of their function: chelators like the ones mentioned above are not natural products and were only developed as recently as the 1930's (*140*). The affinity of these enzymes for such recently available compounds prompts further speculation and debate as to which system, the two-component flavin monooxygenases or their single component counterparts, evolved from the other. The debate may serve to help answer questions pertaining to the role SsuD and its ubiquitous presence throughout known bacterial organisms.

1.4.1 The Sulfur Cycle and Bacterial Organisms

Sulfur is essential for the growth of all living organisms. It is a basic building block used for cysteine, methionine, biotin, coenzyme A, coenzyme M, thiamine, lipoic acid, iron-sulfur centers, and a variety of other cellular compounds. Elemental sulfur alone makes up about 0.1% of the earth's crust and can comprise nearly 1% of the dry cell weight of a bacterial organism (*141*). The majority of this

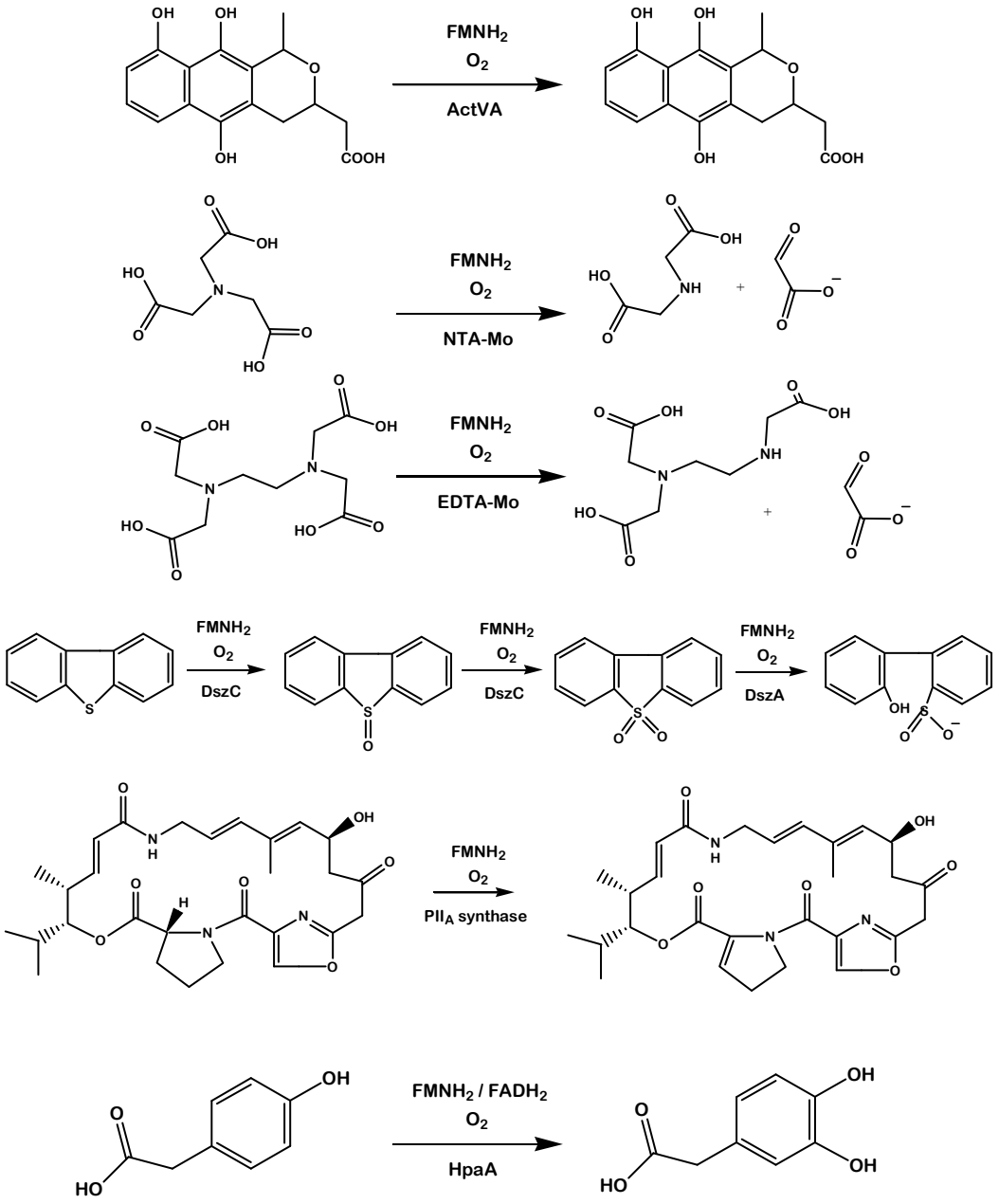

Figure 1.9. Reactions catalyzed by two-component FMN dependent monooxygenases. Note: HpaH can utilize both FMN and FAD.

bioorganosulfur originates from the assimilation of inorganic sulfate by plants and bacteria (*141*). However, inorganic sulfate often constitutes only a limited amount of the total available sulfur in the environment as most organosulfur is locked into extremely stable compounds making it inaccessible to most living organisms. Therefore, these organisms are dependent on alternate, but more ubiquitous, sources like sulfate esters and sulfonates for bioorganic sulfur. Interestingly, plants are not capable of processing xenobiotic and naturally occurring sulfonates and sulfate esters; they must rely on the sulfate and sulfide generated from bacteria (*141*). On the other hand, animals are totally dependent on plants and bacteria for access to bio-available sulfur as they are incapable of assimilating inorganic sulfate. Consequently, methionine is an essential amino-acid for animals and represents the key intermediate in most pathways involving sulfur metabolism in higher organisms. Even the production of cysteine in animals originates from the transsulfurylation of dietary methionine (*142*). In general, cysteine biosynthesis in plants, bacteria, yeast and filamentous fungi begins with the uptake of inorganic sulfate into the cell followed by its conversion to 3′-phosphoadenosine-5′-phosphosulfate (PAPS) via adenosine triphosphate (ATP). The resulting sulfite is further reduced to sulfide where it is condensed with O-acetyl serine to generate cysteine (Figure 1.10) (*143*, *144*). This cysteine then serves as an intermediate in the synthesis of methionine and/or homocysteine depending on the organism.

In recent years, there has been increasing interest in how gram-negative bacteria and certain fungi utilize alternative organosulfur compounds to provide themselves with cysteine and methionine such as sulfate esters ($R\text{-}OSO_3^-$) and sulfonates ($R\text{-}SO_3^-$)

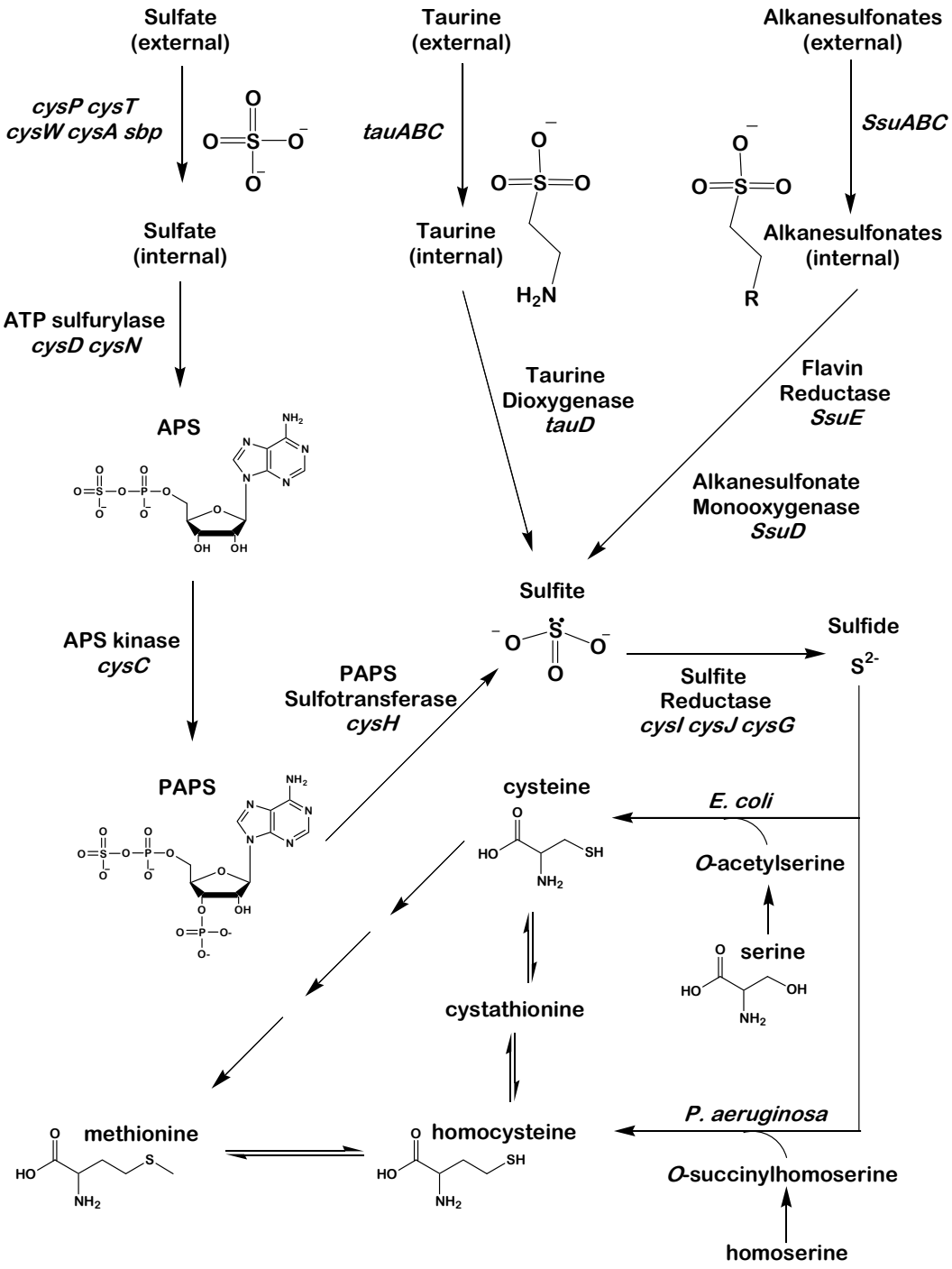

Figure 1.10. Cysteine and methionine biosynthesis in *E. coli and P. aeruginosa*.

for growth (*141*, *145*). Much of this interest is due to the increasing number of genes identified in various organisms, including higher organisms, displaying characteristics pertaining to sulfur metabolism. For instance, while bacteria synthesize a range of sulfatases and sulfonate oxygenases in order to utilize the sulfur available to them, the disruption of genes encoding arylsulfatases in higher organisms have been linked to several human genetic diseases, such as mucopolysaccharidosis VI and X-linked chondrodysplasia punctata, a human genetic disease that causes aberrant bone and cartilage development (*146*, *147*). The link between these genes, which are known to encode for proteins involved in sulfate uptake and activation in bacteria and fungus, and the cause of these serious human genetic diseases remains a subject of active investigation within the medical community.

1.4.2 Sulfate-Starvation Induced Proteins

The widespread availability of sulfonates in natural environments has resulted in the evolution of bacteria to degrade these compounds. Studies have demonstrated that aerobic bacteria can use a wide range of sulfonates as sulfur sources (*141*). In these organisms, desulfonation has been shown to occur via an α-ketoglutarate-dependent dioxygenase (TauD) or SsuD: each enzyme has been shown to be expressed when bio-available sulfate is limiting, earning them the name sulfate-starvation induced (SSI) proteins (Figure 1.9) (*129*). Consequently, the genes encoding these enzymes, *tauABCD* and *ssuEADCB*, have been shown to be repressed in the presence of sulfate in *E. coli*, and the expression of both the *tau* and the *ssu* operons have been shown to be dependent on the CysB protein under the *cys* regulon as well as the closely related regulator protein, the 'CysB-like' protein, Cbl (*141*, *148–150*). CysB, a global

transcriptional activator involved in regulating cysteine biosynthesis, organosulfur metabolism, and acid resistance in *E. coli*, was shown to induce expression of Cbl by binding to the promoter region of the *cbl* gene; the complementary regulation of Cbl by CysB places a tight control on the cellular response to sulfate starvation (*151*). Such tight control over expression suggests the TauD and SsuD systems may do more than simply relieve cellular sulfur starvation, but assist in protection during oxidative stress as well. However, the role of sulfonates within the bacterial life cycle has only been recognized recently. Interestingly, while open reading frames exhibiting characteristics of *E. coli* TauD have been identified in eukaryotic organisms like *Saccharomyces cerevisiae* (32% identity; accession number Z47973), SsuD appears to be exclusive to prokaryotic organisms (*141*). An alternative mechanism for sulfur acquisition has also been identified via the dibenzothiophene (DBT) desulfurization pathway, which is utilized by different strains of *Rhodococcus* sp. and the thermophilic bacterium *Paenibacillus* sp. strain A11-2 (*152*). In these organisms, two separate FMN-dependent monooxygenases are involved in the acquisition of sulfur from DBT (*153*). The DszC FMN-dependent monooxygenase catalyzes the first two steps in the pathway, converting DBT to DBT sulfone, while a second FMN-dependent monooxygenase, DszA, converts DBT sulfone to 2-hydroxybiphenyl-2-sulfinite (Figure 1.9). This system represents the first pathway identified that utilizes a single FMN reductase to service two separate FMN-dependent monooxygenases in a reaction pathway. Nevertheless, discrete desulfonation systems with overlapping substrate ranges have been identified in most bacterial organisms in which sulfur-controlled sulfonate metabolism has been studied, suggesting an ever important necessity on the organism's part to ensure execution of this

process. For instance, *E. coli* TauD exhibits a distinct preference for taurine as substrate, although it will also desulfonate short-chain alkanesulfonates (C_4–C_6), while SsuD has been shown to act on a wide range of sulfonated substrates with the noted exception of taurine (Table 1.2) (*129*, *150*).

Both *tauABCD* and *ssuEADCB* operons encode also for an ABC-type transporter system that assists in the scavenging and importation of extracellular sulfonates from the environment into the cell (*129*, *150*). Once in the cell, the SSI proteins catalyze the generation of sulfite, which can then be further reduced through the sulfur assimilation pathway before being incorporated into sulfur-containing biomolecules. Initial studies showed that SsuD has a broad substrate range, and is capable of desulfonating C_2 to C_{10} alkanesulfonates and several substituted sulfonated compounds (*129*) (Table 1.2). However, one of the more intriguing physiological aspects of the *ssu* gene is the two-component nature of the system: what, if any, is the evolutionary advantage to the monooxygenase component dependent on a separate FMN-dependent reductase (SsuE)?

1.5 The Alkanesulfonate Monooxygenase System: Flavin Reductase Component

With the exception of the FMN reductase involved in EDTA degradation, the FMN reductases of two-component systems that have been characterized are homodimers, and are usually smaller than their monooxygenase partner (*107*). The specificity for NADH or NADPH differs among FMN reductases with some capable of utilizing both. They can also differ as to whether a flavin is a tightly bound cofactor or a substrate in catalysis: for those that have a bound FMN cofactor, a second FMN substrate can either bind and be reduced by the bound flavin cofactor before being subsequently transferred to the monooxygenase. However, the latter mechanism has only been

Sulfonated substrate	Relative activity	
	SsuD	TauD
	%	
Taurine	**0.0**	**100.0**
***N*-Phenyltaurine**	**65.6**	**0.0**
4-Phenyl-1-butanesulfonic acid	**42.4**	**2.5**
HEPES	**10.6**	**5.0**
MOPS	**36.4**	**34.2**
PIPES	**29.2**	**3.1**
2-(4-Pyridyl)ethanesulfonic acid	**87.4**	**0.5**
1,3-Dioxo-2-isoindolineethanesulfonic acid	**100.0**	**30.1**
Sulfoacetic acid	**19.8**	**—[a]**
L-Cysteic acid	**0.0**	**0.0**
Isethionic acid	**14.3**	**1.2**
Methanesulfonic acid	**0.7**	**0.0**
Ethanesulfonic acid	**5.2**	**0.8**
Propanesulfonic acid	**14.0**	**2.3**
Butanesulfonic acid	**17.8**	**8.4**
Pentanesulfonic acid	**40.4**	**22.5**
Hexanesulfonic acid	**43.8**	**11.3**
Octanesulfonic acid	**46.3**	**—[a]**
Decanesulfonic acid	**43.2**	**—[a]**
Dodecanesulfonic acid	**20.1**	**3.3**
Tetradecanesulfonic acid	**2.9**	**—[a]**

[a] relative activity was not determined

Table 1.2. Substrate ranges for SsuD and TauD. Research was originally presented in reference (*128*)

observed for FRaseI in the presence of bacterial luciferase (*154*). Reductases that do not contain a bound flavin cofactor transfer the reduced flavin substrate to the monooxygenase enzyme following reduction by the pyridine nucleotide. Interestingly, the amino acid sequences of these enzymes share few similarities. The SsuE enzyme was shown to utilize flavin as a substrate with no flavin being bound to the enzyme when purified (*129*, *155*). Gel filtration and analytical ultracentrifugation experiments demonstrated SsuE to exist as a dimer in solution (*155*). SsuE showed a higher preference for FMN over FAD a well as a 1000-fold higher affinity for the oxidized FMN substrate over the reduced product (*129*, *155*, *156*). In single-enzyme kinetic assays, SsuE followed an ordered sequential mechanism, with NADPH as the first substrate to bind and $NADP^+$ as the last product to dissociate (*155*, *156*).

Results from studies on SsuE and SsuD indicate that each enzyme can influence the other's kinetic parameters and mechanistic properties. For instance, although the steady-state kinetic parameters for SsuE were not altered with varying ratios of SsuD, the SsuE kinetic mechanism was changed to an equilibrium ordered mechanism in the presence of SsuD and saturating levels of octanesulfonate. This suggests the NADPH substrate and $NADP^+$ product are in equilibrium with free enzyme (*155–157*). Additionally, a 10-fold increase in the K_d value for FMN was observed when SsuD and octanesulfonate were included in the reaction (*155*). This lower affinity for oxidized or reduced FMN by SsuE was proposed to be a mechanism designed to favor the rate of reduced flavin transfer to SsuD. The results demonstrate that the two enzymes serve to influence each other; the two-component nature of this system could have evolved as an efficient form of regulatory control, though the overall advantage remains unclear.

1.6 The Structural and Mechanistic Features of Alkanesulfonate Monooxygenase

The location of both SsuE and SsuD on the same operon ensures that a flavin reductase is available to supply reduced flavin for the monooxygenase reaction during sulfur limitation. While the three-dimensional structure of SsuE remains a matter of some speculation, the members of monooxygenase components of the bacterial luciferase family have been shown to form a triosephosphate isomerase (TIM)-barrel fold, with the active site located at the C-terminal end of the β barrel (Figure 1.11) (*120*, *127*, *128*, *158*). Each of the monooxygenases in this family exhibit several insertion regions throughout their TIM-barrel structures, one of which was largely unresolved in the three-dimensional structure in SsuD, suggesting conformational mobility in this region (Figure 1.12) (*128*, *159*). This disordered region lies near the putative active site of SsuD and is highly conserved in all SsuD homologs, suggesting loop closure over the active site occurs following the binding of substrate(s). The dynamics of this loop closure may be responsible for the conformational changes observed in kinetic studies (*159*, *160*). In several TIM-barrel proteins, flexible loops have been shown to contribute to the structure of the enzyme active site and/or play a functional role both in the binding of substrates and in enzyme catalysis as closure of the loop over the active site protects the substrate and catalytic intermediates from exposure to bulk solvent (*161–163*).

Recently, a structuring of the analogous loop in the α subunit of bacterial luciferase was observed in the three-dimensional structure of the enzyme: the loop was found to close over the active-site where oxidized FMN was bound (*120*). A similar structuring of the unresolved loop region in SsuD may also occur with the binding of substrates. Although SsuD variants containing partial deletions of the loop region are

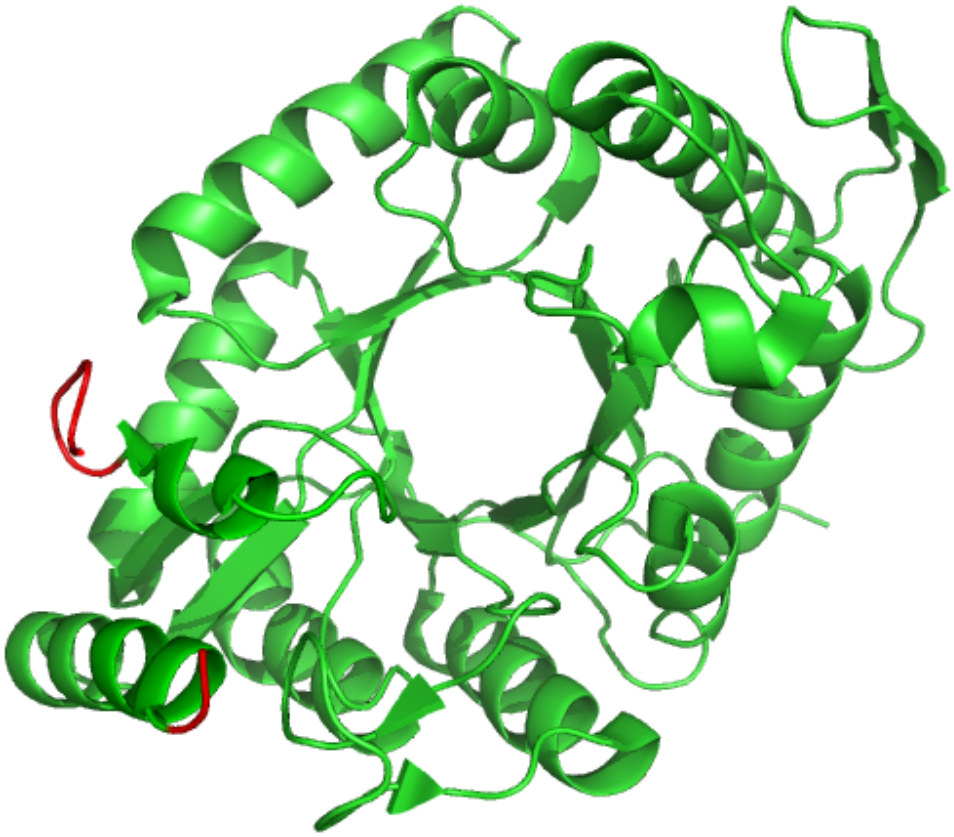

Figure 1.11. Three-dimensional representation of TIM-barrel structure of the SsuD monomer. The residues flanking the unresolved portion of the structure are highlighted in red. PDB ID:1M41

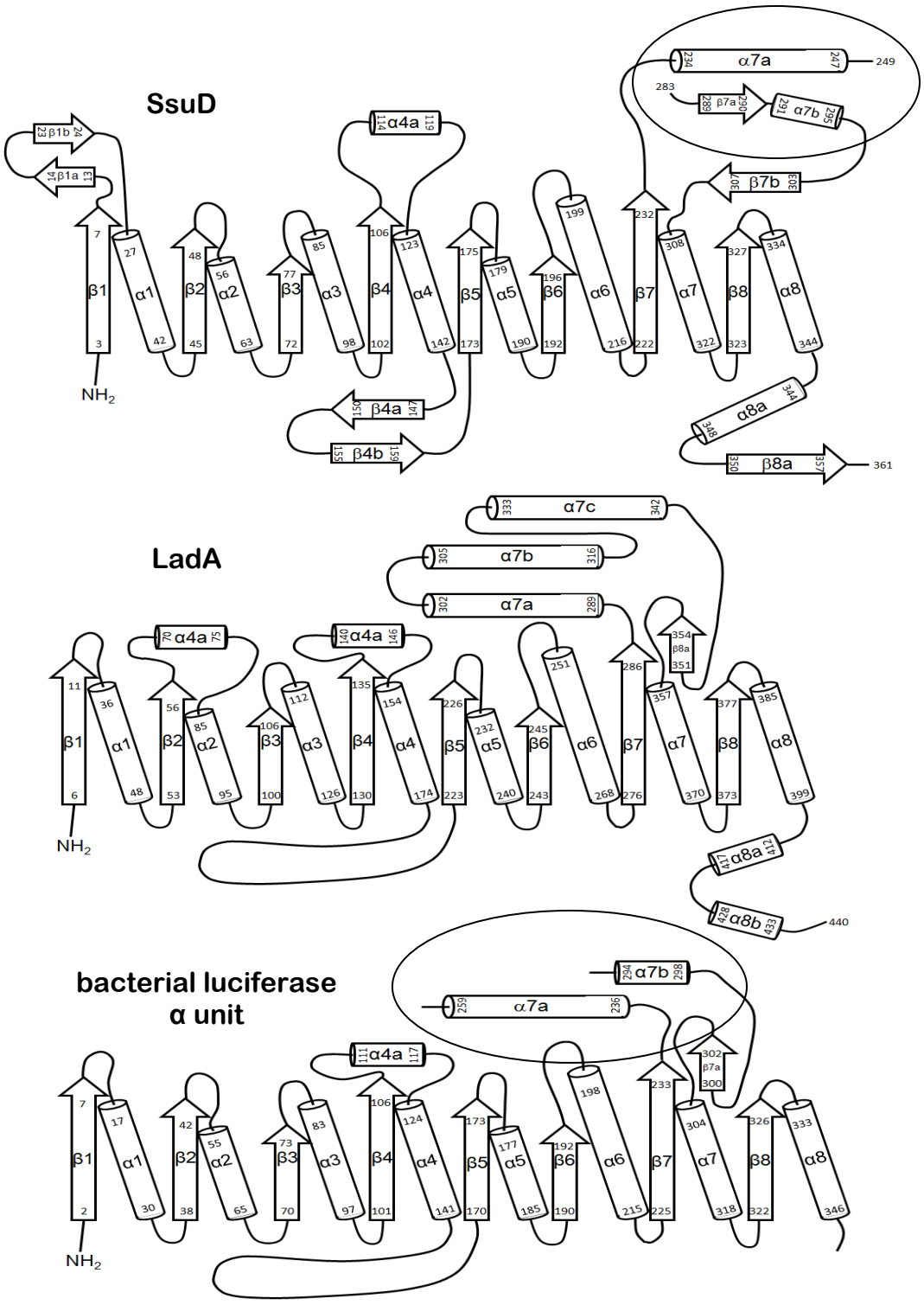

Figure 1.12. Topology diagrams illustrating the insertion regions of the bacterial luciferase family's TIM-barrel structures. The unresolved regions of SsuD and bacterial luciferase are circled.

able to bind reduced flavin and exhibit no gross changes in secondary structure when compared to wild-type SsuD, they are ultimately catalytically inactive (*159*). This result indicates that these variants are unable to undergo the lid-gating conformational change necessary for catalysis. Rapid-reaction kinetic analyses also indicated that the SsuD deletion variants failed to protect reduced flavin from unproductive oxidation (*159*). This result gives rise to the possibility that the lid-gating mechanism may also be involved in mediating the transfer of reduced flavin from SsuE to SsuD as well as protecting flavin intermediates generated during catalysis from solvolysis.

1.6.1 The Conserved Residues in Active-Site of SsuD

Although a low level of overall sequence identity exists between members of the bacterial luciferase family, the active-sites of each enzyme are structurally similar and contain several conserved amino acid residues necessary for enzymatic activity (*119*, *120*, *127–129*, *158*, *164–168*). *E. coli* SsuD in particular shares only a 15% sequence identity with *V. harveyi* lucifase LuxAB and a 16% sequence identity with thermophilic bacillus *Geobacillus thermodenitrificans* LadA. Nevertheless, an examination of the three-dimensional structure of each enzyme's active site reveals conserved amino acid residues in similar, if not identical, spatial arrangements. These conserved residues are separated into two categories: those responsible for flavin binding and those involved directly in catalysis (Figure 1.13) (*127–129*).

The degree of conservation of those amino acid residues involved in flavin binding is high. In SsuD, these amino acid residues are Val107, Phe7, Leu194, Thr195,

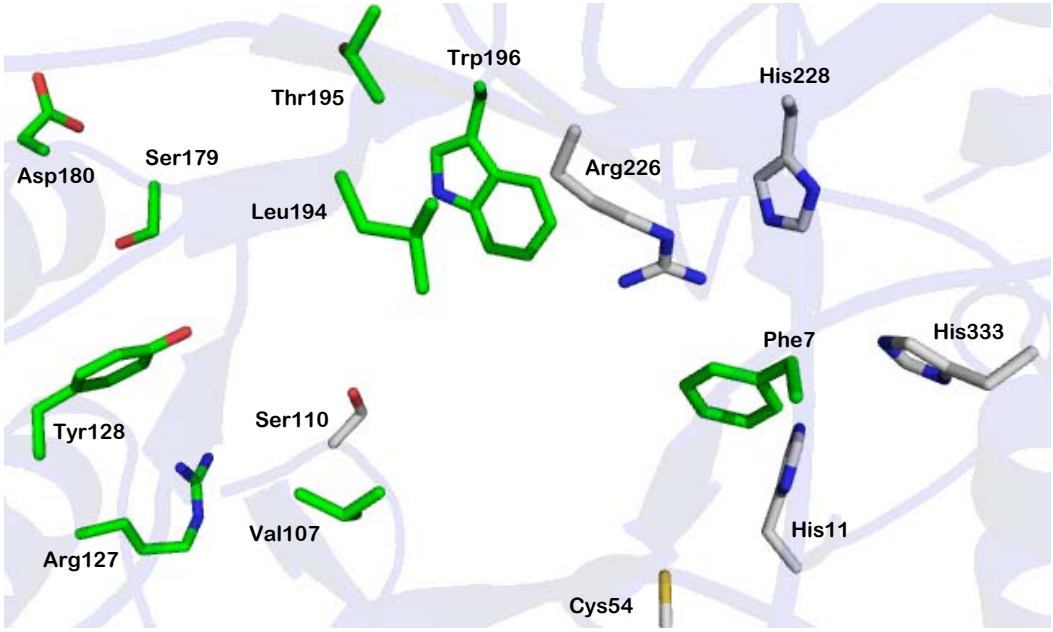

Figure 1.13. Three-dimensional structure of SsuD active-site. Conserved residues proposed to be involved in flavin binding are shown in green. Conserved amino acid residues proposed to be directly involved in catalysis are shown in grey.

Trp196, Arg127, Tyr128, Glu180 and Ser179 (Figure 1.13). The amino acid residues Val173, Phe6, Ile191, Ser193, Trp194, Arg107, Glu175 and Ser176 are required for flavin binding in LuxA, while Val135, Phe10, Leu246, Val244, Trp348, Arg157, Tyr 158, Glu155 and Ser230 serve this purpose in LadA. Not only are the spatial arrangements of these amino acid residues similar in each enzyme, they form identical interactions with oxidized flavin in the three-dimensional structures of bacterial luciferase LuxAB and LadA.

Although there are several conserved amino acid residues throughout the bacterial luciferase family, the importance of each amino acid varies depending on the enzyme. Amino acid residues Cys106, His44 and Tyr110 of LuxA and at Cys14, His17, Tyr63, Gln79, and His311 of LadA have all been identified as important to catalysis by site-directed mutagenesis (Figure 1.13) (*119*, *120*, *127–129*, *158*, *164–168*). To date, only the three-dimensional structures of bacterial luciferase LuxAB and LadA have been determined with oxidized FMN bound to the enzyme, while a three-dimensional structure with reduced $FMNH_2$ bound has yet to be determined for any member of the bacterial luciferase family. Substrate binding studies performed on bacterial luciferase and on SsuD have indicated a conformational change occurs in each enzyme (*107*, *120*, *155*, *157*, *160*, *165*, *169*). As a result, the spatial arrangement of amino acid residues in the active-site during catalysis may be altered from that of the three-dimensional structure with oxidized FMN bound. The lack of a clear three-dimensional structure of the active enzyme conformer provides an additional challenge to understanding the catalytic mechanisms employed by each member of bacterial luciferase family.

1.6.2 The SsuD Catalytic Mechanism

Despite extensive investigations, the details of the catalytic mechanisms employed by SsuD and related members of the bacterial luciferase family remain an enigma. In general, flavin monooxygenases activate O_2 by generating a covalent flavin-oxygen adduct at the C4a position of the flavin isoalloxazine ring (*60*, *65*, *72*, *75*, *107*). Although the individual steps vary, the formation of this C4a-(hydro)peroxyflavin intermediate subsequently promotes a nucleophilic or electrophilic reaction that is integral to enzyme catalysis. In the bacterial luciferase family, proper coordination and stabilization of the enzyme intermediates during catalysis appear to be dependent on one or more conformational changes (*107*, *120*, *155*, *157*, *160*, *165*, *169*). For the bacterial luciferase and alkanesulfonate monooxygenase mechanisms, these intermediates have been proposed to proceed through a complex Baeyer-Villiger like reaction prior to the formation and release of their respective products (*107*, *120*, *125*, *155*, *157*, *160*, *165*, *169*). The structural and catalytic similarities observed between members of the bacterial luciferase family suggest that the catalytic mechanisms employed by each member share common characteristics.

1.6.3 Proposed Mechanism for the SsuD Desulfonation reaction

The reaction mechanism of SsuD involves a flavin mediated oxygenolytic cleavage of a primary alkanesulfonate substrate's carbon-sulfur bond yielding a sulfite and a corresponding aldehyde as products (*107*, *128*, *129*, *155*, *157*, *160*, *169*, *170*). The process of cleaving a stable carbon-sulfur bond is energetically demanding; the process of cleaving a carbon-sulfur bond via a flavin substrate is a mechanistically intriguing. As a result, a mechanism for the desulfonation of alkanesulfonate by SsuD was proposed and

several strategies for investigating the individual mechanistic steps were developed. One challenge to the elucidation of catalytic mechanisms involving two-component monooxygenases is that the reduced flavin cofactor acts as a substrate and not a prosthetic group. As a result, the binding of reduced flavin provides an additional substrate binding step that must be accounted for in the mechanism. It was demonstrated previously through a combination of biochemical and kinetic approaches that the alkanesulfonate substrate was able to bind to SsuD only after $FMNH_2$ had bound first (*160*). The results indicated the SsuD reaction proceeds via an ordered binding substrate mechanism. Stopped-flow analyses also demonstrated the formation of a C4a-hydroperoxyflavin intermediate during SsuD catalysis in the absence or at low concentrations of octanesulfonate substrate (*160*, *171*). The relative stability of this C4a-hydroperoxyflavin intermediate varies between the monooxygenases that comprise two-component systems. In most flavin-dependent monooxygenases, the active-site forms a packed hydrophobic cavity that prevents the rapid breakdown of unstable flavin intermediates via a solvent-free environment (*60*, *65*, *72*, *75*, *95*, *96*). In bacterial luciferase, the C4a-hydroperoxyflavin intermediate is stabilized sufficiently in the absence of aldehyde substrate to be isolated at 4 °C and identified with stopped-flow spectrophotometry using a photo-diode array (*122*, *124*, *165–167*). Conversely, the C4a-hydroperoxyflavin intermediate signal is weak for the SsuD reaction and decomposes relatively rapidly even in the absence or at low concentration of octanesulfonate substrate (*160*, *171*). Although the reason for this lack of C4a-hydroperoxyflavin intermediate stability in the SsuD reaction is unclear, several charged residues near the site of oxygen

activation have been identified as serving to stabilize this intermediate while also playing a direct role in the proposed mechanism.

In the proposed mechanism, the C4a-peroxyflavin performs a nucleophilic attack on the sulfur group of the alkanesulfonate substrate followed by a Baeyer-Villiger rearrangement and the cleavage of the carbon-sulfur bond to generate the alkane peroxyflavin intermediate (Scheme 1.5, II). The release of the aldehyde product from the enzyme occurs following abstraction of a proton from the alkane peroxyflavin intermediate via a catalytic base (Scheme 1.5, III). Finally, a general acid is proposed to donate a proton to the $FMNO^-$ intermediate triggering a conformational change that opens the enzyme to solvation and promotes product release (Scheme 1.5, IV). The research presented in this dissertation serves as evidence to support the proposed mechanism.

1.7 Summary

The field of biochemistry represents an amalgam of disciplines which originated and developed independently of each other. As a result, modern biochemists have several techniques with and directions in which to approach the study of an enzyme. The mechanistic enzymologist utilizes kinetic and mechanistic techniques developed from organic, inorganic, and physical chemistry to better understand the line that separates random chemical processes from the deliberate manipulation of such processes exhibited by living organisms. In doing so, the mechanistic enzymologist explores the molecular framework of the enzyme itself in hopes of understanding better the processes governing the organism as a whole.

In *E. coli*, SsuD is expressed when sulfate becomes limiting. The limitation induces the synthesis of a set of proteins involved in acquiring sulfur from

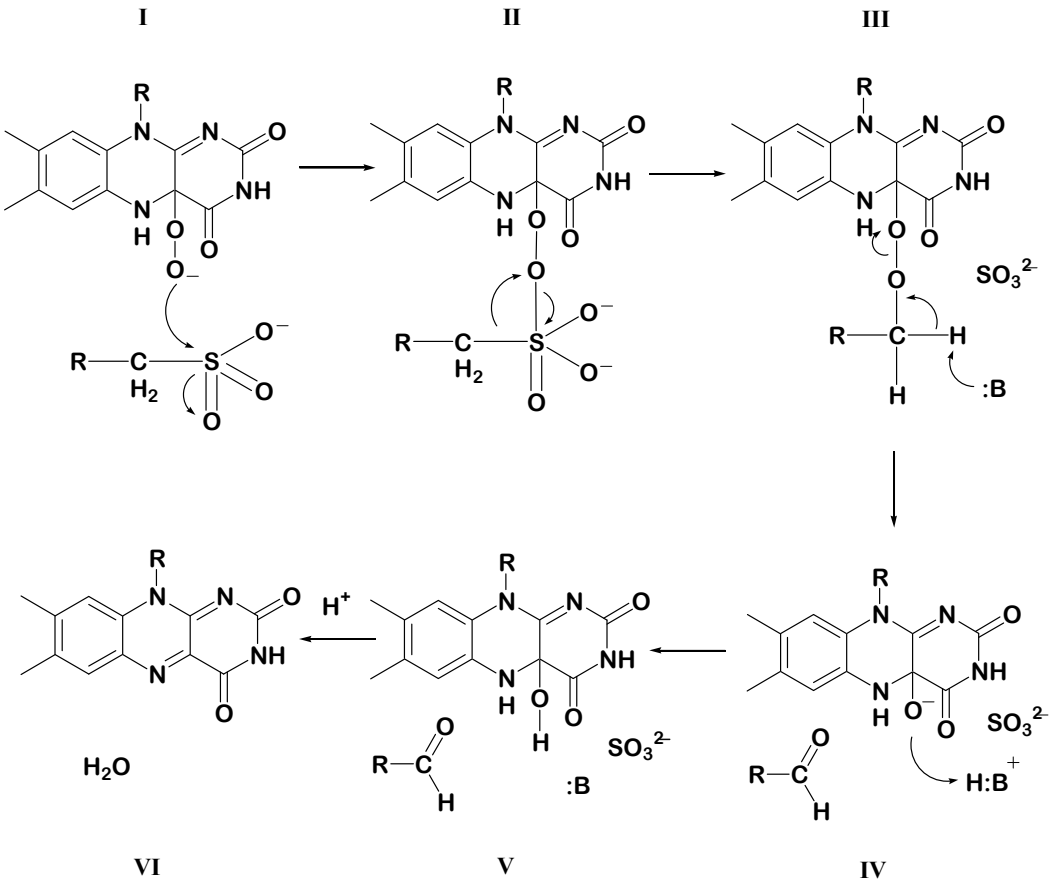

Scheme 1.5. The proposed chemical mechanism for the SsuD desulfonation reaction

alternative sources, primarily alkanesulfonates (*107*, *129*, *150*, *170*). The enzyme is part of a two-component flavin-dependent monooxygenase system that has been identified in a diverse range of bacterial organisms. It is comprised of an independent NAD(P)H-dependent FMN reductase (SsuE) and a monooxygenase (SsuD). Together, they enable the organism to utilize a broad range of alkanesulfonates as alternative sulfur sources (*107*, *129*, *170*). Unlike a traditional flavin monooxygenase where both oxidative and reductive half reactions occur on the same enzyme, the alkanesulfonate monooxygenase system utilizes $FMNH_2$ supplied by SsuE to alleviate periods of limited sulfur bioavailability. SsuE transfers $FMNH_2$ to SsuD which activates dioxygen in order cleave the carbon-sulfur bond of alkanesulfonates releasing sulfite and the corresponding aldehyde (Scheme 1.5) (*107*, *160*).

Flavoproteins are capable of catalyzing various reactions including oxidation, dehydrogenation, reduction, and oxygenation. Like many flavin monooxygenases, SsuD is proposed to activate dioxygen by generating a covalent flavin-oxygen adduct at the C4a position of the flavin isoalloxazine ring (*60*, *72*, *95*, *107*, *160*). Although the individual steps vary between enzymes, the formation of this C4a-(hydro)peroxyflavin intermediate typically promotes a nucleophilic or electrophilic reaction that is integral to enzyme catalysis (*60*, *61*, *72*, *75*, *95*, *96*). The relative stability of this C4a-hydroperoxyflavin intermediate varies between the monooxygenases that comprise two-component systems and is often dependent on the active site environment (*107*, *122*, *165*, *169*, *172*). Typically, the active-sites of flavin monooxygenases are lined with hydrophobic amino acid residues that limit the rapid breakdown of unstable flavin intermediates by preventing solvation during catalysis (*60*, *65*, *72*, *104*, *120*). Previous

studies on SsuD have indicated that proper coordination and stabilization of the enzyme intermediates during catalysis appear to be dependent on one or more conformational changes (*159*, *169*, *171*). These conformational changes have been proposed to stabilize the flavin intermediate via formation of the hydrophobic cavity necessary to prevent solvation.

SsuD has been proposed to promote the oxygenolytic cleavage of a carbon-sulfur bond via acid-base catalysis. Despite extensive investigations, the details of the catalytic mechanism employed by the alkanesulfonate monooxygenase system remain an enigma (*107*, *160*, *169*, *171*). As a result, the catalytic mechanism for SsuD was evaluated using several different kinetic approaches including steady-state pH dependence studies, solvent deuterium and substrate deuterium kinetic isotope effects, temperature dependent studies, and single turnover kinetics. These combined results have served to identify key chemical steps of the proposed catalytic mechanism.

CHAPTER TWO

Identification of Critical Steps Governing the Two-Component Alkanesulfonate Monooxygenase Catalytic Mechanism

2.1 INTRODUCTION

In *Escherichia coli*, sulfur limitation induces the synthesis of a set of proteins involved in acquiring sulfur from alternative sources (*107*, *150*). The two-component alkanesulfonate monooxygenase system, composed of a flavin reductase (SsuE) and an alkanesulfonate monooxygenase (SsuD), enables the organism to utilize a broad range of alkanesulfonates as alternative sulfur sources (*150*). The SsuE enzyme catalyzes the reduction of FMN by NAD(P)H, and the reduced flavin is transferred to SsuD (Scheme 2.1). In the proposed mechanism for desulfonation, $FMNH_2$-bound SsuD activates dioxygen to form a C4a-(hydro)peroxyflavin intermediate that is thought to cleave the carbon-sulfur bond of the alkanesulfonate substrate resulting in the release of sulfite and the corresponding aldehyde (Scheme 2.2) (*157*).

Efforts to elucidate the catalytic mechanisms of flavin-dependent monooxygenase systems continue to be an area of active research. Elucidating catalytic mechanisms of two-component monooxgenases has proven to be particularly challenging in that the

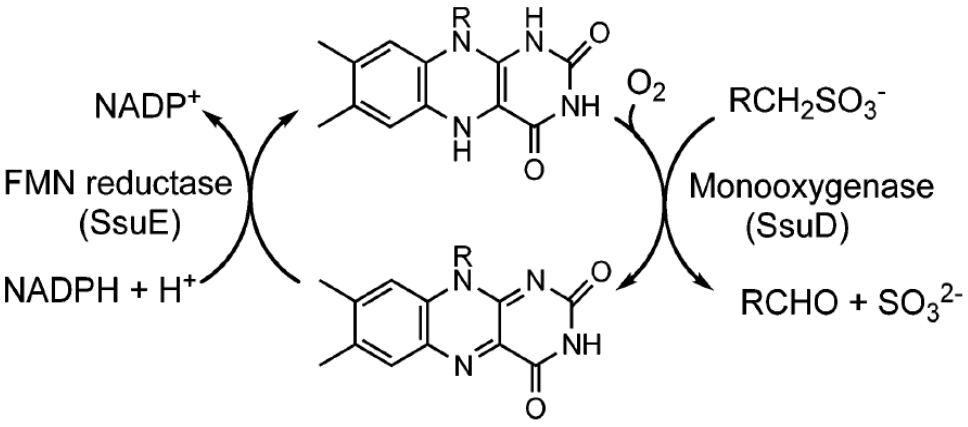

Scheme 2.1. The Catalytic Cycle of the Alkanesulfonate Monooxygenase System

reduced flavin cofactor acts as a substrate and not as a prosthetic group. The binding of the reduced flavin substrate provides an additional step that must be accounted for in the kinetic mechanism, as substrate binding and release steps in both SsuD and bacterial luciferase have been linked to one or more conformational changes during catalysis (*107*, *120*, *127–129*, *148*, *150*, *155–160*, *164*, *165*, *169*, *171*). In our previous studies, the mechanism of SsuD was probed by a combination of biochemical and kinetic approaches (*160*, *169*, *171*). The octanesulfonate substrate was unable to bind to SsuD until $FMNH_2$ was first bound, which implied an ordered substrate binding mechanism in the SsuD reaction. In addition, evidence for the formation of a C4a-(hydro)peroxyflavin intermediate was obtained by stopped-flow kinetic analyses in the absence or at low concentrations of octanesulfonate (*6*, *8*). In the proposed mechanism, the C4a-peroxyflavin performs a nucleophilic attack on the sulfur group of the alkanesulfonate substrate followed by a Baeyer-Villiger rearrangement leading to the cleavage of the carbon-sulfur bond to generate the alkane peroxyflavin intermediate (Scheme 2.2, III). A catalytic base has been proposed to abstract a proton from the alkane peroxyflavin intermediate, leading to the release of the aldehyde product from the enzyme following rearrangement (Scheme 2.2, III). Finally, a general acid is proposed to donate a proton to the $FMNO^-$ intermediate triggering a conformational change that opens the enzyme to solvation and promotes product release (Scheme 2.2, IV). Unfortunately, there is little information regarding the exact structures of proposed SsuD isomers. Therefore, identification of the catalytic base and acid would provide valuable information to support the proposed desulfonation mechanism by SsuD.

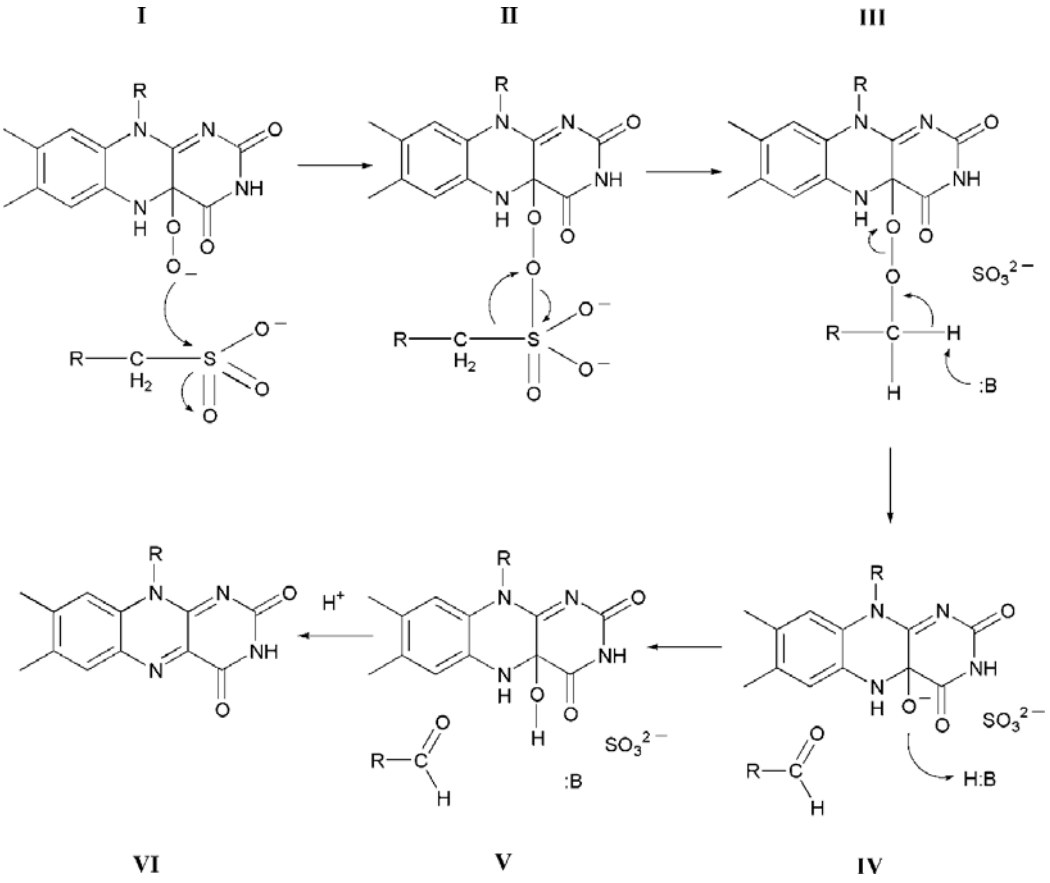

Scheme 2.2. The proposed catalytic mechanism of the SsuD desulfonation reaction

Although the amino acid sequence identity is low, SsuD is similar in overall structure to the flavin-dependent monooxygenases bacterial luciferase and long-chain alkane monooxygenase (LadA) as each of these FMN-dependent monooxygenases display similar TIM barrel architectures (*127–129*, *148*, *158*, *164*, *165*). For bacterial luciferase and SsuD, the binding of reduced flavin induces an apparent conformational change leading to an altered active site environment from the apo-enzyme structure (*120*, *165*, *169*). While three-dimensional structures with oxidized flavin bound within the active site have been obtained for bacterial luciferase and LadA, structures with the reduced flavin bound within the active site have remained elusive for all two-component systems (*120*, *127*). Although there is no three-dimensional structure available for SsuD with substrates bound, the location of the active site of the enzyme has been postulated based on chemical labeling, computer simulations, and structural similarities to bacterial luciferase and LadA (Figure 2.1). Since the K_d value for FMN and SsuD is higher than for $FMNH_2$, it is reasonable to conclude that the active site environment of SsuD would be different between the oxidized and reduced flavin bound enzyme (*120*, *155–157*, *160*, *169*). Therefore, even modeling FMN and 1-octanesulfonate into the active site of SsuD based on its close structural homology to bacterial luciferase and LadA would provide only a limited understanding of the active site environment during catalysis. As a result, site-directed mutagenesis, steady-state kinetic assays, pH dependence, and single-turnover rapid-reaction kinetic studies were employed in order to provide a more complete picture of the active site environment of alkanesulfonate monooxygenase as the desulfonation reaction occurs.

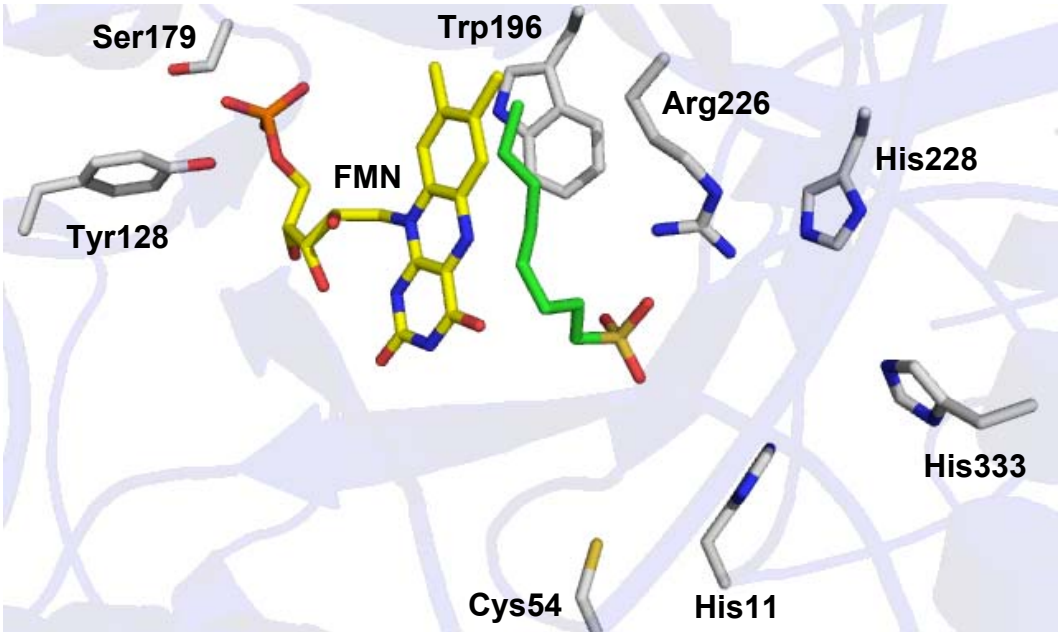

Figure 2.1. The putative active site of SsuD. The Arg226 guanidinium nitrogen is 7.6 Å from the N1 position of the flavin (yellow) and 4.5 Å from the C1 position of the 1-octanesulfonate substrate (green). The His228 Nε2 is 3.9 Å from the guanidinium moiety of Arg226. The Cys54 thiol is 6.6 Å away from the C1 position of the 1-octanesulfonate substrate and 10.2 Å from the guanidinium moiety of Arg226. The active site was rendered with PyMOL (PDB ID:1M41), FMN was modeled using its coordinates in LadA (PDB ID: 3B9O), and AutoDock was used to model octanesulfonate (*127*, *128*).

Several amino acids (His228, His11, His333, Cys54, and Arg226) located in the active site of SsuD are in a similar arrangement as catalytically relevant amino acids from bacterial luciferase and LadA (Figure 2.1) (*120*, *127–129*, *158*, *164*). In our proposed model, an active site base would be involved in proton abstraction from the alkanesulfonate peroxyflavin adduct, leading to the formation of the aldehyde product (Scheme 2.2, III). In bacterial luciferase, His44 in the α-subunit was previously identified as the catalytic base in the bioluminescence reaction as mutation of this histidine residue to an alanine showed a decrease in bioluminescence activity (*166*, *167*). The enzymatic activity could be rescued with the addition of imidazole to the reaction at increasing pH (*167*). Substitution of His311 in LadA to a phenylalanine was also shown to reduce activity of the LadA enzyme (*127*). As a result, His228 of SsuD was suggested as a potential active site base in the desulfonation reaction based on its structural similarity to His44 and His311 in bacterial luciferase and LadA, respectively. (*120*, *127–129*, *158*, *164*, *166*, *167*). Additionally, the proposed catalytic mechanism for SsuD includes an active-site acid that would be involved in protonation of the $FMNO^-$ intermediate prior to product release. Cys54 of SsuD was identified as a residue of potential catalytic importance due to its structural similarity to conserved Cys106 of bacterial luciferase and Cys14 of LadA (*119*, *122*, *124*, *127*, *128*, *166–168*). Although chemical labeling of Cys54 SsuD with methyl mercury led to inactivation of the enzyme, the Cys54 residue was not shown to play a direct role in catalysis (*171*). As a result, Arg226 of SsuD was identified as the possible active-site acid due to its location within the active site and the conserved nature of this residue in bacterial SsuD homologs. Further evaluation of these amino acids in the form of chemical rescue, substrate binding, and single-turnover rapid-

reaction kinetic studies illuminated crucial steps governing the catalytic mechanism of the SsuD desulfonation reaction.

2.2 EXPERIMENTAL PROCEDURES

2.2.1 Materials

E. coli strains (XL-1 and BL21(DE3)) and QuickChange site-directed mutagenesis kit were purchased from Stratagene (La Jolla, CA). Plasmid vectors and pET21a were obtained from Novagen (Madison, WI). DNA primers were synthesized by Invitrogen (Carlsbad, CA). Flavin mononucleotide phosphate (FMN), reduced nicotinamide adenine dinucleotide phosphate (NADPH), ethylenediaminetetraacetic acid (EDTA), potassium phosphate (monobasic anhydrous and dibasic anhydrous), streptomycin sulfate, Trizma base, Bis-Tris, glycine, ammonium sulfate, ampicillin, dimethyl sulfoxide (DMSO), 5,5-dithiobis(2-nitrobenzoic acid) (DTNB), glucose, glucose oxidase, lysozyme, guanidine, and urea were from Sigma (St. Louis, MO). Isopropyl-β-D-thiogalactoside (IPTG), sodium chloride, and glycerol were obtained from Fisher Biotech (Pittsburgh, PA). 1-octanesulfonate and dithiothreitol (DTT) were purchased from Fluka (Milwaukee, WI). The SsuD and SsuE enzymes were expressed and purified as previously described (*155*). The concentrations of SsuD and SsuE proteins were determined from A_{280} measurements using a molar extinction coefficient of 47.9 mM^{-1} cm^{-1} and 20.3 mM^{-1} cm^{-1}, respectively (*155*).

2.2.2 Construction of variant proteins

A recombinant pET21a plasmid containing the *ssuD* gene was used to construct variants of the SsuD enzyme. Primers for each variant were designed as 29 base

oligonucleotides containing the desired mutation. The CAT codon for His228, His11, and His333 was replaced with GCG (H228A, H11A, and H333A). The CGT codon for Arg226 was replaced with CGC (R226A), AAA (R226K), and CAT (R226H). The variant constructs were confirmed by DNA sequencing analysis at Davis Sequencing (University of California, Davis). Confirmed variants were transformed into *E. coli* BL21(DE3) competent cells for protein expression and stored at –80 ˚C. Each SsuD variant protein was purified as previously reported (*155*).

2.2.3 Circular dichroism spectroscopy

Circular dichroism (CD) spectra of wild-type SsuD and variants were obtained by mixing 1.2 μM of enzyme in 10 mM potassium phosphate buffer, pH 7.5, and 100 mM NaCl at 25 ˚C. Spectra were recorded on a Jasco J-810 Spectropolarimeter (Easton, MD). Measurements were taken in 0.1 nm increments from 300 to 185 nm in a 0.1 cm path length cuvette with a bandwidth of 1 nm and a scanning speed of 50 nm/min. Each spectrum is the average of eight scans. Background correction was performed using the default parameters within the Jasco J-720 software.

2.2.4 Dependence of Kinetic Parameters on pH

The activities of the H228A, H11A, H333A, C54A and wild-type SsuD enzymes were routinely assayed at 25 °C as previously described with the following modifications: reactions employed a range of 1-octanesulfonate concentrations (10−5000 μM) in either 50 mM Bis-Tris (pH range of 5.8–7.2), 50 mM Tris-HCl (pH range of 7.2-9.0), or 50 mM glycine (pH range of 9.0-10.0) (*129*, *160*, *171*). Higher enzyme concentrations were utilized for the R226A, R226K, and R226H SsuD enzymes due to decreased activity. For those variants, reactions were initiated by the addition of NADPH

(500 μM) into a reaction mixture containing a SsuD variant (3 μM; R226A, R226K, or R226H SsuD), SsuE (9 μM), FMN (5 μM), and a range of 1-octanesulfonate concentrations (10−5000 μM) in 50 mM Tris-HCl (pH 7.5) at 25 °C. Each buffered solution was supplemented with 100 mM sodium chloride to maintain the ionic strength, and overlapping assays were performed in Bis-Tris and Tris-HCl at pH 7.2 and in Tris-HCl and glycine at pH 9.0 in order to ensure activity was independent of the buffer used. All assays were performed in triplicate, and steady-state kinetic parameters were determined by fitting the data to the Michaelis-Menten equation. The pH dependence of k_{cat} and k_{cat}/K_m were best fit to either a single ionization model (equation 2.1), double ionization model (equation 2.2), or a single ionization model with a sticky proton (equation 2.3).

$$\log y = \log\left[C / \left(1 + \frac{H}{K_1} \right) \right] \qquad \text{(equation 2.1)}$$

$$\log y = \log\left[C / \left(1 + \frac{H}{K_1} + \frac{K_2}{H} \right) \right] \qquad \text{(equation 2.2)}$$

$$\log y = \log\left[C \times \left(1 + \frac{H}{K_1} \right) / \left(\left(1 + \frac{H}{K_2} \right) \times \left(1 + \frac{H}{K_3} \right) \right) \right] \qquad \text{(equation 2.3)}$$

In equations 2.1—2.3, H is $[H^+]$, y is k_{cat} or k_{cat}/K_m, C is the pH independent value of y, and K_1, K_2, and K_3 represent the dissociation constant for groups on the SsuD-$FMNH_2$ complex. The pH stability of SsuD was determined by preincubating 20 μM enzyme in the appropriate buffer (pH 5.8-10.0) at 25 °C for 30 min. The preincubated SsuD (0.2 μM) was then assayed as previously described in 50 mM Tris-HCl, at pH 7.5, and 100 mM NaCl. The activity of SsuE was assayed as previously described monitoring NADPH oxidation at A_{340} in a reaction mixture containing 0.6 μM FMN and 0.04 μM SsuE (*155*).

The effect of pH on the kinetic parameters of wild-type SsuE was determined by performing a series of activity assays with varied NADPH concentrations (10- 200 μM) in 50 mM Bis-Tris (pH range of 5.8–7.2), 50 mM Tris-HCl (pH range of 7.2-9.0), or 50 mM glycine (pH range of 9.0-10.0).

2.2.5 Substrate Binding Affinity

Binding of reduced flavin to the variant SsuD enzymes was monitored by spectrofluorimetric titration as previously described (*160*). $FMNH_2$ solutions containing EDTA (10 mM), glucose (20 mM), and glucose oxidase (10 units) were prepared by bubbling the solution in a glass tonometer with argon gas as previously described (*160*) The resulting anaerobic solution was then photoreduced by irradiation for 30 min. A solution of R226A or R226K SsuD (0.5 μM) in 25 mM potassium phosphate, pH 7.5, 10% glycerol, and 100 mM NaCl (1.0 mL total volume) was titrated with a solution of $FMNH_2$ (0.26-8.26 μM) under anaerobic conditions. After excitation at 280 nm, the fluorescence emission intensity at 344 nm was recorded following each addition of $FMNH_2$. Bound $FMNH_2$ was determined using the following equation:

$$[S]_{bound} = [E]\frac{I_0 - I_c}{I_0 - I_f} \qquad \text{(equation 2.4)}$$

where $[S]_{bound}$ represents the concentration of enzyme-bound substrate. [E] represents the initial concentration of enzyme, I_0 is the initial fluorescence intensity of enzyme prior to the addition of substrate, I_c is the fluorescence intensity of enzyme following each addition, and I_f is the final fluorescence intensity. The concentration of $FMNH_2$ bound was plotted against the free substrate to obtain the dissociation constant (K_d) according to equation 2.5.

$$Y = \frac{B_{max} X}{K_d + X} \qquad \text{(equation 2.5)}$$

Y and X represent the concentration of bound and free substrate, respectively, following each addition. B_{max} is the maximum binding at equilibrium with the maximum concentration of substrate.

Octanesulfonate binding to the SsuD variants was investigated as previously described by similar fluorimetric titration methods employed for flavin binding (*160*). Aliquots of an anaerobic solution of octanesulfonate (2.5—108 μM) in an airtight titrating syringe were added to an anaerobic solution of either R297A or R297K SsuD (1 μM), with $FMNH_2$ (2 μM) in 25 mM potassium phosphate, pH 7.5, 10% glycerol, and 100 mM NaCl (1.0 mL total volume). The fluorescence spectrum for each titration was recorded with an excitation wavelength at 280 nm and emission intensity measurements at 344 nm. The concentration of 1-octanesulfonate bound was determined by equation 2.4, and was plotted against the free substrate to obtain the dissociation constant (K_d) according to equation 2.5.

2.2.6 Rapid reaction kinetic analyses

Stopped-flow kinetic analyses were carried out as previously described using an Applied Photophysics SX.18 MV stopped-flow spectrophotometer (*160*). All experiments were performed by mixing $FMNH_2$ (25 μM) in one drive syringe against SsuD (35 μM) in air-saturated buffer (25 mM Tris-HCl, pH 8.5, 100 mM NaCl) in the other drive syringe. When included in the reaction, varied concentrations of 1-octanesulfonate (20–1000 μM) were added to the SsuD solution in air-saturated buffer. All experiments were carried out in single-mixing mode by mixing equal volumes of the solutions, and the reactions monitored by the change in absorbance at 370 and 450 nm over 100 seconds.

Kinetic traces were fit to the following equation with KaleidaGraph software (Abelbeck Software, Reading, PA):

$$A = A_1 \exp(-k_1 t) + A_2 \exp(-k_2 t) + C \qquad \text{(equation 2.6)}$$

where k_1 and k_2 are the apparent rate constants, A is the absorbance at time t, A_1, and A_2, are amplitudes of each phase, and C is the absorbance at the end of the reaction.

2.2.7 Guanidinium rescue experiments

Two experimental conditions were used in order to evaluate the ability of guanidinium to compensate for the arginine amino acid in R226A SsuD. In the first experiment, the enzymatic activity of R226A SsuD was determined by conducting the previously described activity assay with 1-octanesulfonate (1 mM) and a range of guanidine concentrations (5-200 mM) in 50 mM Bis-Tris (pH range of 5.8–7.2), 50 mM Tris-HCl (pH range of 7.2-9.0), or 50 mM glycine (pH range of 9.0-10.0). The second experiment focused on the effect of guanidinium on the steady-state kinetic parameters of R226A SsuD by measuring the enzymatic activity with varying concentrations of octanesulfonate (10−5000 μM) in the presence of 100 mM guanidine-HCl in 50 mM Bis-Tris (pH 6.2), 50 mM Tris-HCl (pH 7.5), or 50 mM glycine (pH 9.5). For each experimental condition, the reactions were initiated with NADPH (500 μM) into a reaction mixture containing R226A SsuD (3.0 μM), SsuE (9.0 μM), and FMN (5.0 μM). Control experiments were performed where guanidine and/or R226A SsuD were not included in the reaction. The sulfite product was quantified as previously described (*129*, *160*).

2.3 RESULTS

2.3.1 Dependence of wild-type SsuD kinetic parameters on pH

In order to gain insight into catalytically relevant ionizations governing the desulfonation reaction of SsuD, the k_{cat} and k_{cat}/K_m values for wild-type SsuD were measured as a function of pH from pH 5.8-10.0. SsuD showed optimal catalytic activity between pH 7.2-8.5 where the pH independent value was found to be 93 ± 5 min^{-1} for k_{cat}, and 1.9 ± 0.1 μM^{-1} min^{-1} for k_{cat}/K_m (Table 2.1). SsuD was found to be soluble over the entire experimental pH range, as full activity was restored when SsuD that had been preincubated at specific experimental pH values was introduced into an activity assay at pH 7.5. The pH dependence of k_{cat} for SsuD revealed two titratable residues with pK_a values of 6.6 ± 0.1 and 9.5 ± 0.1 (Table 2.1). These results indicate that a group with a pK_a value of around 6.6 must be deprotonated, and a group with a pK_a value of around 9.5 must be protonated to support catalysis up through product release. Interestingly, only one titratable amino acid residue with a pK_a value of 6.9 ± 0.1 was extrapolated from the pH dependence of k_{cat}/K_m, suggesting that a functional group on the free enzyme or substrate must be deprotonated in order to commit through the first-irreversible step. Since the SsuD enzyme works in conjunction with the SsuE enzyme as part of a two-component system, pH dependence controls were performed in order to verify that the experimental pK_a values were not attributable to functional groups participating in

SsuD	k_{cat} (min^{-1})		k_{cat}/K_m (μM^{-1} min^{-1})
	pK_1	pK_2	pK
wild-type	6.6 ± 0.1	9.5 ± 0.1	6.9 ± 0.1
H228A	6.6 ± 0.1	9.6 ± 0.1	7.1 ± 0.1
H11A	6.8 ± 0.2	9.5 ± 0.2	7.0 ± 0.1
H333A	6.6 ± 0.1	9.5 ± 0.1	7.0 ± 0.1
C54A	6.3 ± 0.1	—[a]	7.2 ± 0.2

[a] Value could not be determined within the experimental pH range

Table 2.1. pH dependence of steady-state kinetic parameters for wild-type SsuD and variants

the SsuE reductase half-reaction (data not shown). The SsuE reductase half-reaction did not demonstrate any dependence on pH over the experimental range suggesting that experimental pK_a values can be attributed solely to functional groups on the SsuD enzyme and/or its substrates.

2.3.2 pH Dependence of SsuD variants

In an effort to identify the groups contributing to the pK_a values governing the pH dependence of kinetic parameters for wild-type SsuD, several SsuD variants were constructed with substitutions at amino acid groups likely to be responsible for these pK_a values. The pK_a values of 6.6 ± 0.1 and 6.9 ± 0.1 seen for the pH dependences of k_{cat} and k_{cat}/K_m, respectively, are similar to those that might be expected for a histidine residue acting as an active site base in an enzyme (*119*, *127–129*, *158*, *164*, *166*, *167*, *173*). As a result, pH dependent studies were conducted on H228A, H11A, and H333A SsuD in order to determine whether the absence of the imidazole functional group at these positions resulted in a shift in or absence of the pK_a in the corresponding pH profiles compared to wild-type SsuD. For H228A SsuD, the pH independent value was 57 ± 2 min^{-1} for k_{cat} and 0.54 ± 0.07 μM^{-1} min^{-1} for k_{cat}/K_m. For H11A and H333A SsuD, the pH independent value was 66 ± 3 min^{-1} for k_{cat} and 82 ± 2 min^{-1}, respectively, and 2.1 ± 0.2 μM^{-1} min^{-1} and 1.8 ± 0.2 μM^{-1} min^{-1} for k_{cat}/K_m, respectively (Table 2.2). The pH dependence of k_{cat} and k_{cat}/K_m for each of the SsuD variants revealed titratable groups with pK_a values similar to those determined for the wild-type enzyme (Table 2.1). The results indicated that neither of these histidine residues was contributing exclusively to the lower pK_a value in the k_{cat} nor k_{cat}/K_m pH dependence profile for wild-type SsuD. Interestingly, the presence of a slight "hollow" in the k_{cat} pH profile for H228A and

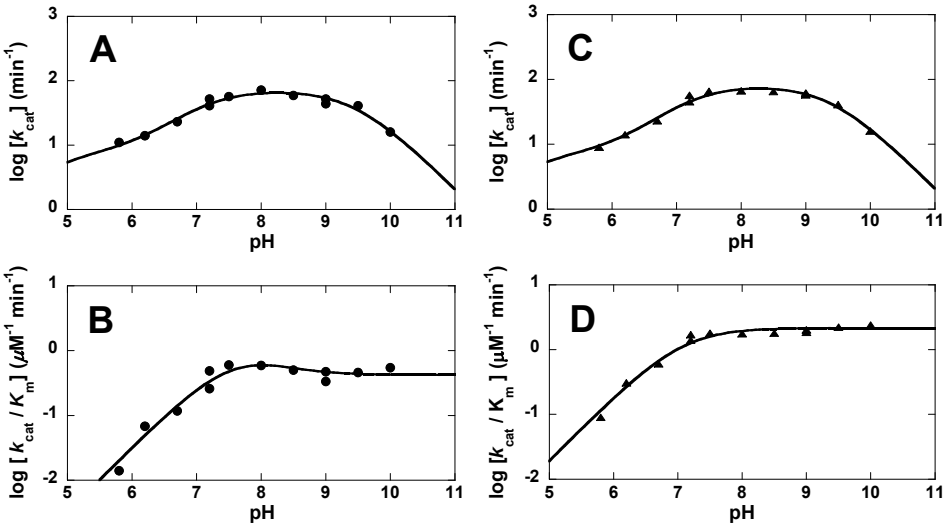

Figure 2.2. pH dependence of H228A and H11A SsuD activity. Reactions were initiated by the addition of NADPH (500 μM) into a reaction mixture containing H228A SsuD (0.2 μM), SsuE (0.6 μM), FMN (2 μM), and a range of octanesulfonate concentrations (10−5000 μM) in either 50 mM Bis-Tris (pH range of 5.8–7.2), 50 mM Tris-HCl (pH range of 7.2-9.0), or 50 mM glycine (pH range of 9.0-10.0) and 100 mM sodium chloride at 25°C. pH dependence of H228A SsuD (●) A: k_{cat} values B: k_{cat}/K_m values; pH dependence of H11A SsuD (▲) C: k_{cat} values D: k_{cat}/K_m values. Each point is the average of at least three separate experiments. Solid lines for A and C are fits of the data to equation 2.3.

	k_{cat} (min^{-1})	k_{cat}/K_m (μM^{-1} min^{-1})
WT SsuD[a]	93 ± 5	1.9 ± 0.1
H228A SsuD	57 ± 2	0.54 ± 0.07
H11A SsuD	66 ± 3	2.1 ± 0.2
H333A SsuD	82 ± 2	1.8 ± 0.2
C54A SsuD[a]	16 ± 1	0.43 ± 0.08
R226A SsuD	ND[b]	ND
R226K SsuD	ND	ND
R226A SsuD with 100 mM Guanidine	1.26 ± 0.08	0.008 ± 0.002

[a] Values were obtained under current experimental conditions. Previously reported values were in 25 mM phosphate buffer.[25, 27]
[b] No activity detected

Table 2.2. pH independent steady-state kinetic parameters for wild-type SsuD and variants

H11A SsuD and "hump" in the k_{cat}/K_m pH profile for H228A SsuD suggested the presence of a sticky substrate with these variants (Figure 2.2). The H228A SsuD variant in particular appears to promote the dissociation of this ionizable group proton when octanesulfonate is present (*173*, *174*). Despite this intriguing result, the overall impact on SsuD activity as a result of the alanine substitutions to these positions was negligible. As a result, neither amino acid residue was considered essential to catalysis.

The upper pK_a value of 9.5 ± 0.1 for the pH dependence of k_{cat} for wild-type SsuD was consistent with the value for a cysteine residue within the active site (*171*, *173*). For C54A SsuD, the pH independent values for k_{cat} and k_{cat}/K_m correspond with the five-fold decrease in activity reported previously (Table 2.2) (*171*). The decrease in activity for C54A SsuD supports the possibility that Cys54 could be contributing to the upper pK_a value at 9.5 ± 0.1 for k_{cat}. Interestingly, the cysteine to alanine substitution resulted in the elimination of the upper pK_a value from the k_{cat} pH profile. The pH dependence of k_{cat} for C54A SsuD revealed only a single titratable group with an apparent pK_a value of 6.3 ± 0.1, and a single titratable group with an apparent pK_a value consistent to that of wild-type SsuD for the pH dependence of k_{cat}/K_m (Table 2.1). These pK_a values are apparent because the pH dependence data were fit to equation 2.1 for comparison with the values obtained for wild-type SsuD. However, "hollows" present in both the k_{cat} and k_{cat}/K_m pH profiles for C54A SsuD indicate the presence of a sticky proton in the enzyme-substrate complex (Figure 2.3C and D)(*173*, *174*). When fitted to equation 2.3, the k_{cat}/K_m pH profile for C54A SsuD revealed three pH dependent terms with values of 7.0 ± 0.5, 7.8 ± 0.2, and 6.0 ± 0.5. Similar pK_a values of 7.1 ± 0.7, 7.4 ± 0.6, and 5.8 ± 0.5 were also obtained for the k_{cat} pH profile. These results indicate that the cysteine to

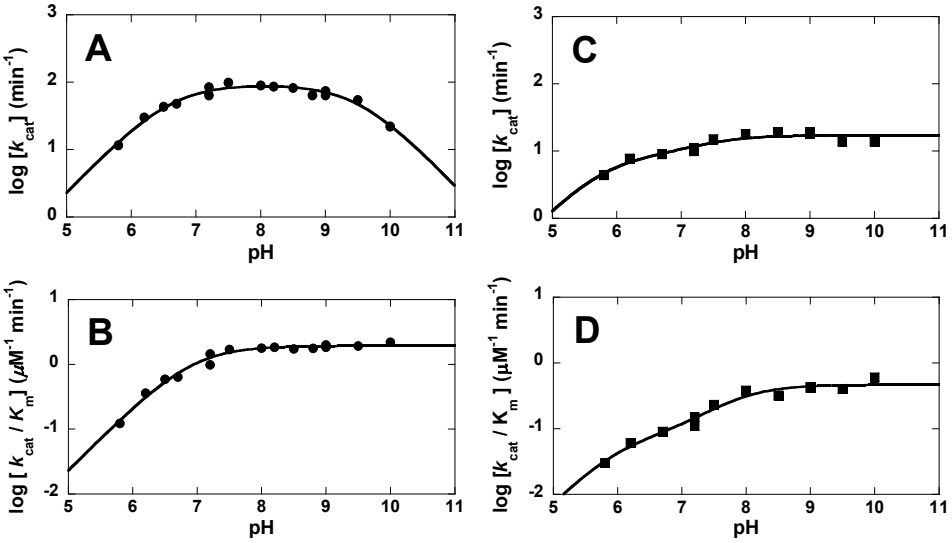

Figure 2.3. pH dependence of wild-type and C54A SsuD activity. Reactions were initiated by the addition of NADPH (500 μM) to a reaction mixture containing wild-type SsuD (0.2 μM), SsuE (0.6 μM), FMN (2 μM), and a range of octanesulfonate concentrations (10−5000 μM) in either 50 mM Bis-Tris (pH range of 5.8–7.2), 50 mM Tris-HCl (pH range of 7.2-9.0), or 50 mM glycine (pH range of 9.0-10.0) and 100 mM sodium chloride at 25°C. Due to decreased activity, reactions with C54A SsuD employed increased concentrations of C54A SsuD (1.2 μM), SsuE (3.6 μM), and FMN (5 μM). pH dependence of wild-type SsuD (●) A: k_{cat} values, B: k_{cat}/K_m values; pH dependence of C54A SsuD (■) C: k_{cat} values, D: k_{cat}/K_m values. Each point is the average of at least three separate experiments. Solid lines for A, B, C, and D are the fits of data to equation 2.2, equation 2.1, equation 2.3, and equation 2.3 respectively.

alanine substitution causes the proton associated with the ionizable group on the acidic limb of the pH profile to become sticky when octanesulfonate is present (*173*, *174*).

Despite arginine having a pK_a of 12.5 in free solution, the active-site residue, Arg226, was identified as a group potentially contributing to the pK_a value at 9.5 ± 0.1 for the pH dependence of k_{cat}. While current and previous experimental evidence dismissed the possibility of Cys54 serving as the active-site acid in SsuD, nearby Arg226 was found to be in close proximity to the pK_a value of an active-site arginine during catalysis (*171*, *173–177*). Interestingly, catalytic sulfite production was not detected over the pH range for those assays involving R226A or R226K SsuD, even at increased protein concentrations. The absorbance values at 412 nm for 2-nitro-5-benzoic acid production were similar to the absorbance values obtained in control experiments in the absence of enzyme. The absorbance values were below the detectable limit for sulfite of 4 μM. As a result, pH independent and dependent k_{cat} and k_{cat}/K_m values could not be determined for R226A or R226K SsuD. The lack of activity seen with these SsuD variants supports Arg226 as the active-site acid contributing to the upper pK_a value at 9.5 ± 0.1 for k_{cat}.

2.3.3 Substrate Binding Affinity

Fluorescent titrations were performed to determine if the lack of detectable activity was due to a disruption in substrate binding. To evaluate flavin binding, $FMNH_2$ was titrated into a sample of R226A or R226K SsuD and the spectra recorded with an excitation wavelength at 280 nm and emission intensity measurements at 344 nm. Each Arg226 SsuD variant had comparable K_d values for $FMNH_2$ binding as wild-type SsuD (1.49 ± 0.24 and 2.02 ± 0.25 μM for R226A or R226K SsuD, respectively) (Figure 2.4),

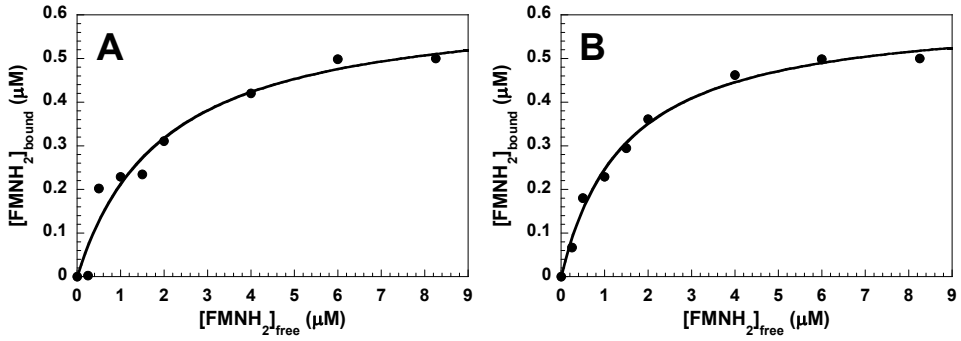

Figure 2.4. Emission intensity measurements at 344 nm were measured using an excitation wavelength at 280 nm. The change in the emission intensity at 344 nm following each addition of $FMNH_2$ was converted to the estimated concentration of bound $FMNH_2$ to SsuD (equation 2.4) and plotted against the concentration of free $FMNH_2$. A: The titration of R226A SsuD enzyme (0.5 μM) with $FMNH_2$ (0.26-8.26 μM). B: The titration of R226K SsuD enzyme (0.5 μM) with $FMNH_2$ (0.26-8.26 μM). The solid line in each plot represents the fit of the titration curve to equation 2.5. Each titration was performed in triplicate.

suggesting that substitution of the arginine residue to either lysine or alanine did not alter the binding affinity of $FMNH_2$ (*160*). Titrations were also performed to determine if there was a measurable change in the affinity for 1-octanesulfonate binding to the Arg226 SsuD variants with $FMNH_2$ bound. The K_d value for 1-octanesulfonate binding to each SsuD variant/$FMNH_2$ complex was 10.5 ± 1.1 and 20.1 ± 2.5 μM for R226A or R226K SsuD, respectively (Figure 2.5). These K_d values are comparable to the values obtained for wild-type SsuD (17.5 ± 0.9 μM) and suggest that substitution of the arginine residue to either lysine or alanine does not alter the binding of 1-octanesulfonate to the SsuD variant/$FMNH_2$ complex in fluorescent titrations (*160*). Therefore, the absence of activity in the Arg226 SsuD variants was not due to substantial changes in the binding affinity for $FMNH_2$ or 1-octanesulfonate.

2.3.4 Rapid Reaction Kinetic Analyses

The role of Arg226 in the desulfonation reaction was further evaluated through rapid reaction kinetic analyses to determine if modification of the flavin oxidation steps were responsible for the lack of activity observed with the Arg226 SsuD variants. The oxidation of $FMNH_2$ by R226A or R226K SsuD in the absence or presence of 1-octanesulfonate (10-500 μM) was monitored at 450 nm by stopped-flow kinetic analyses. The kinetic traces obtained at 450 nm for each variant represent the oxidation of reduced flavin (Figure 2.6A and B). The kinetic traces were best fit to a double exponential equation, and the rate constants obtained either with or without octanesulfonate were within error the same as the values obtained for wild-type SsuD (*160*). Additional studies were performed monitoring the oxidation of $FMNH_2$ by R226A or R226K SsuD in the

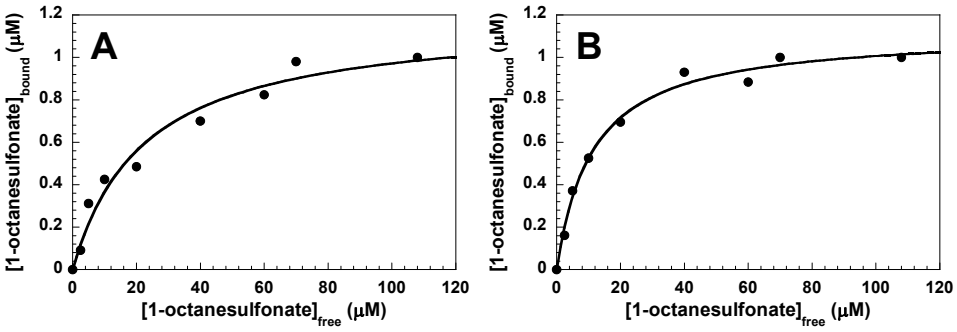

Figure 2.5. Emission intensity measurements at 344 nm were measured using an excitation wavelength at 280 nm. The change in the emission intensity at 344 nm following each addition of 1-octanesulfonate was converted to the estimated concentration of bound 1-octanesulfonate to SsuD-$FMNH_2$ enzyme complex (equation 2.4) and plotted against the concentration of free octanesulfonate. A: The titration of R226A SsuD-$FMNH_2$ enzyme complex. R226A SsuD (1 μM) was premixed with $FMNH_2$ (2 μM) and titrated with 1-octanesulfonate (0.25-108 μM). B: The titration of R226K SsuD-$FMNH_2$ enzyme complex. R226K SsuD (1 μM) was premixed with $FMNH_2$ (2 μM) and titrated with 1-octanesulfonate (0.25-108 μM). The solid line in each plot represents the fit of the titration curve to equation 2.5. Each titration was performed in triplicate.

absence or presence of 1-octanesulfonate (10-500 μM) at 370 nm (Figure 2.6A and B). The kinetic traces at 370 nm for R226A SsuD were best fit to a double-exponential equation with rate constants of 2.24 ± 0.10 s^{-1} (k_1) and 0.41 ± 0.03 s^{-1} (k_2) in the absence of octanesulfonate (Figure 2.6A, ●), and 1.90 ± 0.02 s^{-1} (k_1) and 0.40 ± 0.01 s^{-1} (k_2) with the addition of octanesulfonate (Figure 2.6A, ○). Kinetic traces at 370 nm for R297K SsuD were also best fit to a double-exponential equation with similar rate constants within error as R297A SsuD, 2.09 ± 0.03 s^{-1} (k_1) and 0.26 ± 0.01 s^{-1} (k_2) in the absence of octanesulfonate (Figure 2.6B, ●), and 2.14 ± 0.04 s^{-1} (k_1) and 0.27 ± 0.05 s^{-1} (k_2) with octanesulfonate included in the reaction (Figure 2.6B, ○). The rate constants were similar to the values obtained from the kinetic traces of the Arg226 SsuD variants monitored at 450 nm, indicating that the C4a-(hydro)peroxyflavin intermediate was never formed. The C4a-(hydro)peroxyflavin intermediate has an absorbance peak observable at 370 nm, but not at 450 nm (*160*). In kinetic traces of wild type SsuD at 370 nm in the absence and at low concentrations (<100 μM) of octanesulfonate an initial phase corresponding to the formation of the C4a-(hydro)peroxyflavin intermediate was previously observed (*160*). With the Arg226 SsuD variants, there was no initial phase identified at 370 nm, and the corresponding kinetic trace essentially overlaid with the normalized kinetic trace obtained at 450 nm (Figure 2.6). If the intermediate had formed, these two traces would not have overlaid because the ratio of the extinction coefficients at 370 nm and 450 nm for the C4a-(hydro)peroxyflavin intermediate is greater than the comparable ratio for fully oxidized flavin (*178*). Therefore, if the C4a-(hydro)peroxyflavin were generated in the first phase, the kinetic traces at 370 nm would appear similar to those observed for wild-type SsuD (*60*, *61*, *65*, *72*, *75*, *95*, *96*, *160*). The inability of R226A or R226K SsuD to

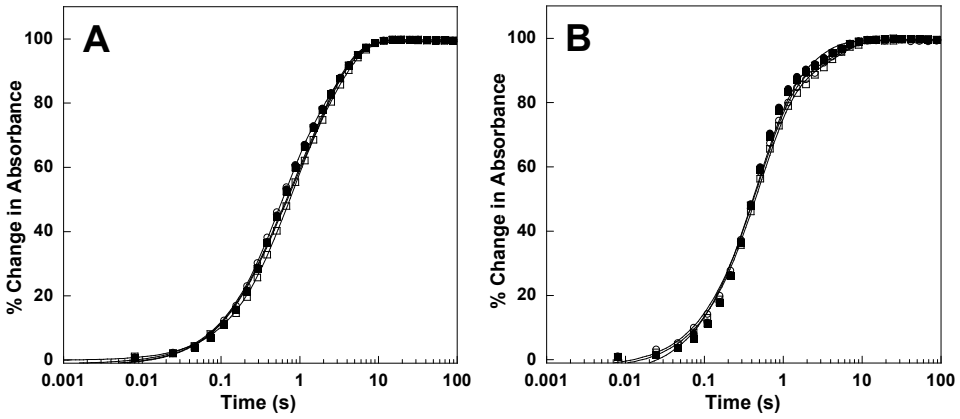

Figure 2.6. Kinetic Traces of flavin oxidation by R226A and R226K SsuD. Single turnover experiments were performed by stopped-flow kinetic analysis at 4 °C in 50 mM Tris-HCl, pH 8.5, and 100 mM sodium chloride. A: Single turnover kinetic traces were obtained after mixing free $FMNH_2$ (25 μM) with R226A SsuD (35 μM) in air-saturated buffer at 370 nm (●) and 450 nm (■), and after mixing free $FMNH_2$ (25 μM) with R226A SsuD (35 μM) and 1-octanesulfonate (100 μM) in air-saturated buffer at 370 nm (○) and 450 nm (□). B: The single turnover traces employ the same conditions described for 2.6A, but with R226K SsuD. The kinetic traces shown represent an average of three separate experiments. The solid lines are the fits of the kinetic traces to equation 2.6.

generate the C4a-(hydro)peroxyflavin intermediate correlates with the absence of activity in steady-state kinetic experiments and suggests the peroxyflavin does not accumulate to detectable levels during turnover.

2.3.5 Guanidinium rescue experiments

From a structural standpoint, the arginine to alanine mutation in the active site of SsuD is equivalent to the removal of a guanido moiety from the side chain of Arg226. The kinetic and biochemical properties that have been affected by such a mutation should be at least partially restored in the presence of exogenous guanidine (*95*, *179–181*). The effect of chemical rescue on the kinetic parameters of R226A SsuD was determined over the experimental pH range. Approximately 1.5% of the wild-type SsuD k_{cat} value was restored by the addition of 100 mM guanidine to the R226A SsuD assay (Table 2.2). The rescue of k_{cat} by guanidinium was pH independent which was attributed not only to free guanidinium cation (pK_a = 13.6) remaining protonated throughout the experimental pH range, but the outwards displacement of pK_a values relative to the wild-type enzyme beyond the experimental pH range. An outward shift, or broadening of pK_a values observed only in the k_{cat} pH profile is indicative of a non-pH dependent, but normally rate limiting, slow step following the catalytic reaction (*173–175*). The pH dependence of k_{cat}/K_m for guandinium rescue of R226A SsuD activity could not be determined due to absorbance values being below the detectable limit for sulfite production (4 μM) at low pH under assay conditions employing low concentrations of 1-octanesulfonate. The lack of activity seen with the lysine variant demonstrates that SsuD activity is not dependent simply on the charge associated with the Arg226 in the active site; the hydrogen bonding interactions of the guanido moiety of Arg226 are also of particular importance to SsuD

catalysis. The combination of low activity and the apparent displacement of pK_a values with the addition of guanidinium suggests Arg226 plays a role in the rate limiting product release step, potentially through mediation of a conformational change (*173–175*).

2.4 DISCUSSION

Similar active-site environments often promote diverse functionalities despite exhibiting nearly identical structural motifs. Although members of the bacterial luciferase superfamily share common structural motifs and some conserved amino acid sequence identities, the catalytic mechanisms employed by each enzyme appear to be quite distinct (*119*, *120*, *122*, *127–129*, *158*, *159*, *164–168*). In the mechanisms of bacterial luciferase and LadA, a histidine residue has been determined to serve as an active-site base in each of these enzymes (*120*, *127–129*, *158*, *164*, *166*, *167*). As a result, the conserved His228 amino acid residue of SsuD had been proposed to serve in this same capacity based on its similar structural orientation to the histidine active-site base in bacterial luciferase and LadA (*120*, *127–129*, *158*, *164*). To further probe the role of active site residues in catalysis, the pH dependence on the k_{cat} and k_{cat}/K_m values of SsuD and SsuE were determined in the pH range of 5.8-10.0. Experiments were limited to this pH range because SsuD reacts with many buffers as aminosulfonic acids are substrates of SsuD. Although previous kinetic parameters were established in potassium phosphate at pH 7.5, use of this buffer was abandoned after it was found to inhibit the SsuD reaction (*160*, *169*, *171*). As a result, Bis-Tris (pH range of 5.8–7.2), Tris-HCl (pH range of 7.2-9.0), and glycine (pH range of 9.0-10.0) were used to establish the kinetic parameters over these pH ranges.

The k_{cat}/K_m pH profile indicates the optimal protonation state of ionizable groups located on the free-enzyme and/or substrates in order for the reaction to commit to the first irreversible step of catalysis, while the pH dependence of k_{cat} reflects ionizable groups on the enzyme-substrate complex that are required for catalysis (*173*, *174*, *182*, *183*). Unlike the pH profile for k_{cat}/K_m, the k_{cat} pH profile reflects the necessary protonation state of groups necessary for catalysis to occur including product release. The k_{cat}/K_m pH profile for the SsuD reaction revealed a single titratable group with a pK_a value of 6.9 ± 0.1. Additionally, the wild-type SsuD pH profile of k_{cat} revealed a similar titratable pK_a value of 6.6 ± 0.1. Despite the differing pK_a values of 6.9 and 6.6 for the k_{cat}/K_m and k_{cat} profiles, respectively, these values likely represent the same group. The altered pK_a value could be the result of a change in the active-site environment upon the formation of the first enzyme-substrate complex where the pK_a value of the group is 6.9 before formation of the enzyme-substrate complex, but is perturbed to 6.6 upon binding of one or more of the substrates (*173*, *184*). Previous studies have indicated that the desulfonation reaction by SsuD occurs through an ordered binding mechanism where $FMNH_2$ must bind to the enzyme first, followed by either 1-octanesulfonate or O_2 (*160*). If the lower pK_a value represents the same group in both the k_{cat}/K_m and k_{cat} profiles, then it can be concluded that the deprotonated form of this group is necessary for both formation of the final enzyme-substrate complex and for catalysis. It is unlikely that this pK_a value can be attributed to the ionization of 1-octanesulfonate because of the relatively low pK_a value of the sulfonate group (*185*).

The pH dependence on the kinetic parameters of SsuD obtained from the current study identified a group with a pK_a consistent with a histidine residue to be essential for

catalysis. However, the present study failed to identify His228 or any other active-site histidine residue serving as an active-site base in the SsuD enzyme. This pK_a value was present in the pH profiles of all His and Cys variants with only minor perturbations in the value (Table 2.1). These minor perturbations were attributed to the presence of a sticky substrate (*173*, *174*). However, the presence of this sticky substrate had a negligible effect on the overall k_{cat}/K_m and k_{cat} pH independent values suggesting that while these amino acid residues may be involved in maintaining the active-site environment through minor substrate binding interactions, they are not critical to catalysis. Therefore, the pH profiles for H228A, H11A, H333A, and Cys54 SsuD confirm that neither of these amino acid residues is contributing solely to this lower pK_a value and that the group responsible for this ionization has yet to be identified.

Previously, deuterium kinetic isotope studies on bacterial luciferase indicated that the N1 position of $FMNH_2$ (pK_a = 6.2) contributes a comparable lower pK_a value of 6.9 (*125*). It is possible the N1 position of $FMNH_2$ is contributing to the lower pK_a value in SsuD as well: as is the case with bacterial luciferase, either the protonated species of $FMNH_2$ does not bind or does not form the C4a-(hydro)peroxyflavin at a significant rate (*125*). An interesting observation was the identification of a "hollow" from fits of the C54A SsuD k_{cat}/K_m and k_{cat} profiles indicating the presence of a sticky proton in the enzyme-substrate complex (*173*, *174*). This "hollow" indicates octanesulfonate dissociates faster than the ionizable proton in the C54A SsuD variant (*173*, *174*). Previously, the formation of the C4a-(hydro)peroxyflavin intermediate has been shown to be stabilized by the presence of Cys54 in SsuD and Cys106 in bacterial luciferase (*122*, *124*, *171*). In the three dimensional structure of bacterial luciferase, Cys106 is directly

interacting with bound FMN (*120*). If the N1 position of $FMNH_2$ is responsible for the lower pK_a value in SsuD, then the observed hollow on the acidic limb of the pH profile indicates Cys54 would be required for the rapid dissociation of the N1 proton from $FMNH_2$ when octanesulfonate is present (*173*, *174*). In this model, rapid dissociation of the N1 proton would be required for the C4a-(hydro)peroxyflavin intermediate to form at a significant rate (*125*). Therefore, these combined results indicate Cys54 of SsuD directly interacts with the C4a-(hydro)peroxyflavin intermediate and promotes its formation by facilitating the dissociation of the proton located at the N1 position of $FMNH_2$.

A conserved but previously uncharacterized arginine residue within the active site, Arg226, was determined to serve a crucial role in SsuD catalysis. Alanine and lysine substitutions to the 226 position of SsuD resulted in complete inactivation of the enzyme. Therefore, the pH dependence on the kinetic parameters of R226A and R226K SsuD could not be determined as neither variant could catalyze detectable levels of sulfite production. The similar substrate affinities of R226A and R226K SsuD to wild type ruled out that substrate binding is altered from these substitutions. Although substrate binding was not affected, there was no observable formation of the C4a-(hydro)peroxyflavin intermediate in rapid reaction kinetic studies (*160*). Kinetic traces at 370 nm obtained for the oxidation of $FMNH_2$ with R226A and R226K SsuD in the absence of octanesulfonate substrate were fitted to a double-exponential equation (equation 2.6). There was no phase (k_1) correlating with the formation of the C4a-(hydro)peroxyflavin intermediate as was previously observed with wild-type SsuD in stopped-flow kinetic studies (*160*). In addition, there was no dependence on k_2 with increasing octanesulfonate concentrations

as previously observed with wild-type SsuD (*160*). The inability of the C4a-(hydro)peroxyflavin intermediate to be generated correlates with the lack of activity for the Arg226 SsuD variants.

In considering the proposed catalytic mechanism for SsuD in combination with the results of the present study, it is reasonable to conclude that Arg226 could possess multiple functions. Positively charged groups, such as an arginine, are highly conserved near the active site of Baeyer-Villiger flavin monooxygenases in order to stabilize peroxyflavin intermediates (*65*, *94*, *104*). The absence of this positively charged stabilizing group near the active site can lead to inactivation of the enzyme due to destabilization of the flavin intermediate. The absence of activity even with the lysine substitution of Arg226 is likely due to an altered position of the positive charge resulting in the inability of this variant to stabilize the C4a-(hydro)peroxyflavin intermediate. Based on the results from the chemical rescue experiments with guanidine, the orientation of and chemical properties associated with the guanido functional group of Arg226 are as crucial to catalysis as its charge. Product release also appears to be affected by the addition of guanidine, given that the recovery of wild-type SsuD k_{cat} is pH independent. This pH independence is likely due to the outwards displacement of pK_a values beyond the experimental pH range, suggesting that while the free guanidinium ion rescues catalytic activity in R226A SsuD, product release remains compromised (*173*–*175*). An active site acid has been proposed to play a role in the SsuD mechanism by protonating the $FMNO^-$ intermediate leading to the release of H_2O and the FMN product through a conformational change (*128*, *129*, *148*, *155*, *159*, *160*, *169*). In the proposed chemical mechanism for SsuD, protonation of the $FMNO^-$ intermediate by the catalytic

acid would be the step prior to product release. If Arg226 is the catalytic acid, and the guanidinium ion is serving the role of this catalytic acid in the R226A SsuD variant, then the product release step could potentially be a limiting factor in guanidinium's ability to rescue k_{cat}. Although exogenous guanidine may be able to compensate for some of the steric and electrostatic interactions normally attributed to Arg226, the guanidinium moiety would be less effective in transferring a proton to the $FMNO^-$ intermediate and signaling the proposed conformational change linked to product release. These combined results support Arg226 playing a dual role in SsuD catalysis by facilitating oxygen activation through stabilization of the C4a-(hydro)peroxyflavin intermediate and by promoting product release through a conformational change associated with protonation of the $FMNO^-$ intermediate.

Experimental results from studies performed on Cys54 SsuD provided support for Arg226 as the active site acid in the SsuD chemical reaction. The protonated form of Cys54 with a pK_a in the free enzyme of 9.3 ± 0.1 was previously shown to be involved in stabilizing the C4a-(hydro)peroxyflavin in SsuD either through direct interactions with the flavin or in helping to maintain the active site environment, but not playing a direct role in SsuD catalysis as the active-site acid (Figure 2.1) (*171*). However, the substitution of Cys54 SsuD with Ala resulted in the elimination of the upper pK_a from the k_{cat} pH profile (Figure 2.3C). Although these combined results indicate Cys54 is contributing to the upper pK_a in the wild-type enzyme, the modest five-fold drop in the k_{cat} and k_{cat}/K_m values compared to wild-type SsuD does not support Cys54 as the catalytic acid (Table 2.1). Two possible models would support the apparent disappearance of the upper pK_a: the pK_a value at 9.5 corresponds to Cys54, and there is a second pK_a value in the wild-

type enzyme occurring outside the experimental pH range corresponding to the catalytic acid; or the pK_a value at 9.5 corresponds to the catalytic acid, and the cysteine to alanine substitution resulted in a shift of this pK_a value to a value outside of the experimental pH range. Both models suggest that Cys54 participates in a step occurring after the first irreversible step through product release, and support Arg226 playing the role of the catalytic acid. Additionally, the cysteine to alanine substitution resulted in the outwards displacement of the lower apparent pK_a value in the k_{cat} pH profile when compared to wild-type SsuD but did not affect the apparent pK_a value seen in the k_{cat}/K_m pH profile (Table 2.1). An outward shift of pK_a values observed only in the k_{cat} pH profile is indicative of a non-pH dependent, but normally rate limiting, slow step following the catalytic reaction (*173–175*). Since the outward pK_a shifts are only present on the pH dependence of k_{cat} for C54A SsuD, the results suggest the rate of product release is slowed by the Cys to Ala substitution (*173–175*). Previous studies have demonstrated that a combination of electrostatic and hydrogen bonding interactions can perturb the pK_a values (≥ 2 units) of catalytic groups in an enzyme active site (*176*). Such studies indicate that the pK_a of an arginine group could be perturbed within the active site of an enzyme through a complex hydrogen bonding network (*173–177*). Considering both Cys54 and Arg226 have been linked to stabilization of the C4a-hydroperoxyflavin intermediate, it would be reasonable to conclude a direct or indirect interaction between the two amino acid side chains. Therefore, the data support the possibility that Cys54 is involved in altering the pK_a of Arg226 from a more typical value of 12.5 to 9.5 during catalysis. This result combined with the absence of detectable SsuD catalytic activity in the SsuD arginine variants, suggest that Arg226 is contributing to the pK_a value at 9.5 ± 0.1 for

wild-type SsuD. Additionally, at least some $FMNO^-$ intermediate must be forming in the reaction with C54A SsuD to account for the catalytic activity of the variant. In this case, the catalytic acid would be required for the protonation of any $FMNO^-$ intermediate that is able to form despite the compromised active site environment (Scheme 2.2, IV). Therefore, it is proposed that Arg226 must be present in order to stabilize the peroxyflavin intermediate and promote product release through a conformational change linked to the protonation of the $FMNO^-$ intermediate.

Similarities between the sequences and three-dimensional structures of related enzymes can offer key insight as to the identity of important groups in catalysis for a particular enzyme. These similarities are evident between the well-characterized bacterial luciferase and the more recently characterized SsuD and LadA two-component monooxygenases. Nevertheless, the present study serves as an example of the different roles conserved groups can play in the mechanisms of such enzymes. The amino acids His44 and His311 were reported to serve as active-site bases in the mechanisms of bacterial luciferase and LadA, respectively (*119*, *120*, *122*, *124*, *127–129*, *158*, *159*, *164–168*). However, results from the characterization of His228 SsuD determined this active-site histidine is not playing this role in SsuD catalysis. Instead, pH dependence studies, steady-state kinetic studies, and single-turnover rapid-reaction kinetic studies highlighted Arg226 to be playing a crucial role as the potential active-site acid in SsuD catalysis. These results are consistent with our proposed mechanism in that conserved arginine residues near the active-site are often crucial players in the mechanisms of Baeyer-Villiger flavin monooxygenases (*65*, *94*, *104*). These results provide an important foundation in the illumination of the SsuD catalytic mechanism. Future studies involving

deuterium solvent isotope effects, kinetic isotope effects, and an expanded characterization of nearby, but previously uncharacterized residues will undoubtedly offer a much clearer window into the intricacies of SsuD catalysis.

The work presented in this chapter was published previously in reference (186).

CHAPTER THREE

Steady-State Kinetic Isotope Effects Support Complex Role of Arg226 in Proposed Desulfonation Mechanism of the Two-Component Alkanesulfonate Monooxygenase System

3.1 INTRODUCTION

Isotope effects are valuable tools for the evaluation of kinetic mechanisms associated with enzyme-catalyzed reactions. Techniques employing isotopically-labeled solvents and substrates have been shown to distinguish several features of an enzyme's mechanism including, but not limited to, the rate-limiting bond-breaking step(s), the commitments to catalysis, the groups directly involved in catalysis, and any conformational change(s) associated with the enzymatic reaction. Kinetic isotope techniques utilizing deuterium have been demonstrated to be particularly useful in identifying enzyme mechanisms promoting acid-base catalysis. In many reactions dependent on acid-base catalysis, the proton transfer step is rate-limiting and can be affected by substituting a deuterium in place of the proton being transferred. The two-component flavin-dependent alkanesulfonate monooxygenase enzyme (SsuD) has been proposed to promote the oxygenolytic cleavage of a carbon-sulfur bond from sulfonated substrates to yield aldehyde and bioavailable sulfite through acid-base catalysis. Despite extensive investigations however, the details of the catalytic mechanism employed by the

alkanesulfonate monooxygenase system remain an enigma (*107*, *160*, *169*, *171*). As a result, deuterium isotope effect studies were performed for SsuD in an effort to further resolve key steps involved in the proposed catalytic mechanism.

In *Escherichia coli*, SsuD is expressed when sulfate becomes limiting. The limitation induces the synthesis of a set of proteins involved in acquiring sulfur from alternative sources, primarily alkanesulfonates (*107*, *129*, *150*, *170*). The two-component alkanesulfonate monooxygenase system is comprised of a flavin reductase (SsuE) that supplies reduced flavin to SsuD and enables the organism to utilize a broad range of alkanesulfonates as alternative sulfur sources (*107*, *129*, *170*). Unlike a traditional flavin monooxygenase where both oxidative and reductive half reactions occur on the same enzyme, only the oxidative half reaction is catalyzed by SsuD. The $FMNH_2$-bound SsuD then activates dioxygen and cleaves the carbon-sulfur bond of alkanesulfonates releasing sulfite and the corresponding aldehyde (Scheme 3.1) (*107*, *160*).

In the SsuD reaction, a C4a-peroxyflavin intermediate is proposed to perform a nucleophilic attack on the sulfur atom of the alkanesulfonate substrate (Scheme 3.1, I). The resulting intermediate then undergoes a Baeyer-Villiger rearrangement leading to the cleavage of the alkanesulfonate carbon-sulfur bond and the generation of sulfite and an alkane peroxyflavin intermediate (Scheme 3.1, II). The release of the aldehyde product from the enzyme occurs following abstraction of a proton from the alkane peroxyflavin intermediate by a catalytic base (Scheme 3.1, III). The abstraction of the α-proton from the alkane peroxyflavin intermediate has been proposed as one of several potential rate-limiting chemical steps in SsuD catalysis. Therefore, substitution of the α-protons

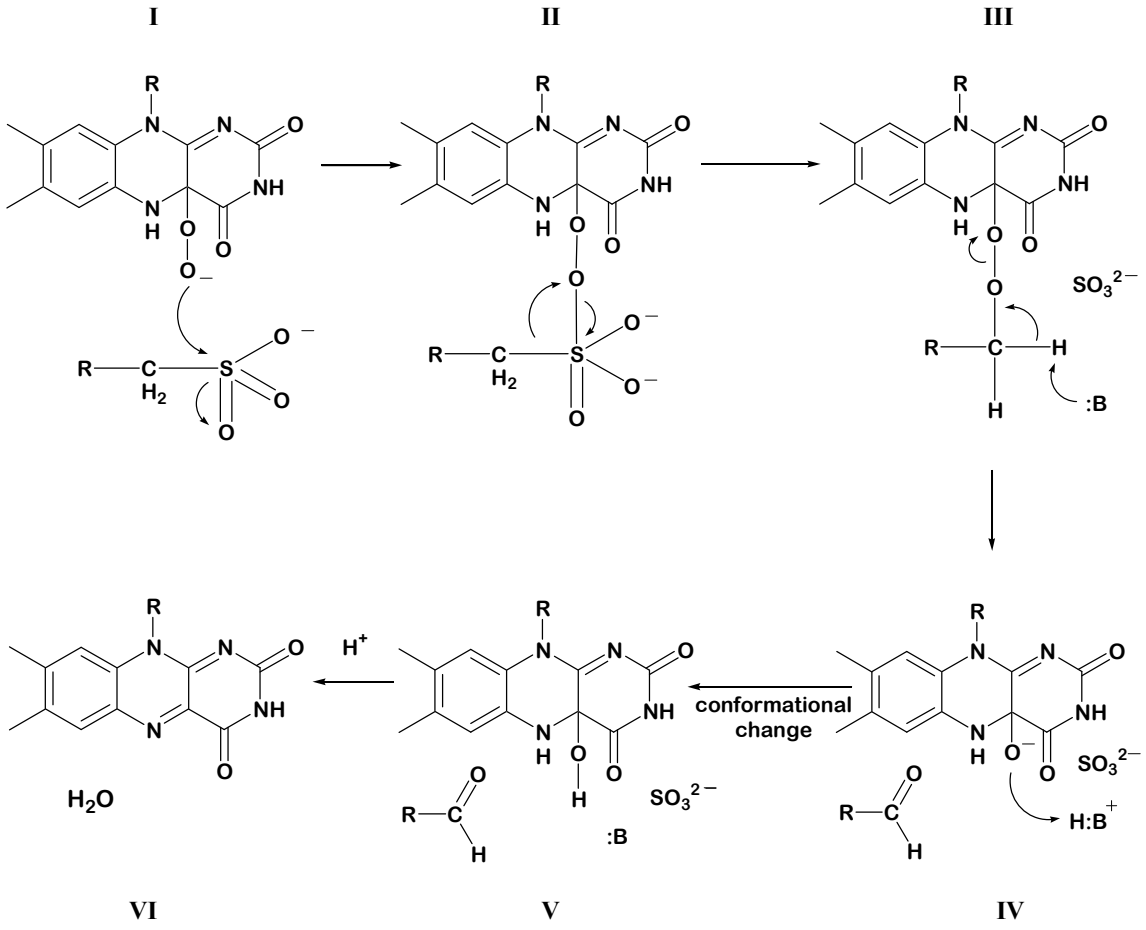

Scheme 3.1. Detailed catalytic mechanism of SsuD catalysis

of octanesulfonate with deuterium should result in a kinetic isotope effect on the proton abstraction step (Scheme 3.1, III). Additionally, results from previous studies have indicated Arg226 playing the role of the active-site acid in the SsuD reaction (*186*). Arg226 has been proposed to donate a proton to the $FMNO^-$ intermediate triggering a proposed conformational change that opens the enzyme to solvation and promotes product release (Scheme 3.1, IV). The reprotonation step should be susceptible to solvent deuterium kinetic isotope effect studies. Therefore, both solvent and kinetic isotope effect studies were performed in order to define the proton transfer steps involved in the SsuD reaction.

3.2 EXPERIMENTAL PROCEDURES

3.2.1 Materials

Potassium phosphate (monobasic and dibasic), flavin mononucleotide phosphate (FMN), reduced nicotinamide adenine dinucleotide phosphate (NADPH), Trizma base, Bis–Tris, glycine, ammonium sulfate, ampicillin, ethylenediaminetetraacetic acid (EDTA), dimethyl sulfoxide (DMSO), streptomycin sulfate, glucose, glucose oxidase, 5,5-dithiobis(2-nitrobenzoic acid) (DTNB), 1-butanesulfonate, 4-pyridineethanesulfonic acid, and lysozyme were purchased from Sigma (St. Louis, MO). Isopropyl-β-D-thiogalactoside (IPTG), sodium chloride, and glycerol were obtained from Fisher Biotech (Pittsburgh, PA). 1-octanesulfonate and dithiothreitol (DTT) were purchased from Fluka (Milwaukee, WI). Deuterium oxide (D_2O), deuterium chloride, and sodium deuteroxide were purchased from Cambridge Isotope Laboratories, Inc (Andover, MA). 1-bromooctane-1,1-d_2 was purchased from CDN Isotopes (Quebec, Canada). Expression and purification of recombinant SsuD and SsuE was performed as previously described (*155*). The concentrations of SsuD and SsuE proteins were determined from A_{280} measurements using a molar extinction coefficient of 47.9 mM^{-1} cm^{-1} and 20.3 mM^{-1} cm^{-1}, respectively (*155*).

3.2.2 Synthesis of 1-octanesulfonate-1,1-d_2

The synthesis of 1-octanesulfonate-1,1-d_2 was performed as previously described with the following modifications (*187*). A solution of sodium sulfite (13.5 mmol, 1.69 g) in 12.5 ml water was slowly added to a refluxing solution of 1-bromoctane-1,1-d_2 (12 mmol, 2.32 g) in ethanol/water (75 mL/12.5 mL). After a reaction time of 48 h, the solution was cooled to room temperature, and the precipitate was removed. The remaining ethanol/water mixture was removed by evaporation, and the resulting precipitate was extracted six times with 25 mL pentane. The remaining solid was re-crystallized from ethanol three times to give 0.47 g (2.0 mmol; 16.7 %). The product was identified by ^{1}H NMR. The chemical shifts obtained for the octanesulfonate ion in DMSO-d_6, OS^-: 3.38 (d, 2H); 1.60 (apparent quintet, 2H); 1.25 (m, 10H); 0.85 (t, 3H). The chemical shifts obtained for the octanesulfonate ion, 1-octanesulfonate-1,1-d_2: 1.7 (apparent t, 2H); 1.25 (m, 10H); 0.85 (t, 3H). The absence of the chemical shift at OS^- (1): 3.38 (d, 2H) for 1-octanesulfonate-1,1-d_2 was used to estimate the degree of deuteration to be over ninety percent.

3.2.3 Dependence of Kinetic Parameters on pL

The activity of SsuD was routinely assayed at 25° C as previously described. Reactions employed a range of 1-octanesulfonate, 1-octanesulfonate-1,1-d_2, 1-butanesulfonate, or 4-pyridineethanesulfonic acid (10−5000 μM) in either 50 mM Bis-Tris (pL range of 5.8–7.2), 50 mM Tris-HCl (pL range of 7.2-9.0), or 50 mM glycine (pL range of 9.0-10.0) with the following modifications (*129*, *160*). Each buffered solution was supplemented with 100 mM sodium chloride to maintain the ionic strength, and overlapping assays were performed in Bis-Tris and Tris-HCl at pL 7.2 and in Tris-HCl

and glycine at pL 9.0 in order to ensure activity was independent of the buffer used. When performing the viscosity experiments, assays were also supplemented with 9% glycerol. All assays were performed in triplicate, and steady-state kinetic parameters were determined by fitting the data to the Michaelis-Menten equation. The pL dependence of k_{cat} and $k_{cat}/K_{[octanesulfonate]}$, $k_{cat}/K_{[butanesulfonate]}$, $k_{cat}/K_{[pyridineeethanesulfonate]}$ were best fit to a single ionization (equation 3.1) model and double ionization (equation 3.2) model, respectively:

$$\log y = \log\left[C / \left(1 + \frac{H}{K_1} \right) \right] \qquad \text{(equation 3.1)}$$

$$\log y = \log\left[C / \left(1 + \frac{H}{K_1} + \frac{K_2}{H} \right) \right] \qquad \text{(equation 3.2)}$$

where H is $[H^+]$, y is k_{cat} or $k_{cat}/K_{[octanesulfonate]}$, C is the pH independent value of y, and K_1, K_2, and K_3 represent the dissociation constant for groups on the SsuD-$FMNH_2$ complex. Both SsuD and SsuE were found previously to be stable throughout the pH range (*186*). The activity of SsuE was determined previously to be pH independent (*186*).

In order to determine the effect of deuterium oxide on the kinetic parameters of SsuD, modifications were made to the standard activity assay. The reaction mixtures were prepared with 99.8% D_2O. Buffer salts were dissolved in D_2O and adjusted with DCl or NaOD to the appropriate pH value (where pD is equal to the pH meter reading + 0.4). Anhydrous FMN, NADPH, SsuD (20 μM), SsuE (60 μM), 1-octanesulfonate, and 1-octansulfonate-1,1-d_2 were suspended in 50 mM Tris-DCl, 100 mM NaCl at pD 7.5. Steady-state kinetic parameters were determined by fitting the resulting plots to the Michaelis-Menten equation, and solvent isotope effects at a given pL were calculated as the ratio of k_{cat} and $k_{cat}/K_{[octanesulfonate]}$ values in H_2O to those in 99.8% D_2O.

For proton inventory measurements, assays were performed as previously described over the experimental pL range. For each pL, the different deuterium fractions (n = 0 to 0.998) were achieved by combining varying volumes of H_2O and D_2O buffers as previously described (*188*). The pH dependence of wild-type SsuD was determined over the pL range in the buffered solutions containing varying isotopic fractions of deuterium. Assays were performed as previously described in triplicate, and steady-state kinetic parameters were determined by fitting the data to the Michaelis-Menten equation (*186*). The pL dependence of k_{cat} and $k_{cat}/K_{m[octanesulfonate]}$ for each isotopic fraction of deuterium were best fit to a single ionization model (equation 3.1) and double ionization model (equation 3.2), respectively. The pH independent kinetic parameters for SsuD in each deuterium fraction concentration (n = 0, 0.124, 0.247, 0.372, 0.495, 0.619, 0.743, 0.870, 0.998) were obtained from these assays, plotted against deuterium fraction n, and best fit to a dome-shaped curve using the following variation of the Gross-Butler equation:

$$k_n = k_o(1 - n + n\phi^T)Z_k^n \qquad \text{(equation 3.3)}$$

where k_n is k_{cat} in mixed isotopic solvent with deuterium atom fraction n, k_o is k_{cat} in the absence of deuterated solvent, ϕ^T is transition state contribution to the isotope effect, and Z_k is medium effect contribution (*188–190*).

3.2.4 Data Analysis

The upper pK_a value for the pD dependence of k_{cat} was determined by the following method: the upper pK_a value for each fraction of D_2O was determined from their respective pL profiles. The [H^+] was calculated for each of these pK_a values and then plotted against deuterium fraction n. The resulting scatter was best fit to a line ($y = mn + z$), where y is the K_a at deuterium fraction n, z is the K_a in pure H_2O, and m is the

slope of the line. The slope m was determined by linear regression, and the K_a at n = 0.998 was calculated.

3.3 RESULTS

3.3.1 Substrate Kinetic Isotope Effects on steady-state kinetic parameters

The kinetic parameters for the wild-type enzyme were established with 1-octanesulfonate-1,1-d_2 as a substrate and plotted as a function of pH from pH 5.8-10.0 to probe the presence of a deuterium kinetic isotope effect on the proposed proton abstraction step (Scheme 3.1, III). SsuD with 1-octanesulfonate-1,1-d_2 showed optimal catalytic activity between pH 7.5-9.5 where the pH independent value was found to be 31 ± 2 min^{-1} for k_{cat}, and 1.9 ± 0.3 μM^{-1} min^{-1} for $k_{cat}/K_{[octanesulfonate]}$ (Figure 3.1A and 3.1B). These pH independent values were compared with those obtained with wild-type SsuD with unlabeled octanesulfonate to reveal a kinetic isotope effect (k_H/k_D) equal to 3.0 ± 0.2 for k_{cat} and 1.0 ± 0.2 for $k_{cat}/K_{[octanesulfonate]}$ (*186*). The pH dependence of k_{cat} for SsuD with deuterated substrate revealed a single titratable residue with a pK_a value of 6.3 ± 0.1 (Table 3.1). The pH dependence of $k_{cat}/K_{[octanesulfonate]}$ with labeled substrate revealed a single titratable amino acid group with a pK_a value of 7.1 ± 0.2. This pK_a value and the pH independent value were consistent with those for the unlabeled substrate indicating that the deuterated substrate had no effect on the $k_{cat}/K_{[octanesulfonate]}$ for SsuD.

3.3.2 Solvent Isotope Effects on steady-state kinetic parameters

The kinetic parameters for the wild-type enzyme were established in 99.8% D_2O and plotted as a function of pD from pD 5.8-10.0 to probe the presence of a deuterium kinetic isotope effect on the proposed catalytic-acid mediated reprotonation step (Scheme

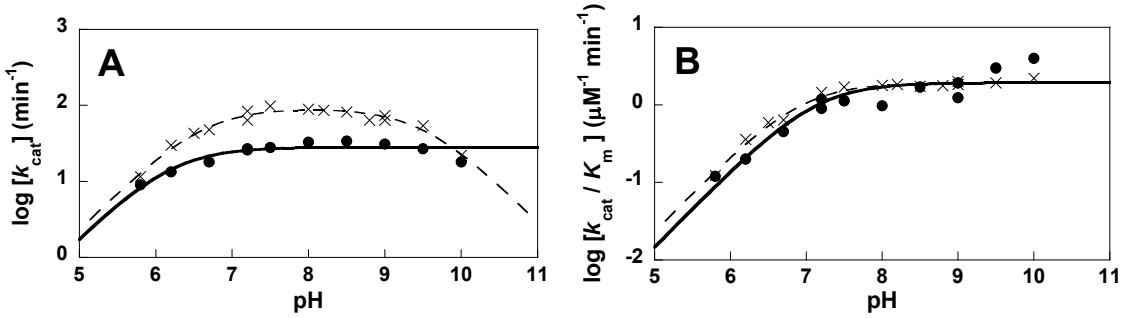

Figure 3.1. pH dependence of SsuD activity at 25°C. Reactions were initiated by the addition of NADPH (500 μM) into a reaction mixture containing SsuD (0.2 μM), SsuE (0.6 μM), FMN (2 μM), and a range of labeled 1-octanesulfonate-1,1-d_2 concentrations (10−5000 μM) in either 50 mM Bis-Tris (pL range of 5.8–7.2), 50 mM Tris-HCl (pL range of 7.2-9.0), or 50 mM glycine (pL range of 9.0-10.0) and 100 mM sodium chloride. A: k_{cat} and B: $k_{cat}/K_{[octanesulfonate]}$ values for SsuD in H_2O (●). The corresponding kinetic parameters for SsuD supplemented with unlabeled 1-octanesulfonate and H_2O (×) were included in each plot as a reference. Each point is the average of at least three separate experiments

3.1, IV). SsuD showed optimal catalytic activity in D_2O between pH 8.5-10.0 where the pH independent value was found to be 123 ± 3 min^{-1} for k_{cat}, and 2.0 ± 0.1 μM^{-1} min^{-1} for $k_{cat}/K_{[octanesulfonate]}$ (Table 3.2). These pD independent values were compared with those obtained with wild-type SsuD in H_2O to reveal a solvent isotope effect ($^{H2O}k/^{D2O}k$) equal to 0.75 ± 0.04 for k_{cat} and 0.95 ± 0.07 for $k_{cat}/K_{[octanesulfonate]}$ (*186*). While no isotope effect on k_{cat} was observed from pL 5.8-7.5, an inverse isotope effect was observed from pL 8.0-10.0 (Figure 3.2A). The isotope effect on k_{cat} increased with increasing pH with a maximum $^{H2O}k/^{D2O}k$ value equal to 0.25 ± 0.02 occurring at pL 10.0. There was no isotope effect observed on $k_{cat}/K_{[octanesulfonate]}$ at any pL (Figure 3.2B). The inverse isotope effect on k_{cat} indicates that deuteration only affects a catalytic step occurring after the first irreversible step in catalysis up through product release (*173*, *174*, *189*).

The resulting pD dependence of SsuD obtained in 99.8% D_2O was compared to the pH dependence previously obtained in H_2O (*186*). The pD dependence of k_{cat} revealed a single titratable amino acid residue with pK_a value of 6.8 ± 0.1 (Table 3.1). While this single pK_a value measured in 99.8% D_2O exhibits a small ΔpK_a value of 0.2 when compared to the lower pK_a value obtained in H_2O, the absence of the upper pK_a value integral to its H_2O counterpart suggests a substantial shift of this pK_a value in D_2O outside of the experimental pL range (Figure 3.2A) (*173*, *188–190*). It was determined from the proton inventory measurements, however, that the value of the upper pK_a value for k_{cat} in D_2O was 10.1 ± 0.2 (Figure 3.3). This pK_a value would fall into the normal limit for an isotope effect on ionization of a catalytic group (ΔpK_a value = 0.4-0.6 units) (*188–190*). The pD dependence of $k_{cat}/K_{[octanesulfonate]}$ revealed a single titratable

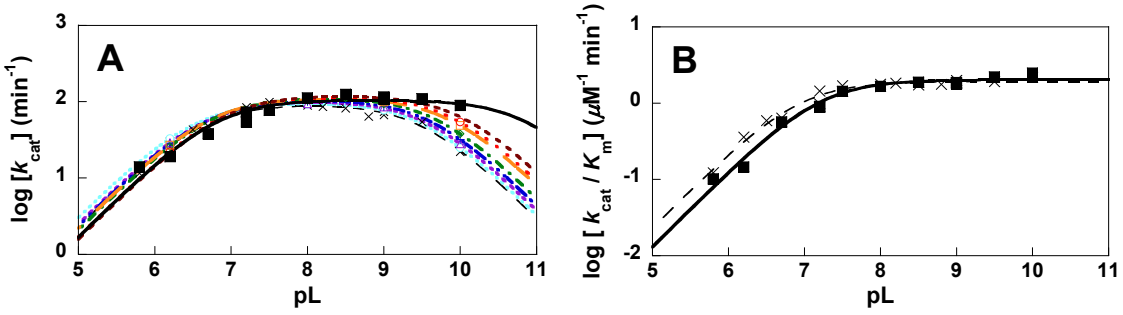

Figure 3.2. pH dependence of A: k_{cat} and B: $k_{cat}/K_{[octanesulfonate]}$ values for SsuD at 25°C supplemented with 0.00 % (×), 12.4 % (—), 24.7 % (—), 37.2 % (—), 49.5 % (—), 61.9 % (—), 74.3 % (—), 87.0 % (—), and 99.8 % (■) D_2O. Reactions were initiated by the addition of NADPH (500 μM) into a reaction mixture containing SsuD (0.2 μM), SsuE (0.6 μM), FMN (2 μM), and a range of unlabeled octanesulfonate concentrations (10−5000 μM) in either 50 mM Bis-Tris (pL range of 5.8–7.2), 50 mM Tris-HCl (pL range of 7.2-9.0), or 50 mM glycine (pL range of 9.0-10.0) and 100 mM sodium chloride. The corresponding kinetic parameters for the SsuD reaction supplemented with unlabeled octanesulfonate and H_2O (×) was included in each plot as a reference. The corresponding kinetic parameters for the SsuD reaction supplemented with unlabelled 1-octanesulfonate and H_2O (×) were included in each plot as a reference. Each point is the average of at least three separate experiments.

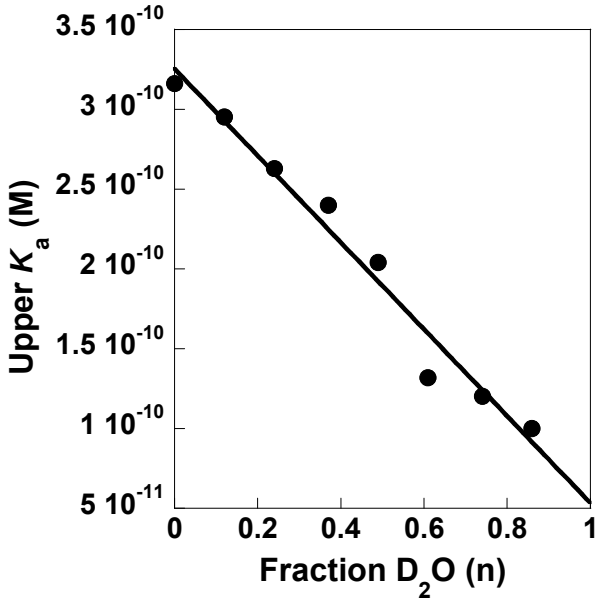

Figure 3.3. Plot of the upper K_a value vs. fraction of D_2O (n). Upper K_a values were determined from respective pL profiles (Figure 3.2A). The upper pK_a for SsuD in 99.8% D_2O was determined by calculating the K_a at $n = 0.998$.

amino acid group with an apparent pK_a value of 7.3 ± 0.1, exhibiting a normal ΔpK_a value of 0.4 when compared to the value obtained in H_2O (*186*, *188–190*).

3.3.3 Proton Inventory Measurements

Proton inventories were conducted in an effort to determine the number and nature of the hydrogenic sites involved in the inverse isotope effect on k_{cat}. Due to the difference in pL optimums for k_{cat} in H_2O (pH 7.2-8.5) compared to D_2O (8.0-9.5), a clear pL independent value necessary to perform a proton inventory could not be identified. As a result, the pL dependence of SsuD was determined for various fractions of D_2O (Figure 3.2A). From these pL dependencies, the pL independent values of k_{cat} and $k_{cat}/K_{[octanesulfonate]}$ for SsuD were determined and used to obtain an accurate proton inventory for each catalytic parameter. Inventory curves were obtained by plotting the pH independent values of k_{cat} and $k_{cat}/K_{[octanesulfonate]}$ as a function of the fraction of D_2O (n = 0 to 99.8%) present in the activity assays. While proton inventories for $k_{cat}/K_{[octanesulfonate]}$ did not demonstrate any curvature and were consistent with plots representing residual error due to the absence of an SIE (data not shown), the proton inventories for k_{cat} at each pL were best described as inverse and dome-shaped or bulging upward (Figure 3.4). Dome-shaped proton inventory curves indicate the presence of offsetting normal and inverse contributions to the overall solvent isotope effect (*182*, *183*, *188–193*). Values of $\phi^T = 0.53 \pm 0.03$ and $Z_k = 2.46 \pm 0.10$ were extrapolated from the proton inventory curve after fitting the data to the best-fit form of the Gross-Butler equation (equation 3.3). Therefore, the results suggest a normal transition state contribution offset by a large

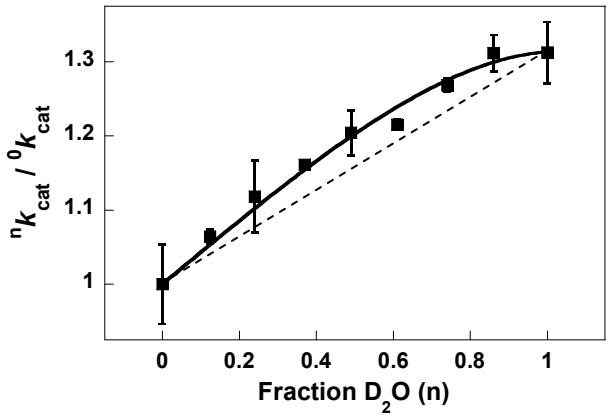

Figure 3.4. Proton inventory on the k_{cat} kinetic parameter. The ratio of k_{cat} in the fraction n of 99.8% D_2O ($^{n}k_{cat}$) to that in 100% H_2O ($^{0}k_{cat}$) plotted as a function of the mole fraction of 99.8% D_2O in the reaction. Each point is the average of at least four separate experiments. The dashed line is theoretical for a linear proton inventory.

inverse medium effect. Proton inventories of the catalytic parameters of SsuD employing 1-octanesulfonate-1,1-d_2 were indistinguishable from those employing unlabeled octanesulfonate.

3.3.4 Dependence of kinetic parameters of SsuD on viscosity

Due to the higher viscosity of D_2O compared to H_2O, activity assays were conducted over the experimental pH range in buffers supplemented with 9% glycerol in order to determine the effect of viscosity on the kinetic parameters of SsuD. It has been demonstrated previously that the viscosity of D_2O is comparable to a solution supplemented with 9% glycerol (*183*, *194–196*). The resulting viscosity dependences of the k_{cat} and $k_{cat}/K_{[octanesulfonate]}$ values for SsuD were compared to those values obtained for pH and pD dependences (Figure 3.5A and 3.5B). The viscosity dependence of k_{cat} revealed two titratable amino acid residues with pK_a values consistent with those measured in H_2O (Figure 3.5A). The pH independent value for k_{cat} was determined to be 80 ± 4 min^{-1}, resulting in a normal viscosity effect (H_2O/glycerol) of 1.2 (Table 3.2). The result indicated that the inverse isotope effect observed with D_2O was independent of viscosity. The viscosity dependence of $k_{cat}/K_{[octanesulfonate]}$ revealed a single ionizable amino acid residue with an apparent pK_a value of 6.4 ± 0.1 with a pH independent value of 1.20 ± 0.07 min^{-1} μM^{-1} (Figure 3.5B). This value resulted in a normal viscosity effect of 1.7 on $k_{cat}/K_{[octanesulfonate]}$ when compared to the $k_{cat}/K_{[octanesulfonate]}$ value in H_2O (Table 3.2). These effects on k_{cat} and $k_{cat}/K_{[octanesulfonate]}$ support a change in the rate of one or more non-pH dependent conformational changes during catalysis as a result of the increased viscosity (*173*, *174*, *182*, *183*, *188*, *189*, *191*, *197*).

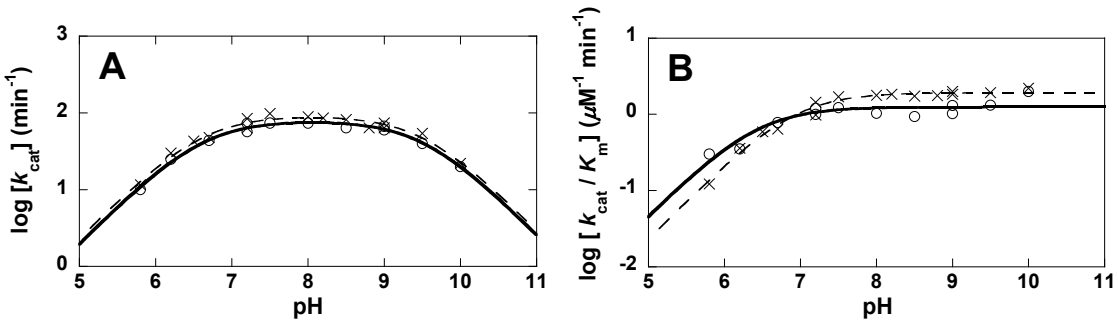

Figure 3.5. pH dependence of A: k_{cat} and B: $k_{cat}/K_{[octanesulfonate]}$ values for SsuD at 25°C in H_2O and supplemented with 9% glycerol (○). Reactions were initiated by the addition of NADPH (500 μM) into a reaction mixture containing SsuD (0.2 μM), SsuE (0.6 μM), FMN (2 μM), and a range of unlabeled octanesulfonate concentrations (10−5000 μM) in either 50 mM Bis-Tris (pL range of 5.8–7.2), 50 mM Tris-HCl (pL range of 7.2-9.0), or 50 mM glycine (pL range of 9.0-10.0) and 100 mM sodium chloride. The corresponding kinetic parameters for SsuD supplemented with unlabeled octanesulfonate and H_2O (×) were included in each plot as a reference. Each point is the average of at least three separate experiments.

3.3.5 Combined Substrate Kinetic and Solvent Isotope Effects on steady-state kinetic parameters

The kinetic parameters for the wild-type enzyme with 1-octanesulfonate-1,1-d_2 were established in 99.8% D_2O and plotted as a function of pD from pD 5.8-10.0 to identify the nature of any proton transfer events involved in the SsuD catalyzed reaction. SsuD with labeled substrate showed optimal catalytic activity in D_2O between pH 8.0-10.0 where the pH independent value was found to be 39.0 ± 0.2 min^{-1} for k_{cat}, and 2.3 ± 0.3 μM^{-1} min^{-1} for $k_{cat}/K_{[octanesulfonate]}$ (Figure 3.6A and 3.6B). These pD independent values were compared with those obtained with wild-type SsuD in H_2O to reveal an SIE+KIE $^{D}k_{D_2O}$ equal to 2.4 ± 0.2 for k_{cat} and 0.83 ± 0.12 for $k_{cat}/K_{[octanesulfonate]}$ (Table 3.2) (*186*). The pD dependence of k_{cat} for SsuD with deuterated substrate revealed a single titratable residue with a pK_a value of 6.6 ± 0.1 consistent with the lower pK_a value in the pH profile for SsuD with unlabeled substrate in H_2O (Table 3.1) (*186*). The upper pK_a value associated pH profile for SsuD with unlabeled substrate in H_2O appeared to have shifted outside of the experimental pH range with the labeled substrate in D_2O (*186*) (Figure 3.6A). The pH dependence of $k_{cat}/K_{[octanesulfonate]}$ with labeled substrate revealed a single titratable amino acid group with a pK_a value of 7.0 ± 0.1 consistent with the pK_a value in the pH profile for SsuD with unlabeled substrate in H_2O (Table 3.1) (*186*). These results demonstrate opposing substrate and solvent isotope effects on the catalytic parameters. The effects appear to be independent of each other indicating that each isotope effect is occurring on a different step in the catalytic mechanism (*173*, *174*, *188*, *189*, *197*).

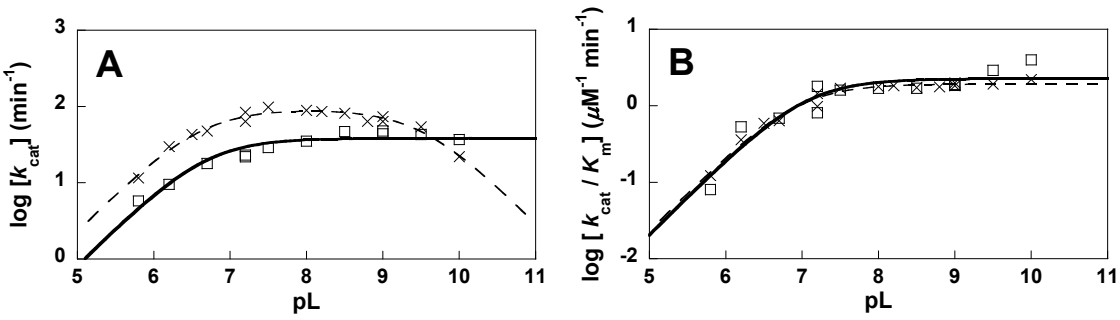

Figure 3.6. pH dependence of A: k_{cat} and B: $k_{cat}/K_{[octanesulfonate]}$ values for SsuD at 25°C supplemented with labeled 1-octanesulfonate-1,1-d_2 in D_2O (□). Reactions were initiated by the addition of NADPH (500 μM) into a reaction mixture containing SsuD (0.2 μM), SsuE (0.6 μM), FMN (2 μM), and a range of labeled 1-octanesulfonate-1,1-d_2 concentrations (10−5000 μM) in either 50 mM Bis-Tris (pL range of 5.8–7.2), 50 mM Tris-HCl (pL range of 7.2-9.0), or 50 mM glycine (pL range of 9.0-10.0) and 100 mM sodium chloride. The corresponding kinetic parameters for SsuD supplemented with unlabeled octanesulfonate and H_2O (×) were included in each plot as a reference. Each point is the average of at least three separate experiments.

3.3.6 Dependence of the kinetic parameters of SsuD on substrate functional groups

In order to determine whether variations in substrate chain length or size could affect the rate of product release and thereby serve as a probe for this step, activity assays from pH 5.8-10.0 were conducted using 1-butanesulfonate or 4-pyridineethanesulfonic acid as substrates for SsuD (Figure 3.7). The resulting pH dependences of the catalytic parameters of SsuD with each alternate substrate were compared to the pH dependences of catalytic parameters of SsuD with unlabeled octanesulfonate as a substrate. SsuD supplemented with 1-butanesulfonate showed optimal catalytic activity between pH 7.2-9.0 where the pH independent value was found to be 86 ± 5 min^{-1} for k_{cat}, and 0.16 ± 0.02 μM^{-1} min^{-1} for $k_{cat}/K_{[butanesulfonate]}$ (Table 3.2). The pH dependence of k_{cat} for SsuD supplemented with 1-butanesulfonate revealed two titratable residues with pK_a values of 6.3 ± 0.1 and 9.9 ± 0.1, and a single titratable residue with an apparent pK_a of 7.0 ± 0.1 for $k_{cat}/K_{[butanesulfonate]}$ (Table 3.1). The $k_{cat}/K_{[butanesulfonate]}$ pK_a values are apparent because the pH dependence data were fit to equation 3.1 for comparison with the values obtained for wild-type SsuD. However, a "hollow" present on the acidic limb of the $k_{cat}/K_{[butanesulfonate]}$ pH profile indicates the presence of a sticky proton in the enzyme-substrate complex, resulting in more than a 10-fold decrease in k_{cat}/K_m when compared to the SsuD reaction with 1-octanesulfonate as a substrate (Figure 3.8B) (*173*, *174*). Additionally, 1-butanesulfonate led to broadening between pK_a values in the k_{cat} pH profile when compared to wild-type SsuD but did not affect the apparent pK_a value seen in the k_{cat}/K_m pH profile (Table 3.1) (Figure 3.8A). SsuD supplemented with 4-pyridineethanesulfonic acid showed optimal catalytic activity between pH 7.2-9.0 where the pH independent value was found to be 164 ± 12 min^{-1} for k_{cat}, and 0.9 ± 0.1

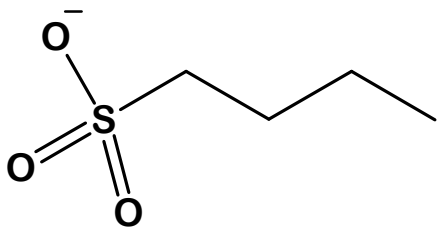

1-butanesulfonate

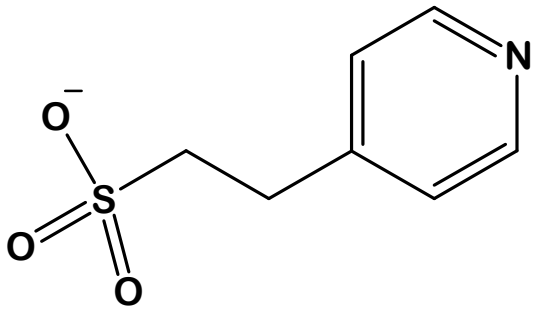

4-pyridineethanesulfonic

Figure 3.7. Structures of alternate substrates used to probe product release step of SsuD reaction. The substrate 1-butanesulfonate was used to probe whether shorter aliphatic chain length results in faster dissociation from the enzyme than octanesulfonate while 4-pyridineethanesulfonic acid was used to probe whether steric hindrance from a bulky aromatic group could disrupt binding interactions and facilitate product dissociation from the enzyme.

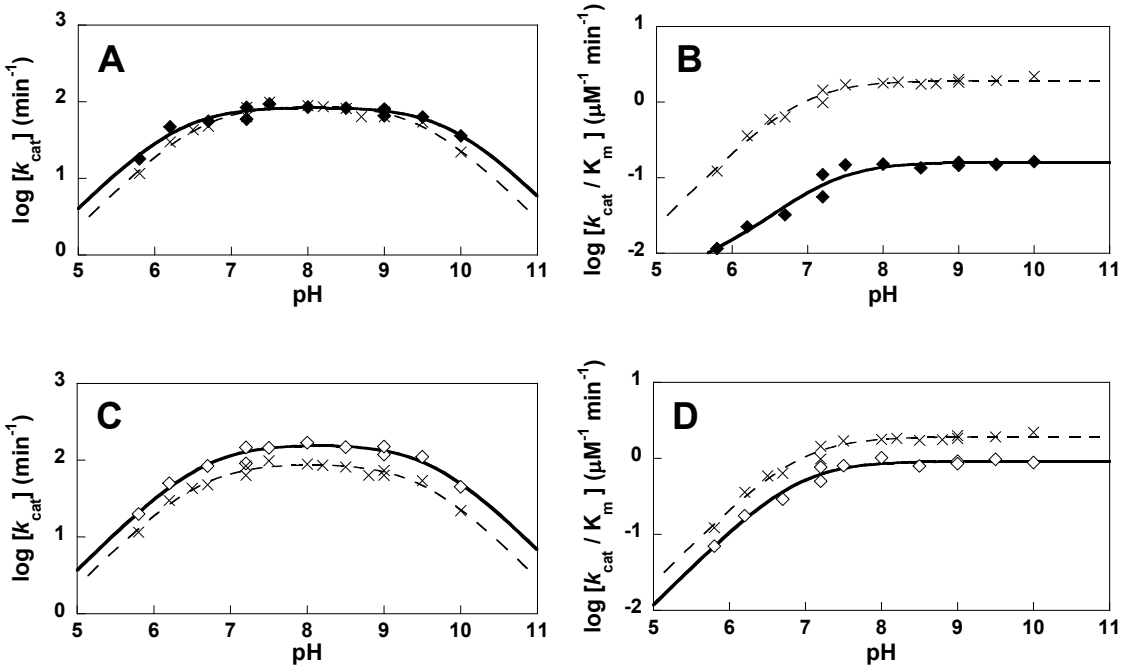

Figure 3.8 pH dependence of A: k_{cat} and B: k_{cat}/K_m values for SsuD at 25°C in H_2O and supplemented with either 1-butanesulfonate (♦) or 4-pyridineethanesulfonic acid (◊). Reactions were initiated by the addition of NADPH (500 μM) into a reaction mixture containing SsuD (0.2 μM), SsuE (0.6 μM), FMN (2 μM), and a range of 1-butanesulfonate or 4-pyridineethanesulfonic acid concentrations (10−5000 μM) in either 50 mM Bis-Tris (pL range of 5.8–7.2), 50 mM Tris-HCl (pL range of 7.2-9.0), or 50 mM glycine (pL range of 9.0-10.0) and 100 mM sodium chloride. The corresponding kinetic parameters for SsuD supplemented with 1-octanesulfonate and H_2O (×) were included in each plot as a reference. Each point is the average of at least three separate experiments.

μM^{-1} min^{-1} for $k_{cat}/K_{[pyridineethansulfonate]}$ (Table 3.2). These values reflect a two-fold increase in k_{cat} and a two-fold decrease in k_{cat}/K_m when compared to the SsuD reaction with 1-octanesulfonate as a substrate (Figure 3.8C and 3.8D). The pH dependence of k_{cat} for SsuD supplemented with 4-pyridineethanesulfonic acid revealed two titratable residues with pK_a values of 6.6 ± 0.1 and 9.6 ± 0.1, and single titratable residue with an apparent pK_a of 6.9 ± 0.1 for $k_{cat}/K_{[pyridineethansulfonate]}$ (Table 3.1). These pK_a values are consistent with the values obtained for SsuD with 1-octanesulfonate as a substrate.

3.4 DISCUSSION

The proposed catalytic mechanism for SsuD involves the abstraction of a proton from the primary carbon of the octanesulfonate substrate (Scheme 3.1, IV). This step has been proposed to be the rate-limiting catalytic step. Therefore, the protium at this position was substituted with deuterium in order to limit the rate of this abstraction step during catalysis. The lack of an isotope effect on $k_{cat}/K_{[octanesulfonate]}$ over the experimental pH range indicates that labeled octanesulfonate substrate does not affect any catalytic steps up through the first-irreversible step (*173*, *174*, *189*, *197*). Alternatively, the k_{cat} pH profile encompasses all steps occurring after the first-irreversible step up through product release which would include the proton abstraction step (*173*, *174*). Therefore, the kinetic isotope effect of 3 on k_{cat} supports proton abstraction being the rate-limiting step. Additionally, comparison of the k_{cat} pH profile of the labeled substrate with the unlabeled substrate revealed a acidic shift of this lower pK_a value from 6.6 to 6.3, while the upper pK_a value associated with unlabeled octanesulfonate appeared to have shifted outside of the experimental pH range with the labeled substrate (Table 3.1) (*186*). An outward shift or broadening of pK_a values observed only in the k_{cat} pH profile is indicative of a non-pH dependent, but normally rate limiting, slow step following the chemical catalytic reaction (*174*, *188–190*). Previously, this step was reported as a conformational change linked to product release (*186*). Therefore, the results suggest that the overall substrate isotope effect originates, at least partially, from product release. Because both

	k_{cat}		k_{cat}/K_m
	pK_1	pK_2	pK
1-octanesulfonate			
H_2O[a]	6.6 ± 0.1	9.5 ± 0.1	6.9 ± 0.1
D_2O	6.8 ± 0.1	10.1 ± 0.2[b]	7.3 ± 0.1
9% glycerol	6.6 ± 0.2	9.5 ± 0.1	6.6 ± 0.5
1-octanesulfonate-1,1-d_2			
H_2O	6.3 ± 0.1	—[c]	7.1 ± 0.1
D_2O	6.6 ± 0.1	—[c]	7.0 ± 0.1
1-butanesulfonate			
H_2O	6.3 ± 0.1	9.9 ± 0.1	7.0 ± 0.1
4-pyridineethanesulfonic acid			
H_2O	6.6 ± 0.1	9.6 ± 0.1	6.9 ± 0.1

[a] previously reported (*186*)
[b] Value was calculated from proton inventory measurements
[c] Value could not be determined within the experimental pH range

Table 3.1. pH dependence of steady-state kinetic parameters for wild-type SsuD isotope effects

alpha carbon protons have been replaced with deuterium in the labeled substrate, an alpha-secondary isotope effect (α-2°) must also be considered. Since the hybridization of the isotopically labeled carbon changes from sp^3 to sp^2 during the reaction (scheme 3.1, III—IV), a normal α-2° would be expected and would account for some of the observed KIE value (*198*).

Solvent isotope effect studies were undertaken in order to probe the reprotonation step in the SsuD reaction (Scheme 3.1, step IV). The pD profile of k_{cat} was fitted to equation 1 to yield a single pK_a value of 7.2 ± 0.1 and an inverse solvent isotope effect of 0.75 ± 0.04. When compared to the lower pK_a value in H_2O, the ΔpK_a value of 0.2 units in D_2O is consistent with that expected for a cysteine amino acid group (*188–190*). Previously, an alanine substitution to Cys54 in SsuD was shown to cause the proton associated with the lower pK_a value to become sticky during catalysis (*186*). These combined results support Cys54 making at least a partial contribution to this lower pK_a value along with the proton at the N1 position of the FMN (*186*). Alternatively, the upper pK_a value in D_2O exhibited the expected shift for a simple carboxylic or ammonium acid groups (ΔpK_a = 0.4-0.6) when compared to its value in H_2O (Table 3.1). Interestingly, previous studies were unable to determine whether Cys54 was the sole group contributing to this upper pK_a value or whether Cys54 was serving to lower the pK_a of Arg226 during catalysis (*186*). The normal shift of this pK_a value in D_2O supports Cys54 serving to lower the pK_a of Arg226 as the ΔpK_a value for a cysteine amino acid group contributing exclusively to the upper pK_a would be much smaller (*186*, *189*). Additionally, cysteine residues like Cys54 have been shown to promote reverse-protonation which can lead to an inverse solvent isotope effect like the one seen on the SsuD k_{cat} parameter (*188*, *199*).

In a reverse-protonation mechanism, the amino acid residue contributing to the lower pK_a value must be protonated while the amino acid residue contributing to the upper pK_a value must be deprotonated in order for catalysis to occur. In order for the D_2O solvent to favor the deprotonated form of the group contributing to the upper pK_a value, this group would need to have a fractionation factor that is less than unity ($ø < 1$) in a mixed isotopic solvent (*188–190*, *193*, *199*). Cysteine residues have been implicated in several reverse-protonation mechanisms as the group contributing to the upper pK_a value, with fractionation factors for cysteine residues ($ø \sim 0.5$) being less than unity in a mixed isotopic solvent (*188–190*, *193*, *199*, *200*). Cys54 was previously shown to be involved in stabilizing the C4a-(hydro)peroxyflavin in SsuD either through direct interactions with the flavin or in helping to maintain the active site environment (*171*). However, previous results have indicated Cys54 must be protonated for activity (*171*). Therefore, the inverse solvent isotope effect is likely the result of a normal protonation event.

Although the change in viscosity that results from substituting D_2O for H_2O can account for apparent solvent isotope effects, k_{cat} values in increased viscosity are normal (decreased) compared to values observed in H_2O over the experimental pH range (Figure 3.4A and 3.4B). A solution containing 99.8% D_2O has the same relative viscosity (η_{rel}~1.24) as a solution containing 9% glycerol (*182*, *183*, *188–190*, *193*, *195*, *196*). However, the k_{cat} pH profile shows that increased viscosity reduces k_{cat} over the experimental pH range, suggesting that the inverse isotope effect on k_{cat} is not the result of increased solvent viscosity (Figure 3.4A). Nevertheless, this normal viscosity effect on the k_{cat} parameter does indicate viscosity affects the rate-limiting step of the mechanism (*173*, *174*). Increased viscosity often affects an enzyme mechanism that is dependent on a

conformational change by favoring closed conformations and slowing the return rate to the open conformation (*195*, *196*). Therefore, increased solvent viscosity may be serving to limit a proposed conformational change from a closed to an open conformation in SsuD.

Alternatively, the proton inventories on k_{cat} suggest that D_2O is contributing to the overall inverse isotope effect by favoring a conformational change to the open conformation during the product release step. The proton inventory was best fit to dome shaped curves suggesting a normal transition state contribution (ϕ^T) opposing multiple inverse effect contributions (Z_k) to yield the overall inverse isotope effect (*182*, *183*, *188–190*, *193*). The transition state contribution (ϕ^T) is consistent with the solvation of a catalytic proton bridge commonly observed for proton transfers among O, N, and S groups (ϕ^T = 0.4-0.6) (*189*). Previously, Arg226 was proposed to be responsible for protonating the FMN-O^- intermediate in the catalytic mechanism for SsuD; the data suggest that the ϕ^T contribution arises from the transfer of a proton from N group Arg226 to the O group of FMN-O^- (*186*). The *Z* term contribution is indicative of multiple reaction state contributions (ϕ^R) occurring on various protein structural sites (ϕ^R = 1.05-1.16) as a result of a conformational change (*189*). These effects in combination with the normal transition state contribution (ϕ^T) support the formation of a transition state intermediate where tighter, stiffer hydrogen bonds (like those corresponding to deuterium bonds) are favored in the committed step for product release. The protonation of FMN-O^- by Arg226 would serve as the committed step. Additionally, proton transfer from an arginine group to a group with a potentially greater fraction factor (FMN-O^-) would be faster with deuterium than with protium. If the fractionation factors of FMN-OOH and

FMN-OH are great and above unity, then the current results would support Schemes 3.1 and 3.2 as well as account for the inverse solvent isotope effect observed on the k_{cat} parameter.

Additionally, since the inverse solvent isotope effect is seen in the k_{cat} pL profile and not the $k_{cat}/K_{[octanesulfonate]}$ pL profile, the results indicate a step occurring after the first-irreversible step up through product release is affected by the deuterated solvent. The lack of an observable isotope effect on $k_{cat}/K_{[octanesulfonate]}$ over the experimental pL range indicates that this ionizable group is not involved in a proton transfer event contributing to an overall rate limitation. Previously, SsuD has been shown to follow a steady-state ordered binding mechanism with $FMNH_2$ binding first to SsuD, followed by either octanesulfonate or O_2 prior to formation of the C4a-peroxyflavin intermediate proposed to govern the desulfonation reaction (Scheme 3.2) (*160*). Since $FMNH_2$ must bind to SsuD first, its binding will represent an on-rate constant that will be insensitive to deuterium isotopic substitution and the affect on $k_{cat}/K_{[octanesulfonate]}$ and $k_{cat}/K_{[O2]}$ will be unity by definition (*197*). Since both the substrate and solvent isotope effect on $k_{cat}/K_{[octanesulfonate]}$ is within experimental error of 1, it can be concluded that octanesulfonate adds to SsuD prior to O_2 under steady-state conditions (*201*). Although dioxygen concentration has been shown to be saturating under these experimental conditions, the kinetic isotope effect on $k_{cat}/K_{[O2]}$ was not explored in the current work; it will be the subject of future studies.

The determination of SsuD kinetic parameters in D_2O and with labeled substrate was performed in an effort to extrapolate the intrinsic substrate and solvent isotope effect from the combined isotope effects data. The pD profile of k_{cat} with the deuterium

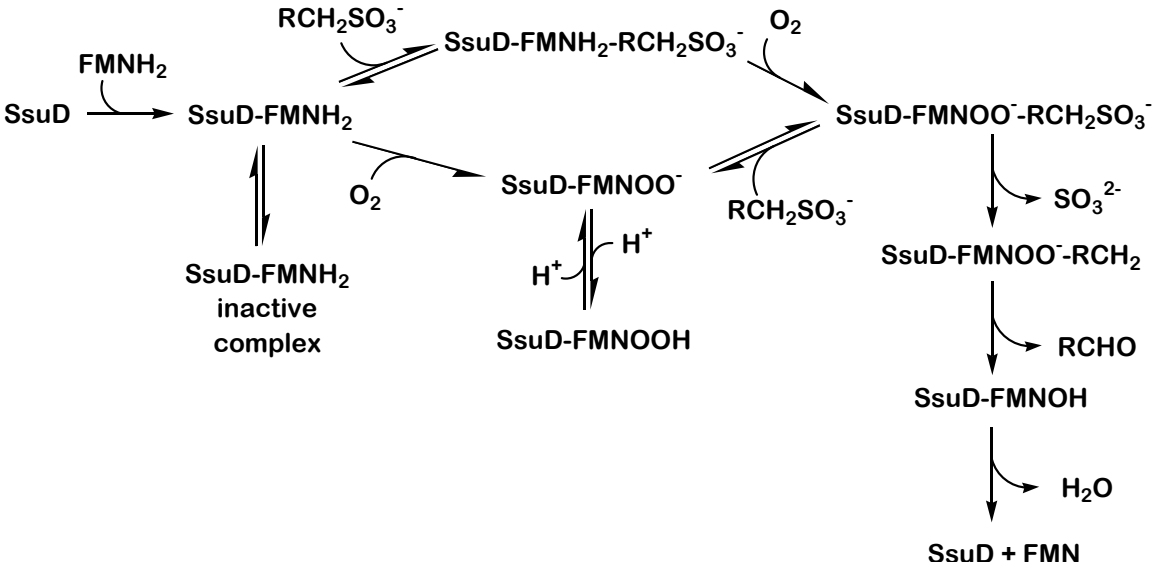

Scheme 3.2. Proposed substrate binding order for SsuD

labeled substrate exhibited features from profiles of the labeled substrate in H_2O and unlabeled substrate in D_2O, while the profile for $k_{cat}/K_{[octanesulfonate]}$ remained unaffected by the combined isotope effects (Figure 3.7A and 3.7B). The reduced pL independent value for k_{cat} combined with the outward shift of the pK_a values for the labeled substrate in D_2O are consistent with the reductions and shifts seen for the labeled substrate in H_2O (Table 3.2). Interestingly, the overall effect on the pL independent value of k_{cat} for the two isotopes together is the product of each individual isotope effect on k_{cat}. The results suggest that there are two separate isotopic sensitive steps in the SsuD reaction. Therefore, while the resuls indicate that the intrinsic isotope effects (^{D}k and ^{D2O}k) affect different mechanistic steps in the reaction, these values could not be determined from steady-state data alone.

A substrate is considered sticky when it dissociates more slowly than it reacts to give products (*188*, *189*). A substrate with a shorter aliphatic chain length (1-butanesulfonate) was used to probe whether the long aliphatic chain of 1-octanesulfonate results in slow dissociation from the enzyme. Interestingly, the results revealed that it is the shorter chain length of 1-butanesulfonate that causes the proton associated with the ionizable group on the acidic limb of the pH profile to become sticky; 1-butanesulfonate dissociates from the enzyme-substrate complex slower than it reacts to give products (*173*, *174*). Furthermore, an outward shift or broadening of pK_a values observed only in the k_{cat} pH profile for SsuD with 1-butanesulfonate as a substrate is indicative of a non-pH dependent, but normally rate limiting, slow step following the catalytic reaction (*173–175*). Since the outward pK_a shifts are only present on the pH dependence of k_{cat}, the

	k_{cat} (min^{-1})	k_{cat}/K_m ($\mu M^{-1}\ min^{-1}$)
1-octanesulfonate		
H_2O	93 ± 5[a]	1.9 ± 0.1[a]
D_2O	123 ± 3	2.0 ± 0.1
9% glycerol	80 ± 4	1.2 ± 0.1
1-octanesulfonate-1,1-d_2		
H_2O	31 ± 2	1.9 ± 0.3
D_2O	39 ± 2	2.3 ± 0.3
k_H/k_D	3.0 ± 0.2	1.0 ± 0.2
$^{H_2O}k_H/^{D_2O}k_H$	0.75 ± 0.04	0.95 ± 0.07
$^{D_2O}k_H/^{D_2O}k_D$	3.1 ± 0.2	0.87 ± 0.12
1-butanesulfonate		
H_2O	86 ± 5	0.16 ± 0.02
4-pyridineethanesulfonic acid		
H_2O	164 ± 12	0.9 ± 0.1

[a] Previously reported in reference (*160*)

Table 3.2. pH Independent steady-state kinetic parameters for wild-type SsuD isotope effects. Reactions were performed at 25°C, and values were determined by fitting pH profiles data to equations 3.1 or 3.2 and solving for C.

results suggest the rate of product release is also slowed by the shorter chain length of 1-butanesulfonate (*173–175*). Despite this broadening between pK_a values, the k_{cat} value for the SsuD reaction with 1-butanesulfonate as a substrate is consistent with the k_{cat} value for the SsuD reaction with 1-octanesulfonate as a substrate, while the k_{cat}/K_m value is decreased more than ten-fold. These results indicate that the rate of the SsuD chemical reaction is increased when 1-butanesulfonate is the substrate, but the overall reaction becomes limited by substrate binding and product release steps. Alternatively, 4-pyridineethanesulfonic acid was used to probe whether steric hindrance from a bulky aromatic group could disrupt binding interactions and facilitate product dissociation from the enzyme. As supported by the two-fold increase in k_{cat} and the absence of an outward shift in pK_a values when compared to the SsuD reaction with 1-octanesulfonate as a substrate, 4-pyridineethanesulfonic acid appears to increase the overall rate of the SsuD reaction by serving to increase the rate-limiting, product release step.

Altogether, the results presented in this study support the proposed mechanism for SsuD. The observed isotope effect of 3.0 ± 0.2 on the k_{cat} parameter when deuterium labelled octanesulfonate is supplemented into the steady-state reaction supports the abstraction of the α-proton from the alkane peroxyflavin intermediate as the rate-limiting chemical step in SsuD catalysis (Scheme 3.1, III). Additionally, the solvent isotope effect data along with the corresponding proton inventory results support Arg226 donating a proton to the $FMNO^-$ intermediate triggering a proposed conformational change that opens the enzyme to solvation and promotes product release (Scheme 3.1, IV).

CHAPTER FOUR

Implications of Rapid-Reaction Studies to Identify Intrinsic Solvent and Kinetic Isotope Effects for the Desulfonation Mechanism of SsuD

4.1 INTRODUCTION

Escherichia coli alkanesulfonate monooxygenase (SsuD) is proposed to activate dioxygen by generating a covalent flavin-oxygen adduct at the C4a position of the flavin isoalloxazine ring (Scheme 4.1) (*60*, *72*, *95*, *107*, *160*). Although the individual steps vary between flavin-dependent monooxygenase enzymes, the formation of the C4a-(hydro)peroxyflavin intermediate typically promotes a nucleophilic or electrophilic reaction that is integral to the particular enzyme's catalytic mechanism (*60*, *61*, *72*, *75*, *95*, *96*). Additionally, the formation of this C4a-(hydro)peroxyflavin intermediate is usually detectable by its distinct UV spectral signal around 370 nm. Unlike many flavin monooxygenases where both oxidative and reductive half reactions occur on the same enzyme, SsuD encompasses only the monooxygenase component of the flavin-dependent two-component alkanesulfonate monooxygenase system and is dependent on a seperate flavin reductase component (SsuE) (*107*, *129*, *170*). SsuE is responsible for catalyzing the reduction of FMN by NAD(P)H prior to transferring it to SsuD. The system is expressed when sulfate becomes limiting, and it is involved in acquiring sulfur from alternative

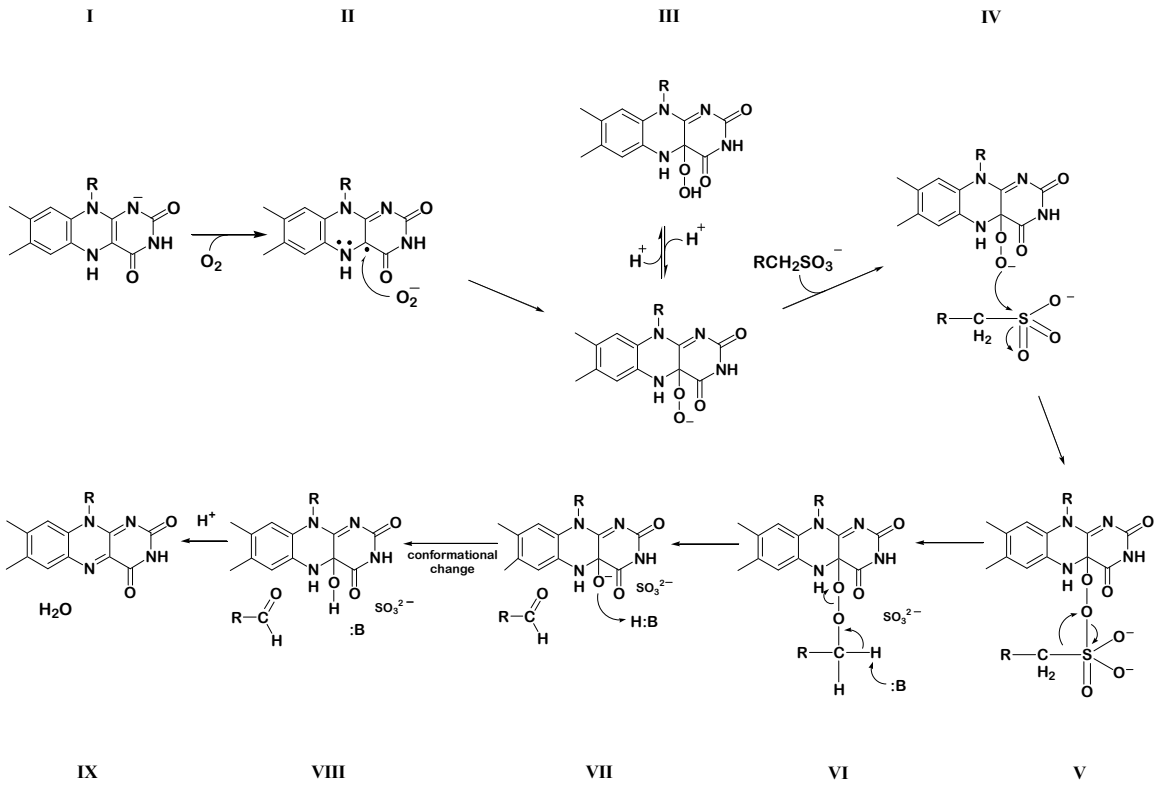

Scheme 4.1. Proposed chemical mechanism for SsuD reaction when octanesulfonate concentration is low.

sources, primarily alkanesulfonates (*107*, *129*, *150*, *170*). For the monooxygenase reaction, $FMNH_2$-bound SsuD is proposed to activate dioxygen and cleave the carbon-sulfur bond of alkanesulfonates releasing sulfite and the corresponding aldehyde through a C4a-peroxyflavin intermediate (Scheme 4.1) (*107*, *160*).

The desulfonation reaction of SsuD has been proposed previously to proceed by an acid-base mechanism via a C4a-peroxyflavin intermediate (*160*, *186*). In many reactions dependent on acid-base catalysis, the proton transfer step is rate-limiting and can be affected by substituting a deuterium in place of the proton being transferred. Although substrate and solvent deuterium isotope effects under steady-state conditions supported this proposed mechanism, the intrinsic isotope effect on individual isotopically sensitive steps and commitments to catalysis were not determined. In the proposed mechanism, the release of the aldehyde product from the enzyme occurs following abstraction of a proton from the alkane peroxyflavin intermediate via a catalytic base. The abstraction of the proton from the alkane peroxyflavin intermediate has been proposed as one of several potential rate-limiting chemical steps in SsuD catalysis. Additionally, a general acid donates a proton to the $FMNO^-$ intermediate triggering a proposed conformational change that opens the enzyme to solvation and promotes product release. As a result, one or more of these mechanistic steps should be observable by monitoring the individual rate constants associated with SsuD-mediated flavin oxidation through rapid-reaction kinetic analysis. Therefore, reactions supplemented with deuterium labeled octanesulfonate substrate and D_2O solvent were observed under single-turnover conditions using rapid-reaction kinetic analysis in an effort to obtain these parameters and further resolve key steps involved in the proposed catalytic mechanism.

4.2 EXPERIMENTAL PROCEDURES

4.2.1 Materials

Potassium phosphate (monobasic and dibasic), flavin mononucleotide phosphate (FMN), reduced nicotinamide adenine dinucleotide phosphate (NADPH), Trizma base, Bis–Tris, glycine, ammonium sulfate, ampicillin, ethylenediaminetetraacetic acid (EDTA), dimethyl sulfoxide (DMSO), streptomycin sulfate, glucose, glucose oxidase, 5,5-dithiobis(2-nitrobenzoic acid) (DTNB), and lysozyme were purchased from Sigma (St. Louis, MO). Isopropyl-β-D-thiogalactoside (IPTG), sodium chloride, and glycerol were obtained from Fisher Biotech (Pittsburgh, PA). 1-Octanesulfonate and dithiothreitol (DTT) were purchased from Fluka (Milwaukee, WI). Deuterium oxide (D_2O), deuterium chloride, and sodium deuteroxide were purchased from Cambridge Isotope Laboratories, Inc (Andover, MA). The synthesis of 1-octanesulfonate-1,1-d_2 was performed as previously described in chapter three of this dissertation. Expression and purification of recombinant SsuD and SsuE was performed as previously described (*155*). The concentrations of SsuD and SsuE proteins were determined from A_{280} measurements using a molar extinction coefficient of 47.9 mM^{-1} cm^{-1} and 20.3 mM^{-1} cm^{-1}, respectively (*155*).

4.2.2 Rapid Reaction Kinetic Analyses

Stopped-flow kinetic analyses were carried out as previously described using an Applied Photophysics SX.18 MV stopped-flow spectrophotometer (*160*, *169*, *171*). All

experiments were performed at pH 8.5 in order to favor equal accumulation of protonated (FMN-OOH) and deprotonated (FMN-OO^-) C4a-(hydro)peroxyflavin intermediates (pK_a = 8.4) (*65*, *96*). Reactions were initiated by mixing $FMNH_2$ (25 μM) in one drive syringe against SsuD (35 μM) in air-saturated buffer (25 mM Tris-HCl, 100 mM NaCl) in the other drive syringe. When included in the reaction, varied concentrations of 1-octanesulfonate or 1-octanesulfonate-1,1-d_2 (20–1000 μM) were added to the SsuD solution in air-saturated buffer. All experiments were carried out in single-mixing mode by mixing equal volumes of the solutions, and monitoring the absorbance at 370 and 450 nm for 100 seconds. Experiments in deuterium oxide were carried out at pD 8.5 using reaction mixtures prepared with 99.8% D_2O instead of H_2O. The single-wavelength traces were fitted to a double or triple exponential using the following equations:

$$A = A_1 \exp(-k_{1(\text{obs})}t) + A_2 \exp(-k_{2(\text{obs})}t) + C \qquad \text{(equation 4.1)}$$

$$A = A_1 \exp(-k_{1(\text{obs})}t) + A_2 \exp(-k_{2(\text{obs})}t) + A_3 \exp(-k_{3(\text{obs})}t) + C \qquad \text{(equation 4.2)}$$

where $k_{1(\text{obs})}$, $k_{2(\text{obs})}$, and $k_{3(\text{obs})}$ are the apparent rate constants, A is the absorbance at time t, A_1, A_2, A_3 are amplitudes of each phase, and C is the absorbance at the end of the reaction.

4.2.3 Data Analysis

The overall equations for kinetic isotope effects on k_{cat} and k_{cat}/K_m will adhere to the following expressions:

$$k_{cat} = \frac{k_9 k_{11}}{k_9 + k_{11}} \qquad \text{(equation 4.3)}$$

$$ {}^{D_2O}k_{cat} = \frac{{}^{D_2O}k_9 + \frac{k_9}{k_{11}}}{1 + \frac{k_9}{k_{11}}} \qquad \text{(equation 4.4)} $$

$$ {}^{D_2O}\left(k_{cat} / K_m\right)_{HA} = \frac{{}^{D_2O}k_9 + c_{fA}}{1 + c_{fA}} \qquad \text{(equation 4.5)} $$

$$ c_{fA} = \frac{k_9(k_2 + k_3 B)}{k_2 k_4} \qquad \text{(equation 4.6)} $$

$$ {}^{D_2O}\left(k_{cat} / K_m\right)_{DA} = \frac{\frac{{}^{D_2O}k_9}{{}^{D}k} + \frac{c_{fA}}{{}^{D}k}}{1 + \frac{c_{fA}}{{}^{D}k}} \qquad \text{(equation 4.7)} $$

$$ {}^{D}\left(k_{cat}\right) = \frac{{}^{D}k + c_{Vf} + c_r({}^{D}K_{eq})}{1 + c_{Vf} + c_r} \qquad \text{(equation 4.8)} $$

where k_2, k_3, k_4, k_9, and k_{11} represent the microscopic rate constants in scheme 4.2, ${}^{D_2O}k_{cat}$ equals the solvent isotope effect on k_{cat} (${}^{H_2O}k_{cat}/{}^{D_2O}k_{cat}$), ${}^{D_2O}(k_{cat}/K_m)_{HA}$ equals the solvent isotope effect on k_{cat}/K_m for octanesulfonate [${}^{H_2O}(k_{cat}/K_m)_H/{}^{D_2O}(k_{cat}/K_m)_H$], ${}^{D_2O}k_9$ represents the solvent isotope effect on the net rate constant for the conversion of enzyme bound reduced flavin to enzyme bound oxidized flavin, c_{fA} equals the forward commitment factor for octanesulfonate, B represents the concentration of dioxygen, ${}^{D_2O}(k_{cat}/K_m)_{DA}$ equals the deuterated substrate kinetic isotope effect on k_{cat}/K_m in D_2O [${}^{D_2O}(k_{cat}/K_m)_H/{}^{D_2O}(k_{cat}/K_m)_D$], ${}^{D}k$ represents the intrinsic kinetic isotope effect (k_{9H}/k_{9D}), c_r represents the reverse commitment factor, and ${}^{D}K_{eq}$ is the equilibrium isotope effect (*197*). The intrinsic kinetic isotope effect (${}^{D}k$), the ratio of catalysis (c_{Vf} or k_9/k_{11}), and the forward

commitment to catalysis (c_{fA}) for the SsuD reaction in D_2O were calculated by solving for the respective value using equations 4.4, 4.5, and 4.7.

4.3 RESULTS

4.3.1 Substrate kinetic isotope effects on kinetic rate constants of SsuD reaction

Stopped-flow kinetic studies were performed using 1-octanesulfonate-1,1-d_2 and compared to studies performed using octanesulfonate substrate in order to evaluate the effect of deuterium labeled substrate on flavin oxidation. All reactions monitored the oxidation of $FMNH_2$ by SsuD in the absence or presence of octanesulfonate (10-500 μM) at 370 and 450 nm for 100 seconds. As a control, single-wavelength kinetic traces were also obtained for the oxidation of free $FMNH_2$ (25 μM) in the absence of SsuD and octanesulfonate. The oxidation of free $FMNH_2$ was best fit to equation 4.1 with rates of 2.36 ± 0.04 s^{-1} ($k_{1,obs}$) and 1.21 ± 0.01 s^{-1} ($k_{2,obs}$) for kinetic traces monitored at 370 nm and 2.5 ± 0.05 s^{-1} ($k_{1,obs}$) and 1.23 ± 0.01 s^{-1} ($k_{2,obs}$) at for kinetic traces monitored at 450 nm. The two phases observed in the kinetic traces at each wavelength can be attributed to non-enzymatic flavin oxidation. At low octanesulfonate concentrations (<100 μM), the kinetic traces at 370 nm and 450 nm were best fit to equations 4.2 and 4.1, respectively. The amplitude of the fast phase ($k_{1,obs}$) observed at 370 nm decreased with increasing octanesulfonate concentration until the rate constant was no longer observable at high octanesulfonate concentrations (≥100 μM) (Figure 4.1A). Previously, this fast phase ($k_{1,obs}$) was attributed to the accumulation and stabilization of the C4a-(hydro)peroxyflavin intermediate integral to the SsuD catalytic mechanism. At higher octanesulfonate concentrations, kinetic traces of reactions monitored at 370 nm were best

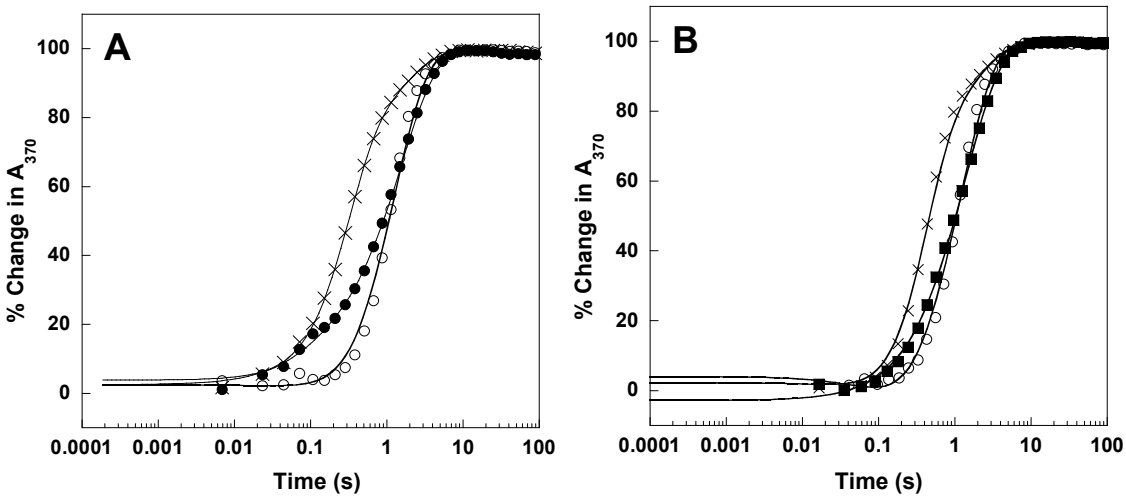

Figure 4.1. Kinetic of flavin oxidation by SsuD monitored at 370 nm in H_2O solvent. A: Free $FMNH_2$ (25 μM) mixed with SsuD (35 μM) in air-saturated H_2O buffer (●). Free $FMNH_2$ (25 μM) mixed with SsuD (35 μM) and octanesulfonate (1000 μM) in air-saturated H_2O buffer (×). B: Free $FMNH_2$ (25 μM) mixed with SsuD (35μM) and 1-octanesulfonate-1,1-d_2 acid (40 μM) in air-saturated H_2O buffer (■). Free $FMNH_2$ (25 μM) mixed with SsuD (35 μM) and 1-octanesulfonate-1,1-d_2 (1000 μM) in air-saturated H_2O buffer (×). Each plot includes the kinetic trace of free $FMNH_2$ (25 μM) mixed with air-saturated buffer (○) as a reference. The kinetic traces shown are the average of at least three separate experiments. The solid lines are the fits of the kinetic traces to equations 4.1 or 4.2.

fit to equation 4.1 and the rate constants were indistinguishable from the rate constants obtained from the corresponding 450 nm kinetic traces (Table 4.1). These results indicated an insufficient accumulation of the C4a-(hydro)peroxyflavin intermediate at higher octanesulfonate concentrations. Interestingly, the initial phase ($k_{1,obs}$) was not observed at any substrate concentration for reactions supplemented with deuterium labeled 1-octanesulfonate-1,1-d_2 (Figure 4.1B). Nevertheless, analyses of kinetic traces from reactions monitored at 370 and 450 nm showed a clear hyperbolic dependence on $k_{2(obs)}$ with both labeled and unlabeled octanesulfonate substrate. A fit of the data monitored at 450 nm gave a K_d value of 18.3 ± 4.0 μM and a limiting rate constant of 2.8 ± 0.1 s^{-1} for reactions supplemented with unlabeled octanesulfonate, and a K_d value of 17.8 ± 2.7 μM and a limiting rate constant of 3.2 ± 0.1 s^{-1} for reactions supplemented with 1-octanesulfonate-1,1-d_2. The results demonstrated that while the value of the second order rate constant was independent of whether labeled or unlabeled octanesulfonate was used in the reaction, the C4a-hydroperoxyflavin intermediate failed to accumulate in reactions supplemented with deuterium labeled substrate. The value of the slowest rate constant ($k_{3,obs}$) was indistinguishable from that obtained with unlabeled substrate indicating that the overall rate of flavin oxidation was not affected by the deuterated octanesulfonate substrate (Table 4.1).

4.3.2 Solvent kinetic isotope effects on kinetic rate constants of SsuD reaction

Stopped-flow kinetic studies of SsuD reactions supplemented with 1-octanesulfonate-1,1-d_2 were performed in 99.8% D_2O and compared to studies performed in H_2O to evaluate the effect of deuterated solvent on flavin oxidation. As a control, single-wavelength kinetic traces were also obtained for the oxidation of free $FMNH_2$ (25

μM) in the absence of SsuD in D_2O and compared to the rate constants obtained in H_2O. In D_2O, the oxidation of free $FMNH_2$ was best fit to equation 4.1 with rates of 1.49 ± 0.05 s^{-1} ($k_{1,obs}$) and 0.73 ± 0.01 s^{-1} ($k_{2,obs}$) for kinetic traces of the reaction monitored at 370 nm and 1.52 s^{-1} ± 0.05 ($k_{1,obs}$) and 0.76 s^{-1} ± 0.01 ($k_{2,obs}$) for traces at 450 nm. The two phases observed for flavin oxidation in H_2O and D_2O were determined to be essentially identical. At low octanesulfonate concentrations (<100 μM), the kinetic traces at 370 nm and 450 nm were best fit to equations 4.2 and 4.1, respectively. Interestingly, the fast phase ($k_{1,obs}$) observed in kinetic traces at 370 nm was present at the highest concentration of unlabeled octanesulfonate (500 μM) for reactions performed in D_2O (Figure 4.2A). These results indicated increased accumulation and stabilization of the C4a-hydroperoxyflavin intermediate in D_2O even at higher octanesulfonate concentrations. Additional analyses of kinetic traces from reactions monitored at 370 and 450 nm also showed a clear hyperbolic dependence ($k_{2,obs}$) on octanesulfonate concentration, with a K_d value of 9.8 ± 2.0 μM and a limiting rate constant of 2.4 ± 0.1 s^{-1} for reactions monitored in D_2O (Table 4.1). These K_d values indicate that unlabeled octanesulfonate binds tighter to SsuD during catalysis in D_2O than in H_2O. The value of the slowest rate constant ($k_{3,obs}$) in D_2O was indistinguishable from that obtained in H_2O indicating that the overall rate of flavin oxidation was not affected by the deuterated solvent (Table 4.1).

4.3.3 Combined substrate and solvent kinetic isotope effects on kinetic rate constants of SsuD reaction

Stopped-flow kinetic studies of SsuD reactions supplemented with 1-octanesulfonate-1,1-d_2 were performed in 99.8% D_2O and compared to reactions

	K_d [a] (μM)	$k_{1(obs)}$ [b] (s^{-1})	$k_{2(obs)}$ (μM^{-1} s^{-1})	$k_{3(obs)}$ (s^{-1})
1-octanesulfonate				
H_2O	18.3 ± 4.0	19 ± 3 [c]	0.132 ± 0.032	0.5 ± 0.2
D_2O	9.8 ± 2.0	35 ± 6	0.245 ± 0.051	0.5 ± 0.2
1-octanesulfonate-1,1-d_2				
H_2O	17.8 ± 2.7	ND[d]	0.179 ± 0.025	0.5 ± 0.2
D_2O	15.5 ± 2.5	40 ± 5 [c]	0.240 ± 0.041	0.8 ± 0.4
k_H/k_D	1.0 ± 0.3		0.73 ± 0.21	—
${}^{H_2O}k_H/{}^{D_2O}k_H$	1.9 ± 0.6	0.54 ± 0.13	0.54 ± 0.17	—
${}^{D_2O}k_H/{}^{D_2O}k_D$	1.2 ± 0.3	0.88 ± 0.18	1.02 ± 0.27	0.6 ± 0.4

[a] K_d is the dissociation constant for octanesulfonate binding determined from single turnover kinetic studies.
[b] Rate constant is only observable at 370 nm
[c] Rate constant is not distinguishable at high octanesulfonate concentrations
[d] Rate is not detectable.

Table 4.1. Single-turnover rapid-reaction kinetic rate constants for wild-type SsuD isotope effects. Reactions were performed at 4°C and pL 8.5. Data reflect the observed k_1, k_2, and k_3 rate constants extrapolated from eqs. 5 and 4 after being fit to kinetic traces of $FMNH_2$ (25 μM) oxidation monitored at A_{370} and A_{450}, respectively.

supplemented with unlabeled octanesulfonate in order to deduce the intrinsic substrate isotope effect. At low 1-octanesulfonate-1,1-d_2 concentrations (<50 μM), the kinetic traces at 370 nm and 450 nm were best fit to equations 4.2 and 4.1, respectively. The amplitude of the fast phase ($k_{1,obs}$) observed at 370 nm decreased with increasing deuterated octanesulfonate concentrations until the rate constant was no longer observable at high deuterated octanesulfonate concentrations (≥50 μM) (Figure 4.2B). At higher 1-octanesulfonate-1,1-d_2 concentrations, kinetic traces of reactions monitored at 370 nm were best fit to equation 4.1 and the rate constants were indistinguishable from the rate constants obtained from the corresponding 450 nm kinetic traces (Table 4.1). These results indicated an insufficient accumulation of the C4a-(hydro)peroxyflavin intermediate at higher octanesulfonate concentrations. Additionally, a fit of the data monitored at 450 nm gave a K_d value of 15.5 ± 2.5 μM and a limiting rate constant of 3.6 ± 0.1 s^{-1} for reactions monitored in D_2O (Table 4.1). These K_d values indicate that labeled octanesulfonate binds slightly tighter to SsuD during catalysis in D_2O than in H_2O, but nearly within experimental error of each other. The value of the slowest rate constant ($k_{3,obs}$) remained unchanged (Table 4.1).

4.3.4 Calculation of intrinsic isotope effect and commitments to catalysis

Calculation and analysis of the intrinsic kinetic isotope effect and commitment factors for the SsuD reaction in D_2O revealed a ^{D}k of 1.9 ± 0.6, a c_{Vf} of 0.84 ± 0.58, and a c_{fA} of 8.20 ± 0.38 (Table 4.2). These results are in agreement with the steady-state pH profiles in that they suggest a large forward commitment to catalysis (c_{fA}) with a ratio of catalysis indicating product release occurring faster than the bond-breaking step ($c_{Vf} = k_9/k_{11}$) (*174*, *197*, *201*). Unfortunately, the intrinsic kinetic isotope effect in H_2O along with commitments to catalysis could not be determined from the rapid-reaction kinetic results due

Table 4.2: Intrinsic isotope effects and commitments for SsuD in D_2O	
${}^{D}k$	1.9 ± 0.6^{a}
c_{Vf}	0.84 ± 0.58^{b}
c_{fA}	8.20 ± 0.38^{c}
${}^{D_2O}k_9$	0.54 ± 0.17^{d}
${}^{D_2O}k_{cat}$	0.75 ± 0.04^{d}
${}^{D_2O}(k_{cat}/K_m)_{HA}$	0.95 ± 0.07^{d}
${}^{D_2O}(k_{cat}/K_m)_{DA}$	0.83 ± 0.12^{d}

[a] Value was calculated from equation 4.7
[b] Value was calculated from equation 4.4. c_{Vf} represents the ratio of k_9/k_{11}.
[c] Value was calculated from equation 4.5
[d] previously reported in Table 4.1 of this dissertation

Table 4.2. Intrinsic isotope effects and commitments for SsuD in D_2O

to the inverse isotope effect of 0.73 ± 0.21 s^{-1} μM^{-1} in H_2O (k_H/k_D) on the second-order rate constant ($k_{2,obs}$) determined from the rapid-reaction kinetic studies (Table 4.1). These results could not be reconciled with the steady-state data and efforts to calculate the net rate constant (k_9) corresponding to scheme 4.2. This perplexing finding suggests that the isotope sensitive step pertaining to the deuterated substrate is not realized while monitoring flavin oxidation during single-turnover conditions.

4.4 DISCUSSION

Studies were employed using rapid-reaction kinetic analyses to examine if the inverse isotope effect observed for the SsuD reaction is dependent on flavin oxidation. SsuD has been proposed to utilize a mechanism comparable to the flavin-dependent enzyme cyclohexanone monooxygenase in that a C4a-peroxyflavin (FMN-OO^-) intermediate acts as a nucleophile in the Baeyer–Villiger oxygenation of alkanesulfonic acid (*96*, *160*, *171*, *186*). As with SsuD, previous studies on the cyclohexanone monooxygenase have attributed a fast phase observed at 370 nm in the rapid reaction kinetics studies to a step involving the formation and accumulation of a relatively stable C4a-hydroperoxyflavin (FMN-OOH) intermediate in the absence of substrate (*65*, *95*, *123*, *130*, *131*, *160*, *172*, *202*). Additionally, this C4a-hydroperoxyflavin (FMN-OOH) intermediate of cyclohexanone monooxygenase has been shown to be in slow protonic equilibrium with the C4a-peroxyflavin (FMN-OO^-) intermediate with an observed pK_a value of 8.4 (*65*, *96*). SsuD has been proposed to utilize a similar mechanism to stabilize its C4a-(hydro)peroxyflavin intermediate.

Previously, SsuD has been shown to follow a steady-state ordered binding mechanism with $FMNH_2$ binding first to SsuD, followed by either octanesulfonate or O_2 prior to formation of the C4a-peroxyflavin intermediate that governs the desulfonation reaction (*160*). The complexity of this ter-reactant mechanism prompted the consideration of a simplified bi-reactant kinetic model for the analysis of the current

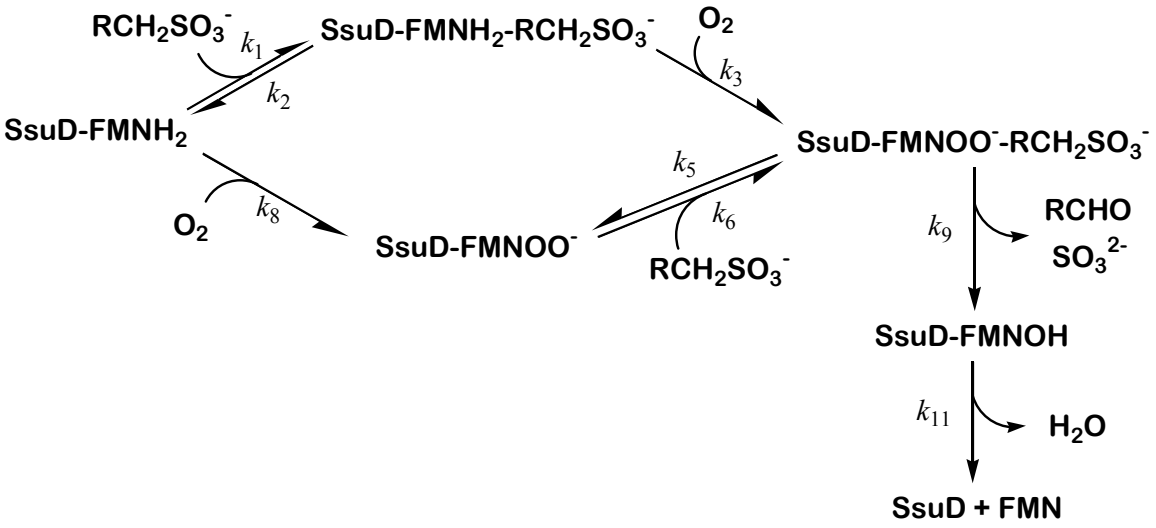

Scheme 4.2. SsuD kinetic mechanism for SsuD reaction adapted from equation 9-63 in reference (*197*)**.**

kinetic isotope effects data (scheme 4.2). The simplified kinetic model works because the first reactant, $FMNH_2$, has been shown previously to bind to SsuD prior to the other substrates. Therefore, $FMNH_2$ binding is reflected by an on-rate constant that will be insensitive to deuterium isotopic substitution; the $k_{cat}/K_{[FMNH2]}$ will be unity and can be ignored in terms of the overall kinetic mechanism (*197*). Previous studies have suggested also that octanesulfonate binds to the SsuD-$FMNH_2$ complex prior to O_2 in order to ensure that formation of the C4a-(hydro)peroxyflavin intermediate is fully coupled to desulfonation (*160*). Additionally, the lack of a substrate and/or solvent isotope effect on $k_{cat}/K_{[octanesulfonate]}$ supports octanesulfonate binding to the SsuD-$FMNH_2$ complex prior to O_2 under steady-state conditions (chapter 3). Nevertheless, the formation of the C4a-(hydro)peroxyflavin intermediate in the absence and at low concentrations of octanesulfonate during rapid-reaction studies supports O_2 binding to SsuD in the absence of octanesulfonate. Therefore, it is possible that the SsuD reaction follows an alternate pathway where O_2 binds prior to octanesulfonate when octanesulfonate concentration is limited (Scheme 4.2) (*160*).

Results from the current study suggest that in the absence of or at low concentrations of octanesulfonate (≤ 100 μM), the formation of FMN-OO^- is immediately followed by a slow protonic equilibrium with FMN-OOH (Scheme 4.2) (*65*, *96*). The rate constant ($k_{1,obs}$) observable even at elevated octanesulfonate concentrations in D_2O but absent in H_2O at increased octanesulfonate concentrations (≥ 100 μM) could correspond to the formation and stabilization of this equilibrium (Table 4.1). In this case, the results suggest that deuterated solvent stabilizes the C4a-(hydro)peroxyflavin intermediate in D_2O, possibly resulting in a pK_a shift that favors accumulation of the FMN-OOH intermediate over the catalytically relevant FMN-OO- intermediate. As a result, the

generation of the C4a-hydroperoxyflavin occurs faster in D_2O than in H_2O resulting in its accumulation and the stabilization of the signal to which it corresponds. For elevated concentrations of octanesulfonate, the C4a-peroxyflavin forms and reacts with the octanesulfonate before protonic equilibrium with FMN-OOH can be established (Scheme 4.1) (*160*). Therefore, it is proposed that the C4a-peroxyflavin is converted to C4a-hydroperoxyflavin in D_2O before it can participate in catalysis resulting in FMN-OOH accumulation even at increased concentrations of octanesulfonate (Figure 4.2A).

Alternatively, the current study also supports the enhanced stabilization of the C4a-peroxyflavin intermediate by Arg226 when in D_2O. In previous studies, the positive charge associated with the protonated form Arg226 was shown to be integral to the stabilization of the C4a-(hydro)peroxyflavin intermediate during rapid-reaction kinetic studies (*186*). Steady-state reaction studies also indicated the pK_a value associated with Arg226 was shifted outwards in D_2O, thus indicating that the protonated, positively charged form of the amino-acid is favored in deuterated solvent (Chapter 3). The increased availability of protonated Arg226 as a result of this pK_a shift may be serving to stabilize the negative charge of the C4a-peroxyflavin intermediate, thus favoring its accumulation in D_2O.

Despite its contributions to the fast rate constant ($k_{1,obs}$), the stabilization of the C4a-(hydro)peroxyflavin intermediate does not appear to limit the overall reaction, as the rate constants extrapolated from kinetic traces of flavin oxidation monitored at 450 nm are similar (within error) in both H_2O and D_2O (Table 4.1). Interestingly, the second order rate constant ($k_{2,obs}$) with a hyperbolic dependence on octanesulfonate concentration exhibits an inverse solvent isotope effect comparable to the steady-state solvent isotope

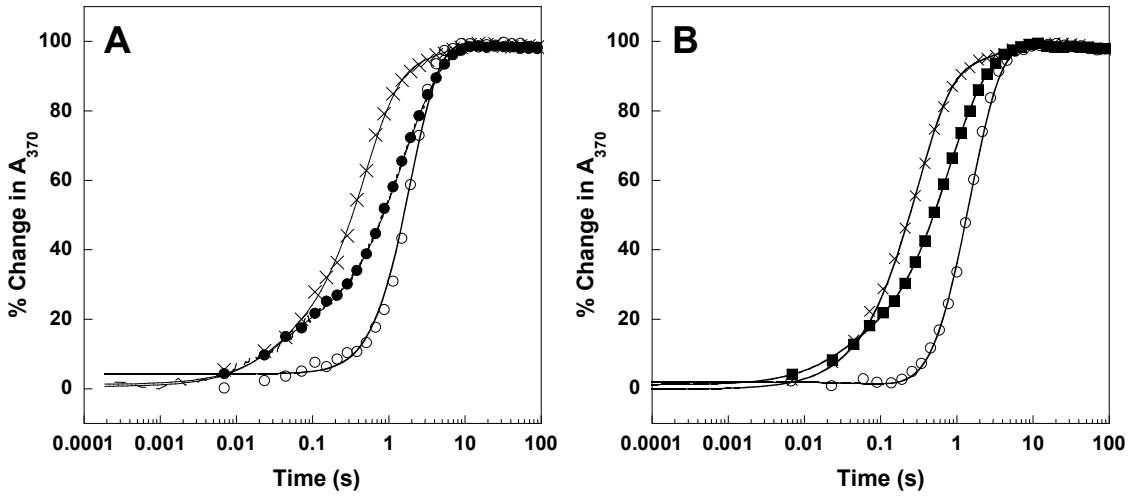

Figure 4.2. Kinetic traces of flavin oxidation by SsuD monitored at 370 nm in D_2O solvent. A: Free $FMNH_2$ (25 μM) mixed with SsuD (35 μM) in air-saturated D_2O buffer (●). Free $FMNH_2$ (25 μM) mixed with SsuD (35μM) and octanesulfonate (1000 μM) in air-saturated D_2O buffer (×). B: Free $FMNH_2$ (25 μM) mixed with SsuD (35μM) and 1-octanesulfonate-1,1-d_2 acid (40 μM) in air-saturated D_2O buffer (■). Free $FMNH_2$ (25 μM) mixed with SsuD (35μM) and 1-octanesulfonate-1,1-d_2 (1000 μM) in air-saturated D_2O buffer (×). All plots include the kinetic trace of free $FMNH_2$ (25 μM) mixed with air-saturated buffer (○) as a reference. The kinetic traces shown are the average of at least three separate experiments. The solid lines are the fits of the kinetic traces to equations 4.1 or 4.2.

effect on k_{cat} suggesting that it may entail the net rate constant (k_9) for SsuD catalysis. In Scheme 4.2, k_9 represents the net rate constant for all steps occurring from the first-irreversible step up to release of the first product; this step will be considered the only step sensitive to isotopic substitution (*197*). In this case, equation 4.3 becomes the expression for k_{cat} based on scheme 4.2 with k_{11} representing the non-pH dependent rate limiting step previously proposed to be a conformational change linked to product release (*186*, *197*). This rate-limiting step is believed to be represented by the slowest of the rate constants from the single-turnover studies, $k_{3(obs)}$. The reverse commitment factor (c_r term) common to the overall expressions for isotope effects on kinetic parameters can be omitted in this case as k_9 is considered a net rate constant that will not be dependent on the concentration of the substrates; thus, the expression for $^{D_2O}k_9$ includes the internal part of the forward as well as all of the reverse commitment (*197*, *201*). As a result, equation 4.4 represents the expression for the isotope effect on k_{cat}. The lack of a kinetic isotope effect on k_{cat}/K_m with varying octanesulfonate gives rise to equation 4.5 and 4.6. In equations 4.5 and 4.6, the value of $^{D}(k_{cat}/K_m)$ becomes unity once O_2 concentration is saturating because octanesulfonate becomes trapped on the enzyme and committed to form product; no isotope effect is observed as a result (*197*).

D_2O also appears to affect either the intrinsic substrate kinetic isotope effect or the equilibrium isotope effect (K_{eq}) for the SsuD reaction. This can be surmised by considering the intrinsic substrate kinetic isotope effect of 1.9 ± 0.6 that was determined from analysis of the SsuD reaction in D_2O. In D_2O, rapid-reaction studies demonstrated that the SsuD reaction follows a textbook steady-state ordered mechanism as the solvent isotope effect ($^{H_2O}k_H/^{D_2O}k_H$) of 0.75 ± 0.04 on k_{cat} is between the limits set by the equilibrium ordered mechanism and Theorell-Chance mechanisms, or $^{D_2O}k_9$ ($^{D_2O}k_{2,obs}$ = 0.54 ± 0.17) and unity,

respectively (Chapter 3). However, the same determination cannot be made from substrate isotope studies in H_2O due to conflicting data obtained from steady-state and single-turnover rapid reaction experimental conditions. By definition, a Theorell-Chance mechanism would require product release to completely limit the overall reaction and the isotope effect on k_{cat} to be unity (*197*, *201*). However, the overall substrate kinetic isotope effect of 3.0 ± 0.2 for k_{cat} and unity for $k_{cat}/K_{[octanesulfonate]}$ determined from the steady-state results eliminates this possibility (Chapter 3). Therefore, the steady-state ordered mechanism requires that the ^{D}k in H_2O be greater than or equal to the overall effect for k_{cat}, unless K_{eq} is normal and large. K_{eq} will be normal and greater than unity if substrate is bonded more tightly, and it will be inverse and less than unity if the product is bonded more tightly (*197*, *201*). The inverse solvent isotope on $k_{2(obs)}$ results from a decrease in the K_d value of unlabeled octanesulfonate in D_2O compared to H_2O (Table 4.1). This decrease in the K_d value may be the result of the enzyme favoring a shift towards product formation in D_2O; tighter, stiffer bonding of the transition state-intermediate resembling the product would favor an inverse isotope effect and is supported by the proton inventory of the SsuD reaction (Chapter 3). Interestingly, the deuterium labeled octanesulfonate K_d value obtained for SsuD reactions performed in D_2O is within error of the value obtained in H_2O (Table 4.1). These results suggest that both the substrate and solvent isotope effects may be due in part to an equilibrium isotope effect. Nevertheless, it should be noted that the two-component nature of the enzyme system implies that the reaction is likely irreversible even under steady-state conditions. If the reaction is irreversible, determination of a true K_{eq} parameter would not be possible.

Although rapid-reaction kinetics studies demonstrated that the rate-limiting step does not occur during flavin oxidation, it is important to understand that these rate constants reflect the kinetics of SsuD under single turnover conditions in the absence of

SsuE. The limiting rate constant ($k_{3,obs}$) of 0.5 s^{-1} (30 min^{-1}) under single-turnover conditions represents a three-fold decrease from the steady-state k_{cat} value (93 min^{-1}), and therefore cannot be catalytically competent (*186*, *203*). This anomaly is likely explained by the absence of SsuE, which is included in the reaction under steady-state conditions. Previous studies have shown that the overall rate of flavin reduction by SsuE is enhanced when SsuD is present in the reaction, potentially as a result of protein-protein interactions occurring between the two enzymes (*155*, *159*). Proton inventories and viscosity studies on SsuD support a rate limiting conformational change as oxidized flavin is released (*178*, *182*, *189*, *196*). If $k_{3(obs)}$ represents a rate-limiting conformational change corresponding to a proton transfer event in the proposed mechanism involving the protonation of FMN-O^- by Arg226, then the presence of SsuE may serve to enhance the rate of this conformational change though protein-protein interactions. This conformational change would result in the enzyme being in an open conformation, and the N5 of the free FMN-OH would be quickly protonated by solvolysis resulting in the rapid dehydration of water and generation of oxidized FMN (Scheme 4.1) (34). Unfortunately, a catalytically competent intrinsic solvent isotope effect for the formation and release of the FMN-OH intermediate could not be determined from the single-turnover experiments.

CHAPTER FIVE

Summary

Two-component flavin-dependent monooxygenases utilize flavin as a co-substrate and are involved in various metabolic and biosynthetic processes in microorganisms. Elucidating the details of the flavin intermediates involved in the catalytic mechanisms of these systems is an area of active investigation. The alkanesulfonate monooxygenase enzyme has been identified in a diverse range of bacterial organisms and utilizes $FMNH_2$ supplied by an independent NAD(P)H dependent FMN reductase (SsuE) to alleviate periods of limited sulfur bioavailability. Catalysis by the monooxygenase enzyme results in the oxygenolytic cleavage of a carbon-sulfur bond from sulfonated substrates to yield free FMN, aldehyde, and metabolically available sulfite. The SsuD mechanism has been determined to be dependent on a C4a-(hydro)peroxyflavin intermediate to catalyze the desulfonation of alkanesulfonates.

5.1 Proposed catalytic mechanism of SsuD

In the SsuD reaction, a C4a-peroxyflavin intermediate is proposed to perform a nucleophilic attack on the sulfur group of the alkanesulfonate substrate (Scheme 3.1, I). The resulting intermediate then undergoes a Baeyer-Villiger rearrangement leading to the cleavage of the alkanesulfonate carbon-sulfur bond and the generation of sulfite and an alkane peroxyflavin intermediate (Scheme 3.1, II). The release of the aldehyde product from the enzyme occurs following abstraction of a proton from the alkane peroxyflavin

intermediate by a catalytic base (Scheme 3.1, III). An active-site acid is then proposed to donate a proton to the $FMNO^-$ intermediate triggering a proposed conformational change that opens the enzyme to solvation and promotes product release (Scheme 3.1, IV).

5.2 Establishment of catalytic active-site acid and active-site base

In order to gain insight into catalytically relevant ionizations governing the desulfonation reaction of SsuD, k_{cat} and k_{cat}/K_m values for wild-type SsuD were measured as a function of pH from 5.8-10.0. The pH dependence of k_{cat} for SsuD revealed two titratable residues with apparent pK_a values of 6.6 ± 0.1 and 9.5 ± 0.1. These results indicate that a group with a pK_a value of around 6.6 must be deprotonated, and a group with a pK_a value of around 9.5 must be protonated in order for the enzyme-substrate complex to convert substrate to product. Interestingly, only one titratable amino acid residue with an apparent pK_a value of 6.9 ± 0.1 was extrapolated from the pH dependence of k_{cat}/K_m, suggesting that a functional group on the free enzyme or substrate must be deprotonated in the conversion of substrate to product.

5.3 Identification of group contributing to pK_a at 6.6.

Despite low amino acid sequence identity, SsuD is similar in overall structure to other flavin-dependent monooxygenases. Structural and functional comparisons of SsuD with bacterial luciferase and LadA have led to the proposal of His228 as the catalytic base. The proposal agrees with the k_{cat} pH profile data in that His228 could contribute the apparent pK_a value of 6.6 ± 0.1. To determine the catalytic role of His228 in the desulfonation reaction by SsuD, several substitutions were introduced into the enzyme, and the mechanistic and catalytic function of these variants evaluated. The H228A SsuD variant showed a two-fold decrease in k_{cat} when compared to the wild-type enzyme. This

slight reduction in activity in conjunction with the presence of sticky proton in the k_{cat} and $k_{cat}/K_{[octanesulfonate]}$ pH dependence profile for the H228A SsuD variant supports the conclusion that His228 serves as a hydrogen bond acceptor and not as an active site base in SsuD.

Cys54 was also evaluated as it is the only cysteine residue present in the wild-type SsuD enzyme. The k_{cat} value for C54A SsuD demonstrated a five-fold decrease in activity from wild-type SsuD as well as the presence of a "hollow" in both the k_{cat} and k_{cat}/K_m pH profiles indicative of a sticky proton during catalysis. The observed hollow on the acidic limb of the pH profile indicates Cys54 would be required for the rapid dissociation of the N1 proton from $FMNH_2$ when octanesulfonate is present. As is the case with bacterial luciferase, the N1 position of $FMNH_2$ is proposed to be contributing to the lower pK_a value in SsuD. Therefore, the results indicate Cys54 of SsuD directly interacts with the C4a-(hydro)peroxyflavin intermediate and promotes its formation by facilitating the dissociation of the proton located at the N1 position of $FMNH_2$.

5.4 Identification of Arg226 as the group contributing to the upper pK_a at 9.5.

Previous studies as well as the elimination of the upper pK_a in the C54A SsuD pH profiles supported Cys54 to be contributing to the pK_a at 9.5. Although these combined results indicate Cys54 is contributing to the upper pK_a in the wild-type enzyme, the modest five-fold drop in the k_{cat} and k_{cat}/K_m values compared to wild-type SsuD did not support Cys54 as the catalytic acid. Given the propensity of an active-site environment to alter the pK_a value of an amino acid, the only other group within the putative active site of SsuD that could be responsible for contributing to the pK_a value at 9.5 is an arginine residue. While SsuD contains several conserved arginine residues, this residue was

estimated to be Arg226 as it is the only arginine residue located within the putative active site. Alanine and lysine substitutions of Arg226 resulted in the inactivation of the enzyme indicating that the amino acid may be responsible for the apparent pK_a value of 9.5 ± 0.1.

5.5 Arg226 serves to stabilize the C4a-hydroperoxyflavin intermediate during SsuD catalysis

Steady-state, pH dependence kinetic studies highlighted Arg226 to be playing a crucial role as the potential active-site acid in SsuD catalysis. As a result, single turnover rapid reaction kinetic studies were performed to investigate the role of Arg226 in catalysis in terms of individual rate constants. Previous studies on SsuD and other flavin-dependent monooxygenases have attributed the initial fast phase observed at 370 nm in the rapid reaction kinetic studies to the formation and accumulation of a relatively stable C4a-hydroperoxyflavin (FMN-OOH) intermediate. This phase was not observed in reactions with R226A and R226K SsuD indicating that Arg226 is serving to stabilize the C4a-(hydro)peroxyflavin intermediate. Results from isotope effect studies further indicted that it is yhe positively charged form of the Arg226 serving to stabilize the C4a-peroxyflavin intermediate.

5.6 Rate-limiting step in SsuD catalysis

The abstraction of the α-proton from the alkane peroxyflavin intermediate has been proposed as one of several potential rate-limiting chemical steps in SsuD catalysis. Therefore, substitution of the α-protons of octanesulfonate with deuterium was performed in order to probe the proton abstraction step (Scheme 3.1, III). Although a substrate kinetic isotope effect of three supported proton abstraction as the rate-limiting chemical

step, steady-state pH dependence and proton inventory experiments indicated product release to be the overall rate limiting step in SsuD catalysis.

5.7 Role of Arg226 during product release

The outwards displacement or broadening observed between of the apparent pK_a values seen in the k_{cat} pH profile for guanidinium rescue experiments is indicative of a non-pH dependent, but normally rate limiting, slow product release step following the catalytic reaction. The result indicates Arg226 plays a role in product release. Additionally, the solvent isotope effect data along with the corresponding proton inventory results support Arg226 donating a proton to the $FMNO^-$ intermediate triggering a proposed conformational change that opens the enzyme to solvation and promotes product release.

5.8 Conclusion

The combined results of these studies support Cys54 and Arg226 of SsuD playing multiple roles in SsuD catalysis. First, Cys54 promotes oxygen activation of $FMNH_2$ by facilitating the dissociation of the proton located at the N1 position. Second, the protonated, positively charged form of Arg226 stabilizes the C4a-(hydro)peroxyflavin intermediate. The stabilization of intermediate is followed by a nucleophilic attack on the C-S bond of the alkanesulfonate substrate and a Baeyer-Villiger rearrangement leading to the cleavage of the alkanesulfonate carbon-sulfur bond and the generation of sulfite and an alkane peroxyflavin intermediate. Finally, Arg226 serves to protonate the $FMNO^-$ intermediate, thereby triggering a conformational change that results in product release.

REFERENCES

1. Fruton, J. S. (1999) Proteins, Enzymes, Genes: The Interplay of Chemistry and Biology. Yale University Press.
2. Bugg, T. D. H. (2001) The development of mechanistic enzymology in the 20th century, *Natural Product Reports 18*, 465–493.
3. Fischer, E. (1894) Einfluss der Configuration auf die Wirkung der Enzyme, *Ber. Chem. 27*, 2985–2993.
4. Naturhistorisch-Medizinischer Verein, H. (1877) Verhandlungen. Cited from http://books.google.com/books?id=jzdMAAAAYAAJ
5. Nobelprize.org.
6. Buchner, E. (1897) Alkoholische Gärung ohne Hefezellen, *Ber. Chem. 30*, 1110–1113.
7. Kresge, N., Simoni, R. D., and Hill, R. L. (2005) Otto Fritz Meyerhof and the Elucidation of the Glycolytic Pathway, *J. Biol. Chem. 280*, e3.
8. Otto Meyerhof and the Physiology Institute: the Birth of Modern Biochemistry. Cited from http://www.nobelprize.org/nobel_prizes/medicine/articles/states/otto-meyerhof.html
9. Harden, A., and Young, W. J. (1906) The Alcoholic Ferment of Yeast-Juice, *Proc. R. Soc. B. Biol. Sci. 77*, 405–420.

10. Raymond, A. L., and Winegarden, H. M. (1927) Cozymase. A Study of Purification Methods., *J. Biol. Chem. 74*, 175 –188.

11. von Euler, H., and Myrback, K. (1927), *Z. Physiol. Chem. 165*, 28.

12. von Euler, H., and Nilsson, R. (1926), *Z. Physiol. Chem. 162*, 72.

13. von Euler, H., and Myraback, K. (1923) Garungs-co-Enzym der Hefe. I., *Z. Physiol. Chem. 131*, 179–203.

14. von Euler, H., Myraback, K., and Nilsson, R. (1928) Neuere Forschungen uber den enzymatischen Kohlenhydratabbau (I). Die Mutation als einleitende Reaktion des Glucose-Abbaues und das dara beteiligte Enzymsystem., *Erg. Physiol. 26*, 531–567.

15. Michaelis, L., and Menten, M. L. (1913) Die Kinetik der Invertinwirkung, *Biochem. Z. 49*, 333–369.

16. Briggs, G. E., and Haldane, J. B. (1925) A Note on the Kinetics of Enzyme Action., *Biochem. J. 19*, 338–340.

17. Eadie, G. S. (1942) The Inhibition of Cholinesterase by Physostigmine and Prostigmine, *J. Biol. Chem. 146*, 85–93.

18. Lineweaver, H., and Burk, D. (1934) The Determination of Enzyme Dissociation Constants, *J. Am. Chem. Soc. 56*, 658–666.

19. Armstrong, E. F. (1930) Enzymes. By J.B.S. Haldane, M.A. Monographs on Biochemistry. Edited by R.H.A. Plimmer, D.Sc., and Sir F. G. Hopkins, M.A., M.B., D.Sc., F.R.S. Pp. vii+235. London: Longmans, Green & Co., 1930., *J. Soc. Chem. Ind. 49*, 919–920.

20. Hartridge, H., and Roughton, F. J. W. (1923) A Method of Measuring the Velocity of Very Rapid Chemical Reactions, *Proc. R. Soc. A. Math. Phys. Eng. Sci. 104*, 376–394.

21. Roughton, F. J. W. (1934) The Kinetics of Haemoglobin VI--The Competition of Carbon Monoxide and Oxygen for Haemoglobin, *Proc. R. Soc. B. Biol. Sci. 115*, 473–495.

22. Sumner, J. B. (1926) The Isolation and Crystallization of the Enzyme Urease, *J. Biol. Chem. 69*, 435 –441.

23. Northrop, J. H. (1929) Crystalline Pepsin, *Science 69*, 580.

24. Northrop, J. H., and Kunitz, M. (1932) Crystalline Trypsin: I. Isolation and Test Purity, *J. Gen. Physiol. 16*, 267–294.

25. Kunitz, M., and Northrop, J. H. (1935) Crystalline Chymo-Trypsin and Chymo-Trypsinogen : I. Isolation, Crystallization, and General Properties of a New Proteolytic Enzyme and Its Precursor, *J. Gen. Physiol. 18*, 433–458.

26. Guzmán-Casado, M., and Parody-Morreale, A. (2002) Notes on the Early History of the Interaction between Physical Chemistry and Biochemistry: The Development of Physical Biochemistry, *J. Chem. Edu. 79*, 327.

27. Rosenfeld, L. (1997) Vitamine--vitamin. The early years of discovery, *Clin. Chem. 43*, 680–685.

28. Wagner, A. (1975) Vitamins and coenzymes. R.E. Krieger Pub. Co, Huntington, N.Y.

29. Pauling, L., and Coryell, C. D. (1936) The Magnetic Properties and Structure of the Hemochromogens and Related Substances, *Proc. Natl. Acad. Sci. U.S.A. 22*, 159–163.

30. Pauling, L., and Coryell, C. D. (1936) The Magnetic Properties and Structure of Hemoglobin, Oxyhemoglobin and Carbonmonoxyhemoglobin, *Proc. Natl. Acad. Sci. U.S.A. 22*, 210–216.

31. Barker, H. A., Smyth, R. D., Weissbach, H., Munch-Petersen, A., Toohey, J. I., Ladd, J. N., Volcani, B. E., and Wilson, R. M. (1960) Assay, Purification, and Properties of the Adenylcobamide Coenzyme, *J. Biol. Chem. 235*, 181 –190.

32. Watson, J. D., and Crick, F. H. (1953) Molecular structure of nucleic acids; a structure for deoxyribose nucleic acid, *Nature 171*, 737–738.

33. Kendrew, J. C., Dickerson, R. E., Strandberg, B. E., Hart, R. G., Davies, D. R., Phillips, D. C., and Shore, V. C. (1960) Structure of myoglobin: A three-dimensional Fourier synthesis at 2 A. resolution, *Nature 185*, 422–427.

34. Perutz, M. F., Rossmann, M. G., Cullis, A. F., Muirhead, H., Will, G., and North, A. C. (1960) Structure of haemoglobin: a three-dimensional Fourier synthesis at 5.5-A. resolution, obtained by X-ray analysis, *Nature 185*, 416–422.

35. Blake, C. C., Koenig, D. F., Mair, G. A., North, A. C., Phillips, D. C., and Sarma, V. R. (1965) Structure of hen egg-white lysozyme. A three-dimensional Fourier synthesis at 2 Angstrom resolution, *Nature 206*, 757–761.

36. Phillips, D. C. (1966) The three-dimensional structure of an enzyme molecule, *Sci. Am. 215*, 78–90.

37. Blake, C. C., Johnson, L. N., Mair, G. A., North, A. C., Phillips, D. C., and Sarma, V. R. (1967) Crystallographic studies of the activity of hen egg-white lysozyme, *Proc. R. Soc. Lond., B, Biol. Sci. 167*, 378–388.

38. Johnson, L. N., and Phillips, D. C. (1965) Structure of some crystalline lysozyme-inhibitor complexes determined by X-ray analysis at 6 Angstrom resolution, *Nature 206*, 761–763.

39. Sinnott, M. L. (1990) Catalytic mechanism of enzymic glycosyl transfer, *Chem. Rev. 90*, 1171–1202.

40. Vocadlo, D. J., Davies, G. J., Laine, R., and Withers, S. G. (2001) Catalysis by hen egg-white lysozyme proceeds via a covalent intermediate, *Nature 412*, 835–838.

41. Hutchison, C. A., 3rd, Phillips, S., Edgell, M. H., Gillam, S., Jahnke, P., and Smith, M. (1978) Mutagenesis at a specific position in a DNA sequence, *J. Biol. Chem. 253*, 6551–6560.

42. Winter, G., Fersht, A. R., Wilkinson, A. J., Zoller, M., and Smith, M. (1982) Redesigning enzyme structure by site-directed mutagenesis: tyrosyl tRNA synthetase and ATP binding, *Nature 299*, 756–758.

43. Wilkinson, A. J., Fersht, A. R., Blow, D. M., and Winter, G. (1983) Site-directed mutagenesis as a probe of enzyme structure and catalysis: tyrosyl-tRNA synthetase cysteine-35 to glycine-35 mutation, *Biochemistry 22*, 3581–3586.

44. Wilkinson, A. J., Fersht, A. R., Blow, D. M., Carter, P., and Winter, G. (1984) A large increase in enzyme-substrate affinity by protein engineering, *Nature 307*, 187–188.

45. Saiki, R. K., Scharf, S., Faloona, F., Mullis, K. B., Horn, G. T., Erlich, H. A., and Arnheim, N. (1985) Enzymatic amplification of beta-globin genomic sequences and restriction site analysis for diagnosis of sickle cell anemia, *Science 230*, 1350–1354.

46. Kunkel, T. A. (1985) Rapid and efficient site-specific mutagenesis without phenotypic selection, *Proc. Natl. Acad. Sci. U.S.A. 82*, 488–492.

47. Kohler, R. E. (1982) From Medical Chemistry to Biochemistry: The Making of a Biomedical Discipline. Cambridge University Press.

48. Blyth, A. W. (1879) The composition of cows' milk in health and disease, *J. Chem. Soc. Trans. 35*, 530.

49. Kühling, O. (1899) Ueber die Reduction des Tolualloxazins, *Ber. Chem. 32*, 1650–1653.

50. Goldberger, J., Wheeler, G. A., Lillie, R. D., and Rogers, L. M. (1926) A Further Study of Butter, Fresh Beef, and Yeast as Pellagra Preventives, with Consideration of the Relation of Factor P-P of Pellagra (and Black Tongue of Dogs) to Vitamin B, *Public Health Reports 41*, 297.

51. Kuhn, R., György, P., and Wagner-Jauregg, T. (1933) Über Lactoflavin, den Farbstoff der Molke, *Ber. Chem. 66*, 1034–1038.

52. György, P., and Eckardt, R. E. (1940) Further investigations on vitamin B(6) and related factors of the vitamin B(2) complex in rats. Parts I and II, *Biochem. J. 34*, 1143–1154.

53. Rajakumar, K. (2000) Pellagra in the United States: a historical perspective, *South. Med. J. 93*, 272–277.

54. Bapurao, S., and Krishnaswamy, K. (1978) Vitamin B6 nutritional status of pellagrins and their leucine tolerance, *Am. J. Clin. Nutr. 31*, 819–824.

55. Szent-Györgyi, A. (1930) On the Mechanism of Biological Oxidation and the Function of the Suprarenal Gland, *Science 72*, 125–126.

56. Ellinger, P., and Koschara, W. (1934) The Lyochromes: a New Group of Animal Pigments, *Nature 133*, 553–556.

57. Theorell, H., Karrer, P., Schapp, K., and Frei, P. (1935) Flavinphosphorsaure aus Leber, *H. Chem. Acta. 18*, 1022–1026.

58. Warburg, O., and Christian, W. (1936) Über Nikotinsäure-amid und Luminoflavin, *Ber. Chem. 69*, 228–228.

59. Kuhn, R., Rudy, H., and Weygand, F. (1936) Synthese der Lactoflavin-5′-Phosphorsäure, *Ber. Chem. 69*, 1543–1547.

60. Massey, V. (1994) Activation of molecular oxygen by flavins and flavoproteins, *J. Biol. Chem. 269*, 22459–22462.

61. Massey, V. (2000) The chemical and biological versatility of riboflavin, *Biochem. Soc. Trans. 28*, 283–296.

62. Warburg, O., and Christian, W. (1938) Isolierung der prosthetischen Gruppe der d-Aminosaureoxydase, *Biochem. Z. 298*, 150–168.

63. Müller, F. (1987) Flavin radicals: chemistry and biochemistry, *Free Radic. Biol. Med. 3*, 215–230.

64. Mewies, M., McIntire, W. S., and Scrutton, N. S. (1998) Covalent attachment of flavin adenine dinucleotide (FAD) and flavin mononucleotide (FMN) to enzymes: the current state of affairs, *Protein Sci. 7*, 7–20.

65. Palfey, B. A., and McDonald, C. A. (2010) Control of catalysis in flavin-dependent monooxygenases, *Arch. Biochem. Biophys. 493*, 26–36.

66. Massey, V., Palmer, G., and Bennett, R. (1961) The purification and some properties of D-amino acid oxidase, *Biochim. Biophys. Acta 48*, 1–9.

67. Bernath, P., and Singer, T. P. (1962) Succinic dehydrogenase, in *Meth. Enzymol.*, pp 597–614. Elsevier.

68. Mize, C. E., and Langdon, R. G. (1962) Hepatic glutathione reductase. I. Purification and general kinetic properties, *J. Biol. Chem. 237*, 1589–1595.

69. Hosokawa, K., and Stanier, R. Y. (1966) Crystallization and properties of p-hydroxybenzoate hydroxylase from Pseudomonas putida, *J. Biol. Chem. 241*, 2453–2460.

70. Venkataram, U. V., and Bruice, T. C. (1984) On the mechanism of flavin-catalyzed dehydrogenation α, β to an acyl function. The mechanism of 1,5-dihydroflavin reduction of maleimides, *J. Am. Chem. Soc. 106*, 5703–5709.

71. Hamilton, G. A., and Brown, L. E. (1970) Model reactions and a general mechanism for flavoenzyme-catalyzed dehydrogenations, *J. Chem. Soc. 92*, 7225–7227.

72. Bruice, T. C. (1984) Oxygen-flavin chemistry, *Israel. J. Chem. 24*, 54–61.

73. Gibson, Q. H., and Hastings, J. W. (1962) The oxidation of reduced flavin mononucleotide by molecular oxygen, *Biochem. J. 83*, 368–377.

74. Francis, K. (2004) Involvement of a Flavosemiquinone in the Enzymatic Oxidation of Nitroalkanes Catalyzed by 2-Nitropropane Dioxygenase, *J. Biol. Chem. 280*, 5195–5204.

75. Kemal, C., Chan, T. W., and Bruice, T. C. (1977) Reaction of 3O2 with dihydroflavins. 1-N3,5-dimethyl-1,5-dihydrolumiflavin and 1,5-dihydroisoalloxazines, *J. Am. Chem. Soc. 99*, 7272–7286.

76. Schopfer, L. M., Massey, V., Ghisla, S., and Thorpe, C. (1988) Oxidation-reduction of general acyl-CoA dehydrogenase by the butyryl-CoA/crotonyl-CoA couple. A new investigation of the rapid reaction kinetics, *Biochemistry 27*, 6599–6611.

77. Ghisla, S., and Edmondson, D. E. (2009) Flavin Coenzymes, in *Encyclopedia of Life Sciences* (John Wiley & Sons, Ltd, Ed.). John Wiley & Sons, Ltd, Chichester, UK.

78. Walsh, C. T., Schonbrunn, A., and Abeles, R. H. (1971) Studies on the mechanism of action of D-amino acid oxidase. Evidence for removal of substrate -hydrogen as a proton, *J. Biol. Chem. 246*, 6855–6866.

79. Porter, D. J., Voet, J. G., and Bright, H. J. (1973) Direct evidence for carbanions and covalent N 5 -flavin-carbanion adducts as catalytic intermediates in the oxidation of nitroethane by D-amino acid oxidase, *J. Biol. Chem. 248*, 4400–4416.

80. Walsh, C., Lockridge, O., Massey, V., and Abeles, R. (1973) Studies on the mechanism of action of the flavoenzyme lactate oxidase. Oxidation and elimination with β-chlorolactate, *J. Biol. Chem. 248*, 7049–7054.

81. Williams, R. F., Shinkai, S., and Bruice, T. C. (1975) Radical mechanisms for 1,5-dihydroflavin reduction of carbonyl compounds, *Proc. Natl. Acad. Sci. U.S.A. 72*, 1763–1767.

82. Novak, M., and Bruice, T. C. (1980) Mechanistic investigation of the oxidation of the carbanion of methyl 2-methoxy-2-phenylacetate by an isoalloxazine, *J. Chem. Soc. Chem. Comm.* 372.

83. Miller, A., and Bruice, T. C. (1979) Oxidations by a 4a-hydroperoxyisoalloxazine hindered in the 9a and 10a positions, *J. Chem. Soc. Chem. Comm.* 896.

84. Bruice, T. C., and Miller, A. (1980) Products of the decomposition of the anion of a 4a-hydroperoxyisoalloxazine hindered in the 9a and 10a positions, *J. Chem. Soc. Chem. Comm.* 693.

85. Strickland, S., and Massey, V. (1973) The mechanism of action of the flavoprotein melilotate hydroxylase, *J. Biol. Chem. 248*, 2953–2962.

86. Entsch, B., Ballou, D. P., and Massey, V. (1976) Flavin-oxygen derivatives involved in hydroxylation by p-hydroxybenzoate hydroxylase, *J. Biol. Chem. 251*, 2550–2563.

87. Massey, V., Müller, F., Feldberg, R., Schuman, M., Sullivan, P. A., Howell, L. G., Mayhew, S. G., Matthews, R. G., and Foust, G. P. (1969) The reactivity of flavoproteins with sulfite. Possible relevance to the problem of oxygen reactivity, *J. Biol. Chem. 244*, 3999–4006.

88. Hemmerich, P., Massey, V., and Weber, G. (1967) Photo-induced Benzyl Substitution of Flavins by Phenylacetate: a Possible Model for Flavoprotein Catalysis, *Nature 213*, 728–730.

89. Sutton, W. B. (1954) Isolation and properties of a lactic oxidative decarboxylase from Mycobacterium phlei, *J. Biol. Chem. 210*, 309–320.

90. Sutton, W. B. (1955) Sulfhydryl and prosthetic groups of lactic oxidative decarboxylase from Mycobacterium phlei, *J. Biol. Chem. 216*, 749–761.

91. Hayaishi, O., and Sutton, W. B. (1957) Enzymatic Oxygen Fixation Into Acetate Concomitant with the Enzymatic Decarboxylation of L-Lactate, *J. Am. Chem. Soc. 79*, 4809–4810.

92. Land, E. J., and Swallow, A. J. (1969) One-electron reactions in biochemical systems as studied by pulse radiolysis. II. Riboflavine, *Biochemistry 8*, 2117–2125.

93. Faraggi, M., and Klapper, M. H. (1979) One-electron reduction of flavodoxin. A fast kinetic study, *J. Biol. Chem. 254*, 8139–8142.

94. Orru, R., Dudek, H. M., Martinoli, C., Torres Pazmiño, D. E., Royant, A., Weik, M., Fraaije, M. W., and Mattevi, A. (2011) Snapshots of enzymatic Baeyer-Villiger catalysis: oxygen activation and intermediate stabilization, *J. Biol. Chem. 286*, 29284–29291.

95. Ryerson, C. C., Ballou, D. P., and Walsh, C. (1982) Mechanistic studies on cyclohexanone oxygenase, *Biochemistry 21*, 2644–2655.

96. Sheng, D., Ballou, D. P., and Massey, V. (2001) Mechanistic studies of cyclohexanone monooxygenase: chemical properties of intermediates involved in catalysis, *Biochemistry 40*, 11156–11167.

97. Entsch, B., Cole, L. J., and Ballou, D. P. (2005) Protein dynamics and electrostatics in the function of p-hydroxybenzoate hydroxylase, *Arch. Biochem. Biophys. 433*, 297–311.

98. Nakamura, S., Ogura, Y., Yano, K., Higashi, N., and Arima, K. (1970) Kinetic studies on the reaction mechanism of p-hydroxybenzoate hydroxylase, *Biochemistry 9*, 3235–3242.

99. Bigi, F., Casiraghi, G., Casnati, G., Sartori, G., Gasparri Fava, G., and Ferrari Belicchi, M. (1985) Asymmetric electrophilic substitution on phenols. Enantioselective ortho-hydroxyalkylation mediated by chiral alkoxyaluminum chlorides, *J. Org. Chem. 50*, 5018–5022.

100. Wessiak, A., Schopfer, L. M., and Massey, V. (1984) pH dependence of the reoxidation of p-hydroxybenzoate hydroxylase 2,4-dihydroxybenzoate complex, *J. Biol. Chem. 259*, 12547–12556.

101. Anderson, R. F., Patel, K. B., and Vojnovic, B. (1991) Absorption spectra of radical forms of 2,4-dihydroxybenzoic acid, a substrate for p-hydroxybenzoate hydroxylase, *J. Biol. Chem. 266*, 13086–13090.

102. Ortiz-Maldonado, M., Ballou, D. P., and Massey, V. (1999) Use of Free Energy Relationships to Probe the Individual Steps of Hydroxylation of p-Hydroxybenzoate Hydroxylase: Studies with a Series of 8-Substituted Flavins., *Biochemistry 38*, 8124–8137.

103. Palfey, B. A., Entsch, B., Ballou, D. P., and Massey, V. (1994) Changes in the Catalytic Properties of p-Hydroxybenzoate Hydroxylase Caused by the Mutation Asn300Asp, *Biochemistry 33*, 1545–1554.

104. Malito, E., Alfieri, A., Fraaije, M. W., and Mattevi, A. (2004) Crystal structure of a Baeyer-Villiger monooxygenase, *Proc. Natl. Acad. Sci. U.S.A. 101*, 13157–13162.

105. Mirza, I. A., Yachnin, B. J., Wang, S., Grosse, S., Bergeron, H., Imura, A., Iwaki, H., Hasegawa, Y., Lau, P. C. K., and Berghuis, A. M. (2009) Crystal Structures of Cyclohexanone Monooxygenase Reveal Complex Domain Movements and a Sliding Cofactor, *J. Am. Chem. Soc. 131*, 8848–8854.

106. Fraaije, M. W., Kamerbeek, N. M., van Berkel, W. J. H., and Janssen, D. B. (2002) Identification of a Baeyer–Villiger monooxygenase sequence motif, *FEBS Letters 518*, 43–47.

107. Ellis, H. R. (2010) The FMN-dependent two-component monooxygenase systems, *Arch. Biochem. Biophys. 497*, 1–12.

108. Tu, S.-C. (2001) Reduced Flavin: Donor and Acceptor Enzymes and Mechanisms of Channeling, *Antioxidants & Redox Signaling 3*, 881–897.

109. Arunachalam, U., Massey, V., and Vaidyanathan, C. S. (1992) p-Hydroxyphenylacetate-3-hydroxylase. A two-protein component enzyme, *J. Biol. Chem. 267*, 25848–25855.

110. Kantz, A., Chin, F., Nallamothu, N., Nguyen, T., and Gassner, G. T. (2005) Mechanism of flavin transfer and oxygen activation by the two-component flavoenzyme styrene monooxygenase, *Arch. Biochem. Biophys. 442*, 102–116.

111. Xun, L., and Webster, C. M. (2004) A monooxygenase catalyzes sequential dechlorinations of 2,4,6-trichlorophenol by oxidative and hydrolytic reactions, *J. Biol. Chem. 279*, 6696–6700.

112. Gisi, M. R., and Xun, L. (2003) Characterization of chlorophenol 4-monooxygenase (TftD) and NADH: flavin adenine dinucleotide oxidoreductase (TftC) of Burkholderia cepacia AC1100, *J. Bacteriol. 185*, 2786–2792.

113. Parry, R. J., and Li, W. (1997) Purification and characterization of isobutylamine N-hydroxylase from the valanimycin producer Streptomyces viridifaciens MG456-hF10, *Arch. Biochem. Biophys. 339*, 47–54.

114. Yeh, E., Cole, L. J., Barr, E. W., Bollinger,, J. M., Ballou, D. P., and Walsh, C. T. (2006) Flavin Redox Chemistry Precedes Substrate Chlorination during the Reaction of the Flavin-Dependent Halogenase RebH, *Biochemistry 45*, 7904–7912.

115. Kirchner, U., Westphal, A. H., Müller, R., and van Berkel, W. J. H. (2003) Phenol hydroxylase from Bacillus thermoglucosidasius A7, a two-protein component monooxygenase with a dual role for FAD, *J. Biol. Chem. 278*, 47545–47553.

116. Sucharitakul, J., Chaiyen, P., Entsch, B., and Ballou, D. P. (2006) Kinetic mechanisms of the oxygenase from a two-component enzyme, p-hydroxyphenylacetate 3-hydroxylase from Acinetobacter baumannii, *J. Biol. Chem. 281*, 17044–17053.

117. Chaiyen, P., Suadee, C., and Wilairat, P. (2001) A novel two-protein component flavoprotein hydroxylase, *Eur. J. Biochem. 268*, 5550–5561.

118. Strehler, B. L., Harvey, E. N., Chang, J. J., and Cormier, M. J. (1954) The Luminescent Oxidation of Reduced Riboflavin or Reduced Riboflavin Phosphate In the Bacterial Luciferin-Luciferase Reaction, *Proc. Natl. Acad. Sci. U.S.A. 40*, 10–12.

119. Nicoli, M. Z., Meighen, E. A., and Hastings, J. W. (1974) Bacterial luciferase. Chemistry of the reactive sulfhydryl, *J. Biol. Chem. 249*, 2385–2392.

120. Campbell, Z. T., Weichsel, A., Montfort, W. R., and Baldwin, T. O. (2009) Crystal structure of the bacterial luciferase/flavin complex provides insight into the function of the beta subunit, *Biochemistry 48*, 6085–6094.

121. Meighen, E. A. (1991) Molecular biology of bacterial bioluminescence, *Microbiol. Rev. 55*, 123–142.

122. Abu-Soud, H. M., Clark, A. C., Francisco, W. A., Baldwin, T. O., and Raushel, F. M. (1993) Kinetic destabilization of the hydroperoxy flavin intermediate by site-directed modification of the reactive thiol in bacterial luciferase, *J. Biol. Chem. 268*, 7699–7706.

123. Hastings, J. W., and Balny, C. (1975) The oxygenated bacterial luciferase-flavin intermediate. Reaction products via the light and dark pathways, *J. Biol. Chem. 250*, 7288–7293.

124. Paquatte, O., and Tu, S. C. (1989) Chemical modification and characterization of the alpha cysteine 106 at the Vibrio harveyi luciferase active center, *Photochem. Photobiol. 50*, 817–825.

125. Francisco, W. A., Abu-Soud, H. M., DelMonte, A. J., Singleton, D. A., Baldwin, T. O., and Raushel, F. M. (1998) Deuterium kinetic isotope effects and the mechanism of the bacterial luciferase reaction, *Biochemistry 37*, 2596–2606.

126. Feng, L., Wang, W., Cheng, J., Ren, Y., Zhao, G., Gao, C., Tang, Y., Liu, X., Han, W., Peng, X., Liu, R., and Wang, L. (2007) Genome and proteome of long-chain alkane degrading Geobacillus thermodenitrificans NG80-2 isolated from a deep-subsurface oil reservoir, *Proceedings of the National Academy of Sciences 104*, 5602–5607.

127. Li, L., Liu, X., Yang, W., Xu, F., Wang, W., Feng, L., Bartlam, M., Wang, L., and Rao, Z. (2008) Crystal structure of long-chain alkane monooxygenase (LadA) in complex with coenzyme FMN: unveiling the long-chain alkane hydroxylase, *J. Mol. Biol. 376*, 453–465.

128. Eichhorn, E., Davey, C. A., Sargent, D. F., Leisinger, T., and Richmond, T. J. (2002) Crystal structure of Escherichia coli alkanesulfonate monooxygenase SsuD, *J. Mol. Biol. 324*, 457–468.

129. Eichhorn, E., van der Ploeg, J. R., and Leisinger, T. (1999) Characterization of a two-component alkanesulfonate monooxygenase from Escherichia coli, *J. Biol. Chem. 274*, 26639–26646.

130. Valton, J., Filisetti, L., Fontecave, M., and Nivière, V. (2004) A two-component flavin-dependent monooxygenase involved in actinorhodin biosynthesis in Streptomyces coelicolor, *J. Biol. Chem. 279*, 44362–44369.

131. Valton, J., Mathevon, C., Fontecave, M., Nivière, V., and Ballou, D. P. (2008) Mechanism and regulation of the two-component FMN-dependent monooxygenase ActVA-ActVB from Streptomyces coelicolor, *J. Biol. Chem. 283*, 10287–10296.

132. Thibaut, D., Ratet, N., Bisch, D., Faucher, D., Debussche, L., and Blanche, F. (1995) Purification of the two-enzyme system catalyzing the oxidation of the D-proline residue of pristinamycin IIB during the last step of pristinamycin IIA biosynthesis, *J. Bacteriol. 177*, 5199–5205.

133. Blanc, V., Lagneaux, D., Didier, P., Gil, P., Lacroix, P., and Crouzet, J. (1995) Cloning and analysis of structural genes from Streptomyces pristinaespiralis encoding enzymes involved in the conversion of pristinamycin IIB to

pristinamycin IIA (PIIA): PIIA synthase and NADH:riboflavin 5'-phosphate oxidoreductase, *J. Bacteriol. 177*, 5206–5214.

134. Uetz, T., Schneider, R., Snozzi, M., and Egli, T. (1992) Purification and characterization of a two-component monooxygenase that hydroxylates nitrilotriacetate from "Chelatobacter" strain ATCC 29600, *J. Bacteriol. 174*, 1179–1188.

135. Knobel, H. R., Egli, T., and van der Meer, J. R. (1996) Cloning and characterization of the genes encoding nitrilotriacetate monooxygenase of Chelatobacter heintzii ATCC 29600, *J. Bacteriol. 178*, 6123–6132.

136. Xu, Y., Mortimer, M. W., Fisher, T. S., Kahn, M. L., Brockman, F. J., and Xun, L. (1997) Cloning, sequencing, and analysis of a gene cluster from Chelatobacter heintzii ATCC 29600 encoding nitrilotriacetate monooxygenase and NADH:flavin mononucleotide oxidoreductase, *J. Bacteriol. 179*, 1112–1116.

137. Nissen, M. S., Youn, B., Knowles, B. D., Ballinger, J. W., Jun, S.-Y., Belchik, S. M., Xun, L., and Kang, C. (2008) Crystal structures of NADH:FMN oxidoreductase (EmoB) at different stages of catalysis, *J. Biol. Chem. 283*, 28710–28720.

138. Payne, J. W., Bolton, H., Jr, Campbell, J. A., and Xun, L. (1998) Purification and characterization of EDTA monooxygenase from the EDTA-degrading bacterium BNC1, *J. Bacteriol. 180*, 3823–3827.

139. Bohuslavek, J., Payne, J. W., Liu, Y., Bolton, H., Jr, and Xun, L. (2001) Cloning, sequencing, and characterization of a gene cluster involved in EDTA degradation from the bacterium BNC1, *Appl. Environ. Microbiol. 67*, 688–695.

140. Münz, F. (1929) Anwendung von dispergierenden Mitteln bei durch hartes Wasser entstehenden Ausscheidungen, *Zeitschrift für Angewandte Chemie 42*, 734–736.

141. Kertesz, M. A. (2000) Riding the sulfur cycle--metabolism of sulfonates and sulfate esters in gram-negative bacteria, *FEMS Microbiol. Rev. 24*, 135–175.

142. Stipanuk, M. H. (1986) Metabolism of sulfur-containing amino acids, *Annu. Rev. Nutr. 6*, 179–209.

143. Hell, R. (1997) Molecular physiology of plant sulfur metabolism, *Planta 202*, 138–148.

144. Verschueren, K. H., and Wilkinson, A. J. (2005) Sulfide: Biosynthesis from Sulfate, in *Encyclopedia of Life Sciences* (John Wiley & Sons, Ltd, Ed.). John Wiley & Sons, Ltd, Chichester, UK.

145. Marzluf, G. A. (1997) Molecular genetics of sulfur assimilation in filamentous fungi and yeast, *Annu. Rev. Microbiol. 51*, 73–96.

146. Evers, M., Saftig, P., Schmidt, P., Hafner, A., McLoghlin, D. B., Schmahl, W., Hess, B., von Figura, K., and Peters, C. (1996) Targeted disruption of the arylsulfatase B gene results in mice resembling the phenotype of mucopolysaccharidosis VI, *Proc. Natl. Acad. Sci. U.S.A. 93*, 8214–8219.

147. Franco, B., Meroni, G., Parenti, G., Levilliers, J., Bernard, L., Gebbia, M., Cox, L., Maroteaux, P., Sheffield, L., Rappold, G. A., Andria, G., Petit, C., and Ballabio, A. (1995) A cluster of sulfatase genes on Xp22.3: mutations in chondrodysplasia punctata (CDPX) and implications for warfarin embryopathy, *Cell 81*, 15–25.

148. Quadroni, M., Staudenmann, W., Kertesz, M., and James, P. (1996) Analysis of global responses by protein and peptide fingerprinting of proteins isolated by two-

dimensional gel electrophoresis. Application to the sulfate-starvation response of Escherichia coli, *Eur. J. Biochem. 239*, 773–781.

149. Dainese, P., Staudenmann, W., Quadroni, M., Korostensky, C., Gonnet, G., Kertesz, M., and James, P. (1997) Probing protein function using a combination of gene knockout and proteome analysis by mass spectrometry, *Electrophoresis 18*, 432–442.

150. van Der Ploeg, J. R., Iwanicka-Nowicka, R., Bykowski, T., Hryniewicz, M. M., and Leisinger, T. (1999) The Escherichia coli ssuEADCB gene cluster is required for the utilization of sulfur from aliphatic sulfonates and is regulated by the transcriptional activator Cbl, *J. Biol. Chem. 274*, 29358–29365.

151. Iwanicka-Nowicka, R., and Hryniewicz, M. M. (1995) A new gene, cbl, encoding a member of the LysR family of transcriptional regulators belongs to Escherichia coli cys regulon, *Gene 166*, 11–17.

152. Gray, K. A., Mrachko, G. T., and Squires, C. H. (2003) Biodesulfurization of fossil fuels, *Current Opinion in Microbiology 6*, 229–235.

153. Oldfield, C., Pogrebinsky, O., Simmonds, J., Olson, E. S., and Kulpa, C. F. (1997) Elucidation of the metabolic pathway for dibenzothiophene desulphurization by Rhodococcus sp. strain IGTS8 (ATCC 53968), *Microbiology 143*, 2961–2973.

154. Lei, B., and Tu, S.-C. (1998) Mechanism of Reduced Flavin Transfer from Vibrio harveyi NADPH−FMN Oxidoreductase to Luciferase†, *Biochemistry 37*, 14623–14629.

155. Gao, B., and Ellis, H. R. (2005) Altered mechanism of the alkanesulfonate FMN reductase with the monooxygenase enzyme, *Biochem. Biophys. Res. Commun. 331*, 1137–1145.

156. Gao, B., and Ellis, H. R. (2007) Mechanism of flavin reduction in the alkanesulfonate monooxygenase system, *Biochim. Biophys. Acta 1774*, 359–367.

157. Abdurachim, K., and Ellis, H. R. (2006) Detection of protein-protein interactions in the alkanesulfonate monooxygenase system from Escherichia coli, *J. Bacteriol. 188*, 8153–8159.

158. Fisher, A. J., Raushel, F. M., Baldwin, T. O., and Rayment, I. (1995) Three-dimensional structure of bacterial luciferase from Vibrio harveyi at 2.4 A resolution, *Biochemistry 34*, 6581–6586.

159. Xiong, J., and Ellis, H. R. (2012) Deletional studies to investigate the functional role of a dynamic loop region of alkanesulfonate monooxygenase, *Biochimica et Biophysica Acta (BBA) - Proteins and Proteomics 1824*, 898–906.

160. Zhan, X., Carpenter, R. A., and Ellis, H. R. (2008) Catalytic importance of the substrate binding order for the FMNH2-dependent alkanesulfonate monooxygenase enzyme, *Biochemistry 47*, 2221–2230.

161. Farber, G. K., and Petsko, G. A. (1990) The evolution of alpha/beta barrel enzymes, *Trends Biochem. Sci. 15*, 228–234.

162. Malabanan, M. M., Amyes, T. L., and Richard, J. P. (2010) A role for flexible loops in enzyme catalysis, *Curr. Opin. Struct. Biol. 20*, 702–710.

163. Miller, B. G., Hassell, A. M., Wolfenden, R., Milburn, M. V., and Short, S. A. (2000) Anatomy of a proficient enzyme: the structure of orotidine 5'-

monophosphate decarboxylase in the presence and absence of a potential transition state analog, *Proc. Natl. Acad. Sci. U.S.A. 97*, 2011–2016.

164. Fisher, A. J., Thompson, T. B., Thoden, J. B., Baldwin, T. O., and Rayment, I. (1996) The 1.5-A resolution crystal structure of bacterial luciferase in low salt conditions, *J. Biol. Chem. 271*, 21956–21968.

165. Sparks, J. M., and Baldwin, T. O. (2001) Functional implications of the unstructured loop in the (beta/alpha)(8) barrel structure of the bacterial luciferase alpha subunit, *Biochemistry 40*, 15436–15443.

166. Xin, X., Xi, L., and Tu, S. C. (1991) Functional consequences of site-directed mutation of conserved histidyl residues of the bacterial luciferase alpha subunit, *Biochemistry 30*, 11255–11262.

167. Huang, S., and Tu, S. C. (1997) Identification and characterization of a catalytic base in bacterial luciferase by chemical rescue of a dark mutant, *Biochemistry 36*, 14609–14615.

168. Baldwin, T. O., Chen, L. H., Chlumsky, L. J., Devine, J. H., and Ziegler, M. M. (1989) Site-directed mutagenesis of bacterial luciferase: analysis of the “essential” thiol, *J. Biolumin. Chemilumin. 4*, 40–48.

169. Carpenter, R. A., Xiong, J., Robbins, J. M., and Ellis, H. R. (2011) Functional role of a conserved arginine residue located on a mobile loop of alkanesulfonate monooxygenase, *Biochemistry 50*, 6469–6477.

170. Ellis, H. R. (2011) Mechanism for sulfur acquisition by the alkanesulfonate monooxygenase system, *Bioorganic Chemistry 39*, 178–184.

171. Carpenter, R. A., Zhan, X., and Ellis, H. R. (2010) Catalytic role of a conserved cysteine residue in the desulfonation reaction by the alkanesulfonate monooxygenase enzyme, *Biochim. Biophys. Acta 1804*, 97–105.

172. Beaty, N. B., and Ballou, D. P. (1980) Transient kinetic study of liver microsomal FAD-containing monooxygenase, *J. Biol. Chem. 255*, 3817–3819.

173. Cleland, W. W. (1982) The use of pH studies to determine chemical mechanisms of enzyme-catalyzed reactions, *Meth. Enzymol. 87*, 390–405.

174. Cook, P. F., and Cleland, W. W. (2007) pH Dependence of Kinetic Parameters and Isotope Effects, in *Enzyme kinetics and mechanism*, pp 325–366. Garland Science, New York.

175. Schimerlik, M. I., Grimshaw, C. E., and Cleland, W. W. (1977) Determination of the rate-limiting steps for malic enzyme by the use of isotope effects and other kinetic studies, *Biochemistry 16*, 571–576.

176. Harris, T. K., and Turner, G. J. (2002) Structural basis of perturbed pKa values of catalytic groups in enzyme active sites, *IUBMB Life 53*, 85–98.

177. Czerwinski, R. M., Harris, T. K., Johnson, W. H., Jr, Legler, P. M., Stivers, J. T., Mildvan, A. S., and Whitman, C. P. (1999) Effects of mutations of the active site arginine residues in 4-oxalocrotonate tautomerase on the pKa values of active site residues and on the pH dependence of catalysis, *Biochemistry 38*, 12358–12366.

178. Mallett, T. C., and Claiborne, A. (1998) Oxygen reactivity of an NADH oxidase C42S mutant: evidence for a C(4a)-peroxyflavin intermediate and a rate-limiting conformational change, *Biochemistry 37*, 8790–8802.

179. Rynkiewicz, M. J., and Seaton, B. A. (1996) Chemical rescue by guanidine derivatives of an arginine-substituted site-directed mutant of Escherichia coli ornithine transcarbamylase, *Biochemistry 35*, 16174–16179.

180. Boehlein, S. K., Walworth, E. S., Richards, N. G., and Schuster, S. M. (1997) Mutagenesis and chemical rescue indicate residues involved in beta-aspartyl-AMP formation by Escherichia coli asparagine synthetase B, *J. Biol. Chem. 272*, 12384–12392.

181. Lehoux, I. E., and Mitra, B. (2000) Role of arginine 277 in (S)-mandelate dehydrogenase from Pseudomonas putida in substrate binding and transition state stabilization, *Biochemistry 39*, 10055–10065.

182. Xu, H., Alguindigue, S. S., West, A. H., and Cook, P. F. (2007) A proposed proton shuttle mechanism for saccharopine dehydrogenase from Saccharomyces cerevisiae, *Biochemistry 46*, 871–882.

183. Vashishtha, A. K., West, A. H., and Cook, P. F. (2009) Chemical mechanism of saccharopine reductase from Saccharomyces cerevisiae, *Biochemistry 48*, 5899–5907.

184. Brant, D. A., Barnett, L. B., and Alberty, R. A. (1963) The Temperature Dependence of the Steady State Kinetic Parameters of the Fumarase Reaction, *J. Am. Chem. Soc. 85*, 2204–2209.

185. McCallum, C., and Pethybridge, A. D. (1975) Conductance of acids in dimethyl-sulphoxide—II. Conductance of some strong acids in DMSO at 25°C, *Electrochim. Acta. 20*, 815–818.

186. Robbins, J. M., and Ellis, H. R. (2012) Identification of Critical Steps Governing the Two-Component Alkanesulfonate Monooxygenase Catalytic Mechanism., *Biochemistry 51*, 6378–6387.

187. Persson, G., Edlund, H., Hedenström, E., and Lindblom, G. (2004) Phase Behavior of 1-Alkylpyridinium Octane-1-sulfonates. Effect of the 1-Alkylpyridinium Counterion Size, *Langmuir 20*, 1168–1179.

188. Schowen, K. B., and Schowen, R. L. (1982) Solvent isotope effects of enzyme systems, *Meth. Enzymol. 87*, 551–606.

189. Quinn, D. M., and Sutton, L. D. (1991) Theoretical Basis and Mechanistic Utility of Solvent Isotope Effects, in *Enzyme mechanism from isotope effects* (Cook, P. F., Ed.), pp 73–126. CRC Press, Boca Raton.

190. Schowen, R. L. (1977) Solvent Isotope Effects on Enzymic Reactions, in *Isotope effects on enzyme-catalyzed reactions* (Cleland, W. W., O'Leary, M. H., and Northrop, D. B., Eds.), pp 64–99. University Park Press, Baltimore, MD.

191. Quinn, D. M., Elrod, J. P., Ardis, R., Friesen, P., and Schowen, R. L. (1980) Protonic reorganization in catalysis by serine proteases: acylation by small substrates, *J. Am. Chem. Soc. 102*, 5358–5365.

192. Harmony, J. A., Himes, R. H., and Schowen, R. L. (1975) The monovalent cation-induced association of formyltetrahydrofolate synthetase subunits: a solvent isotope effect, *Biochemistry 14*, 5379–5386.

193. Schowen, K. B. (1978) Solvent Hydrogen Isotope Effects, in *Transition states of biochemical processes* (Gandour, R. D., and Schowen, R. L., Eds.), pp 225–279. Plenum Press, New York.

194. Bazelyansky, M., Robey, E., and Kirsch, J. F. (1986) Fractional diffusion-limited component of reactions catalyzed by acetylcholinesterase, *Biochemistry 25*, 125–130.

195. Karsten, W. E., Lai, C.-J., and Cook, P. F. (1995) Inverse Solvent Isotope Effects in the NAD-Malic Enzyme Reaction Are the Result of the Viscosity Difference between D2O and H2O: Implications for Solvent Isotope Effect Studies, *J. Am. Chem. Soc. 117*, 5914–5918.

196. Raber, M. L., Freeman, M. F., and Townsend, C. A. (2009) Dissection of the stepwise mechanism to beta-lactam formation and elucidation of a rate-determining conformational change in beta-lactam synthetase, *J. Biol. Chem. 284*, 207–217.

197. Cook, P. F., and Cleland, W. W. (2007) Isotope Effects as a Probe of Mechanism, in *Enzyme kinetics and mechanism*, pp 253–324. Garland Science, New York.

198. Hengge, A. C. (2006) Secondary Isotope Effects, in *Isotope effects in chemistry and biology* (Kohen, A., and Limbach, H.-H., Eds.), pp 955–974. Taylor & Francis, Boca Raton.

199. Frankel, B. A., Kruger, R. G., Robinson, D. E., Kelleher, N. L., and McCafferty, D. G. (2005) Staphylococcus aureus sortase transpeptidase SrtA: insight into the kinetic mechanism and evidence for a reverse protonation catalytic mechanism, *Biochemistry 44*, 11188–11200.

200. Knuckley, B., Bhatia, M., and Thompson, P. R. (2007) Protein arginine deiminase 4: evidence for a reverse protonation mechanism, *Biochemistry 46*, 6578–6587.

201. Cook, P. F. (1991) Enzyme mechanism from isotope effects. CRC Press, Boca Ra ton. ISBN: 0849353122 9780849353123

202. Sucharitakul, J., Prongjit, M., Haltrich, D., and Chaiyen, P. (2008) Detection of a C4a-hydroperoxyflavin intermediate in the reaction of a flavoprotein oxidase, *Biochemistry 47*, 8485–8490.

203. Phillips, R. S. (1989) Mechanism of tryptophan indole-lyase: insights from pre-steady-state kinetics and substrate and solvent isotope effects, *J. Am. Chem. Soc. 111*, 727–730.